UNIVERSITY OF
LIVERPOOL

Planar Inverted-F Antennas for Wireless Communication

Thesis submitted in accordance with
the requirements of the University of Liverpool
for the degree of Doctor of Philosophy

by

Hassan Tariq Chattha

September 2010

Department of Electrical Engineering and Electronics

Acknowledgement

First of all, I thank to ALLAH ALMIGHTY who has given me the courage and confidence to do this work. This thesis could not be finished without the help and support of many people who are gratefully acknowledged here. At the very first, I would like to express my deepest gratitude to my supervisor, Dr. Yi Huang. He has always given me valuable ideas, suggestions and comments with his profound knowledge and rich research experience and guided me in the right direction. He was easily available and accessible and willing to discuss whenever I needed his guidance and support. I have learnt from him a lot not only about research, but also about the professional ethics. I am very much obliged to his efforts of helping me to complete this dissertation. I also would like to thank Dr. X. Zhu for supporting and guiding me in my research.

In addition, I wish to extend my thanks to the Department of Electrical and Electronics for its support of this study. I owe special thanks to Mr. John Lynch of the core services for his help and guidance in making and fabrication of my antenna designs.

I would like to thank my wife, Aqsa, for her patience and support during this work. She has to live alone a lot of times at home

when I was busy in doing research at University. This would not be possible without her support and encouragement.

Thanks are also due to my postgraduate friends, who never failed to give me great encouragement and suggestions. Special thanks should go to Mr. Shafayat Abrar, Mr. Yang Lu, Mr. Stephan Boyes, and Di Li for their brainstorming with me when I failed coming up with ideas. I am also indebted to Mr. Ping Cao, Miss Jingwei Zhang, and Miss Nida Khiabani for their support.

At last but not the least, I would like to thank my father and mother for their support, thoughtfulness and encouragement, all the way from the very beginning of my study. I am thankful to all my other family members, my sisters and my younger brother for their support. I also wish to thank all of my teachers at my school and college for their support, encouragement and guidance without whom I would not be able to achieve my goals.

Abstract

The Planar Inverted-F Antenna (PIFA) has evolved from a quarter-wavelength monopole antenna and is now widely used in mobile and portable radio applications due to its many attractive features such as simplicity of design, light-weight, low-cost, low-profile, conformal nature and reliable performance. Many antenna types for portable applications are extensions of PIFA antenna, which is considered as one of the strongest candidates for Multiple-Input Multiple-Output (MIMO) systems. In this work, PIFA is taken as a main element of study. Three different areas related to the PIFA antenna are investigated in this thesis.

First area related to PIFA investigated in this work is a comprehensive parametric study and a new empirical equation of PIFA. This work presents a thorough numerical and experimental study of Planar Inverted-F Antennas (PIFA) involving all the parameters which may affect the characteristics of PIFA. It is found that PIFA characteristics are affected by a number of parameters including the dimensions of the ground plane, length, width, height and position of the top plate, positions and widths of shorting pin/plate and feed pin/plate. Based on this parametric study, a new empirical

equation for predicting the resonant frequency of the PIFA is introduced; taking into account all the important parameters which significantly affect the resonant frequency. The comparisons between the new and the previously used empirical equations are provided to show the comparative accuracy of the new equation. The average percentage error found between the proposed and the actual operational frequencies is less than 3%. This proposed equation should be very useful to aid the antenna design.

The second investigation related to the PIFA concerns bandwidth enhancement techniques. PIFA is not yet employed as an ultra wide band antenna as this antenna is perceived as a narrow band antenna. This work introduces three techniques for enhancing the impedance bandwidth of PIFA, which are a) changes in the widths of feed plate and shorting plate, b) addition of an inverted-L shaped parasitic element and c) adding a rectangular shaped parasitic element. It is found that the width of feed plate plays an important role in broadening the antenna bandwidth. It is shown that a fractional impedance bandwidth up to 65% can be obtained by optimizing the widths of the feed and shorting plates. The 2nd technique introduces a PIFA antenna having an inverted-L shaped parasitic element. It is shown that due to the addition of this parasitic element, this PIFA antenna can achieve a very wide bandwidth (more than 100%). Further enhancement to this is achieved by adding another rectangular shaped

parasitic element at a right place. In this way, PIFAs with very wide fractional bandwidths (more than 120%) can be achieved by using the aforementioned techniques.

The third investigation involves the use of PIFA antenna as a diversity and / or MIMO antenna. This work presents three new and novel designs of dual-feed Planar Inverted-F Antenna (PIFA) for different heights suitable for wireless diversity / MIMO applications. The theme used is to employ only one PIFA antenna with multiple feeds / ports and using pattern and / or polarization diversity to produce diversity gain. First PIFA antenna design is dual-feed PIFA antenna with parallel feed plates for antenna height h = 10 mm. By exploiting the pattern diversity, we have successfully made a provision of two isolated feeding ports using one common radiating plate. The main technique introduced is to etch and modify the ground plane under the radiating plate to reduce the mutual coupling between the two ports which produces anti-resonance between the two ports. It is found that the envelope cross-correlation is less than 0.02 and the ratio of the mean effective gain between the two ports is close to unity. Thus, this new PIFA antenna can provide a better solution than two separate antennas for diversity and MIMO applications by saving the space and cost.

The 2nd PIFA antenna design presents a new and novel dual-feed Planar Inverted-F Antenna (PIFA) with perpendicular feed plates suitable for wireless applications such as Wireless Local Area Network (WLAN) and Long Term Evolution (LTE) as a diversity and MIMO antenna. Instead of two antenna elements, there is only one top radiating element with two isolated ports which save the space and the cost. The two feed plates are placed perpendicular to each other due to which polarization diversity as well as pattern diversity is exploited to achieve diversity gain. The isolation between the two antenna ports is achieved by the modifying the ground plane under the top radiating element.

The 3rd design presents a new low profile dual-feed planar Inverted-F Antenna (PIFA) suitable for wireless LAN applications for height h = 5 mm. Pattern diversity is utilized using one common radiating plate and two isolated feeding ports. The isolation is successfully achieved mainly by modifying the ground plane under the radiating plate and producing anti-resonance between the two ports. Thus, this single PIFA antenna can act as two separate antennas for diversity and MIMO applications with reduced space and cost.

Contents

List of Figures

Patent Applications

1. **H. T. Chattha** and Yi Huang, "Planar Inverted F Antenna with Parasitic Element", United Kingdom Patent Application No. GB0902679.0, February 2009.
2. **H. T. Chattha** and Yi Huang, "A dual-feed PIFA diversity and MIMO Antenna", United Kingdom Patent Application No. GB0920286.2, March 2010. (Under Extensive Examination)

List of Publications

1. **H. T. Chattha**, Y. Huang, X. Zhu and Y. Lu, "An ultra wideband planar inverted-F antenna", *Microwave and Optical Technology Letters,* volume 52, page(s): 2285-2288, 2010.
2. **H. T. Chattha**, Y. Huang, X. Zhu and Y. Lu, "Dual-feed PIFA diversity antenna for wireless applications", *Electronics Letters*, volume 46, page(s): 189 – 190, 2010.
3. **H. T. Chattha**, Y. Huang, X. Zhu and Y. Lu, "An empirical equation for predicting the resonant frequency of planar inverted-F antennas", *IEEE Antennas and Wireless Propagation Letters*, volume 8, page(s): 856 – 860, 2009.
4. **H. T. Chattha**, Y. Huang and Y. Lu, "PIFA bandwidth enhancement by changing the widths of feed and shorting plates", *IEEE Antennas and Wireless Propagation Letters*, volume 8, page(s): 637-640, 2009.
5. **H. T. Chattha**, Y. Huang, X. Zhu and Y. Lu, "A dual feed PIFA diversity antenna for MIMO systems", *International Workshop on Antenna Technology (iWAT)*, page(s): 1 – 4, 2010.
6. **H. T. Chattha**, Y. Huang, X. Zhu, and Y. Lu, "A further study of planar inverted-F antenna", *International Workshop on Antenna Technology (iWAT)*, page(s): 1 – 4, 2009.
7. **H. T. Chattha**, Y. Huang, X. Zhu, and Y. Lu, "A study of parameter changes on the characteristics of planar inverted-F antenna", *3rd European Conference on Antennas and Propagation (EuCAP)*, page(s): 1 – 4, 2009.
8. **H. T. Chattha**, Y. Huang, X. Zhu, and Y. Lu, "Further bandwidth enhancement of PIFA by adding a parasitic element", *Loughborough Antennas & Propagation Conference (LAPC)*, page(s): 213 – 216, 2009.
9. Y. Lu, Y. Huang, and **H. T. Chattha**, "Size reduction of a wideband slot antenna", *3rd European Conference on Antennas and Propagation (EuCAP)*, page(s): 1455 - 1458, 2009.

10. Y. Lu, Y. Huang, Y. Shen and **H. T. Chattha**, "A further study of planar UWB monopole antennas", *Loughborough Antennas & Propagation Conference (LAPC)*, page(s): 353 – 356, 2009.
11. Y. Lu, Y. Huang, and **H. T. Chattha**, "Effects of wheeler cap loss on wideband antenna efficiency measurement results", *International Workshop on Antenna Technology (iWAT)*, page(s): 1 – 4, 2009.
12. Y. Huang, Y. Lu, **H. T. Chattha**, X. Zhu, I. Hewitt, and S. Hussain, "UWB antennas for radio positioning systems", *3rd European Conference on Antennas and Propagation (EuCAP)*, page(s): 3779 - 3782, 2009.
13. Y. Huang, Y. Lu, S. Boyes, **H. T. Chattha** and N. Khiabani, "Wideband antenna efficiency measurements", *International Workshop on Antenna Technology (iWAT)*, page(s): 1 – 4, 2010.
14. Y. Lu, Y. Huang, **H. T. Chattha**, Y. Shen and S. Boyes, "An elliptical UWB monopole antenna with reduced ground plane effects", *International Workshop on Antenna Technology (iWAT)*, page(s): 1 – 4, 2010.
15. **Hassan Tariq Chattha**, Yi Huang and S. J. Boyes, "Polarization and pattern diversity based dual-feed planar inverted-F antenna", Submitted in *IEEE Trans. on Antennas & Propagation*, October 2010.
16. **Hassan Tariq Chattha**, Yi Huang and M. K. Ishfaq, "Bandwidth enhancement techniques for planar inverted-F antenna", Submitted in *IET Trans. on Microwaves, Antennas & Propagation*, October 2010.
17. **Hassan Tariq Chattha**, Yi Huang and S. J. Boyes, "Low profile dual-feed planar inverted-F antenna for wireless LAN applications", Submitted in *Microwave and Optical Technology Letters*, September 2010.

CHAPTER

1

Introduction

Over the last two decades, the wireless mobile communication technology has made a spectacular progress from first-generation (1G) analogue voice-only communication to second-generation (2G) digital voice communication. Currently, the third generation (3G) mobile communication technology not only providing digital voice services, but also providing video telephony, internet access and videos download services. Furthermore, the forthcoming fourth-generation (4G) mobile telephone technology is aiming to provide on-demand high quality video and audio services. Wireless Local Area Network (WLAN) technology has also made a giant stride by introducing Wi-Fi (Wireless Fidelity). Wi-Fi is a set of product compatibility standards for WLAN technology based on the IEEE 802.11 specifications. It enables a person with a wireless-enabled computer, laptop or personal digital assistant (PDA) to connect to the internet within proximity of an access point at a maximum data rate of 54 Mbps. Now a day, Wi-Fi is not only used solely

for internet connections, but it is also used to broadcast quality multimedia content throughout the entire home. WiMax (Worldwide Interoperability for Microwave Access) is a wireless technology which is designed for Metropolitan Area Networks (MAN) based on the IEEE 802.16 specifications. It aims to provide high speed wireless internet connectivity over long distances. Both the 4G and WiMax technologies require high data rates and longer range to provide quality services to the end users. These advancements in the communication technology and ever increasing demands of the consumers have tremendously increased the need for communications with high data rates, more reliability, power efficient, and cheaper wireless services. To achieve these high quality services, wireless communication technology has to be pushed to the physical limits of the radio channels. The channel capacity or data rate of a communication system is limited by the bandwidth and the transmitted power. A well known upper bound on the maximum achievable data rate for the ideal band-limited additive white Gaussian noise (AWGN) channel is given by the Shannon-Nyquist criterion [1]. Having an available channel bandwidth, W and signal-to-noise ratio (SNR) over this bandwidth, the maximum transmit data rate is:

$$C = W \log_2 (1 + SNR) \quad \text{bits / s} \tag{1.1}$$

From equation (1.1), it is clear that data rates can only be increased by increasing the bandwidth occupation or transmission power. However, the radio spectrum available for the wireless systems is very limited and expansive, and therefore it is crucial to increase the channel capacity and the reliability of the wireless systems without additional spectrum usage. Also, the signal power cannot be readily increased as the communication systems are interference limited.

Until a few years ago, these limits have been expanded by introducing the spatial domain to mobile communication antennas. By introducing an array of antenna elements at both receivers and transmitters, the channel capacity of that system can grow linearly with the number of

antennas under ideal conditions. This system with multiple antennas at both link-ends of a wireless communication technology is called a Multiple-Input Multiple-Output (MIMO) system. In 1987, Winters reported that the capacity of the multi-antenna fading channels can be enhanced by applying multiple antennas at both the transmitters and receivers [2]. Lately, the potential capacity of the MIMO system was theoretically demonstrated by Foschini and Gans [3-4], and Telatar [5]. Since then, MIMO systems have attracted a considerable interest in both the academic and industry worlds, and significant amount of efforts have been put into the researches and developments of MIMO systems [6-15]. The MIMO system can enhance not only the channel capacity, but also the reliability (Quality of Service) of the wireless communication system by exploiting different coding schemes.

Antenna arrays can improve reliability and capacity in two ways. First, diversity combining or adaptive beam forming techniques can combine the signals from multiple antennas in a way that mitigates multi-path fading. Second, adaptive beam forming using antenna arrays can provide capacity improvement through interference reduction.

1.1 Motivation of the Work

The requirements of the antenna elements at the small devices like mobiles, laptops and PDA terminals are low-profile, conformal nature, light weight and low cost while maintaining high bandwidth, good isolation and low envelope cross-correlation [16]. The application of MIMO technology on small terminals causes a problem that the antenna array must be installed inside the small terminal chassis. This causes a high degree of mutual coupling and the spatial correlation between antenna elements and it affects the MIMO channels capacity. For ideal diversity antenna array (i.e. zero correlation), the antenna elements should have zero mutual coupling between them [17]. The strong surface current on the ground plane of the antennas has been one of the main reasons for the high mutual coupling between the antennas and results in high correlation [18]. Conventionally, low correlation

can be achieved at the base stations by spacing the antennas an appropriate distance a part i.e. spatial diversity. However, in small portable terminals, the space is very limited to place more than one antenna elements. When the antennas are spaced closely, this will result in high correlation and no diversity gain could be achieved. Therefore, the motivation of this work is to explore other antenna diversity techniques such as polarization and pattern diversities to achieve low correlation and similar mean power levels between the antennas for MIMO terminals.

As Planar Inverted-F Antenna (PIFA) is now widely used in small portable applications, it is chosen as main antenna element for study in this work. PIFA antenna is investigated in depth by doing a comprehensive parametric study as it was found that a comprehensive parametric study of PIFA does not exist in literature taking into account all those parameters which affect the characteristics of PIFA such as resonant frequency, impedance bandwidth and radiation pattern. PIFA antenna is generally considered a narrow band antenna therefore this work includes the investigation of bandwidth enhancing techniques for PIFA antenna to make this antenna a broadband antenna. Then the PIFA is adopted as a MIMO and diversity antenna to produce diversity gain. The theme is to use one antenna with only one radiating element with multiple ports and then diversity gain is achieved by exploiting the pattern and/or polarization diversity. Due to only one antenna element, it can easily fit into the chassis/body of the small portable system.

1.2 Organization of the Thesis

The rest of the thesis is organized as follows.

Chapter 2 describes the types of antennas which are being implemented on small portable terminals such as mobiles, laptops and PDAs over the last decade.

Chapter 3 covers the Planar Inverted-F Antenna (PIFA) in detail. It includes the comprehensive parametric analysis of planar inverted-F antenna (PIFA) taking into account all those parameters which significantly affect the characteristics of PIFA. Based on the parametric study, a new empirical equation for PIFA is developed and validated.

Chapter 4 introduces three bandwidth enhancement techniques for PIFA which significantly increase the impedance bandwidth of PIFA. Based on these techniques, Ultra Wide Band (UWB) PIFA antennas are made and tested which are discussed in detail.

Chapter 5 discusses the MIMO systems, its signaling schemes and its channel capacity. This chapter also includes the diversity, its combining schemes and its types in detail. It also discusses the conditions necessary to achieve the diversity gain from diversity antennas.

Chapter 6 describes three new designs for different heights in which PIFA is used as a diversity and MIMO antenna with only one common radiating element and multiple feeds. The antenna designs of dual-feed PIFAs are presented for Bluetooth/WLAN 2.45 GHz frequency band.

Chapter 7 discusses the conclusions and some thoughts of the future work.

References

[1] C. E. Shannon, "A Mathematical theory of communication," Bell Syst. Tech. J., Vol. 27, pp. 379-423, 623-656, July & October 1948.

[2] J. Winters, "On the capacity of radio communication system with diversity in a Rayleigh fading environment", *IEEE Journal on Selected Areas in Communications*, vol. 5, no. 5, pp. 871-878, June 1987.

[3] G. J. Foschini, "Layered space-time architecture for wireless communication in a fading environment when using multi-element antennas," Bell Labs Tech J., vol. 1, no. 2, pp. 41-59, 1996.

[4] G. J. Foschini and M. J. Gans, "On limits of wireless communications in a fading environment when using multiple antennas", *Wireless Personal Communications*, page(s): 311-335, March 1998.

[5] I. E. Telatar, "Capacity of multi-antenna gaussian channels", *European Transaction on Telecommunications*, vol. 10, no. 6, pp. 585-595, Nov. 1999.

[6] D. Chizhik, J. Ling, P. W. Wolniansky, R. A. Valensuela, N. Costa and K. Huber, "Multiple-input multiple-output measurements and modeling in Manhattan", *IEEE Journal on Selected Areas on Communications*, vol. 21, no. 3, pp. 321-331, April 2003.

[8] D. Chizhik, J. Ling, D. Samardzija and R. A. Valenzuela, "Spatial and polarization characterization of MIMO channels in rural environment", *IEEE 61st Vehicular Technology Conference*, vol. 1, pp. 161-164, 2005.

[9] A. J. Paulraj, D. A. Gore, R. U. Nabar and H. Bolcskei, "An overview of MIMO communications-a key to gigabit wireless", *Proceedings of the IEEE*, vol. 92, no. 2, pp. 198-218, February 2004.

[10] A. Goldsmith, S. A. Jafar, N. Jindal and S. Vishwanath, "Capacity limits of MIMO channels", *IEEE Journal on Selected Areas in Communications*, vol. 21, no. 6, pp. 684-702, June 2003.

[11] L. Dong, H. Choo, R. W. Heath and H. Ling, "Simulation of MIMO channel capacity with antenna polarization diversity", *IEEE Transactions on Wireless Communications*, vol. 4, no. 4, pp. 1869-1873, July 2005.

[12] F. Tila, P. Shepherd and S. R. Pennock, "Theoretical capacity evaluation of indoor micro and macro MIMO systems at 5 GHz using site specific ray tracing", *Electronics Letters*, vol. 39, no. 5, pp. 471-472, March 2003.

[13] A. F. Molisch, "A generic model for MIMO wireless propagation channels in macro and micro cells", *IEEE Transactions on Signal Processing*, vol. 52, no. 1, pp. 61-71, January 2004.

[14] A. Paulraj, D. Gore and R. Nabar, *Introduction to space-time wireless communications*, Cambridge University Press, 2003.

[15] M. Martoner, *Multiantenna digital radio transmission*, Artech House Publishers, 2002.

[16] S. Yeap, X. Chen, C. C. Chiau, J. Dupuy and C. G. Parini, "Integrated diversity antenna for laptop and PDA terminals", *IEE Proc. Microwaves, Antennas & Propagation*, vol. 152, no. 6, pp. 495-504, December 2005.

[17] R. G. Vaughan and J. B. Andersen, "Antenna diversity in mobile communications", *IEEE Trans. on Vehicular Technology*, vol. 36, pages(s): 147-172, Nov. 1987.

[18] K. Wong, *Planar antennas for wireless communications*, John Wiley & Sons, New York, 2003.

CHAPTER

2

Antennas for Small Portable Systems

2.1 Introduction

Antennas for small portable systems include those used in cellular phones, walkie-talkie for private and emergency service applications and data terminals such as laptops and Personal Digital Assistants (PDAs). These systems require carefully designed antennas at both the base station and the user terminal end for efficient operation. It is essential to carefully control radiation patterns to target the desired coverage areas while minimizing the outside interference. The antenna structure should minimize interactions with its surroundings, such as supporting structures and the human body, while maximizing the efficiency for radiation and reception. The requirements of antennas which make them suitable for small terminals are examined in this chapter, together with an outline of the main structures of antennas which are

suitable and being used on smaller terminals and their key design issues are discussed in this chapter.

2.2 Antenna Performance Requirements

Antennas for the small portable systems are subjected to a wide range of variations in the environment which they encounter. The propagation conditions vary from very wide multipath arrival angles to a strong line-of-sight component. The orientation of the terminal is often random, particularly when a portable device is in a standby mode. The antennas must be able to operate in the close proximity of the user's head and hand. They must also be suitable for manufacturing in very large volumes at an acceptable cost. Increasingly, the users prefer the antenna to be fully integrated with the casing of the terminal rather than being separately identifiable [1]. In general, these challenging requirements may be summarized as follows:

Radiation Pattern: Approximately omni-directional in azimuth plane and wide beam widths in the vertical planes, although the precise pattern are usually uncritical and given the random orientations, the large degree of multi-paths and the pattern disturbances which are inevitable and given the close proximity of the user.

Input Impedance: The input impedance should be stable and well-matched to the source impedance over the whole bandwidth of interest, even in the presence of detuning from proximity of the user and other objects. Many user terminals now operate over a wide variety of standards, so multi-band, multi-mode operations via several resonances are increasingly a requirement.

Efficiency: Given the low gain of the antenna, it is important to achieve a high translation of input RF power into radiation over the whole range of conditions of use.

Manufacturability: Efficient antenna manufacturing at large scale should be possible, without the need for tuning of individual elements, while being robust enough against mechanical and environmental hazards encountered while moving.

Size and Integrability: The antenna size should be as small as possible, consistent with meeting the performance requirements. Furthermore, the ability to fit into the chassis of the portable system acceptable to a consumer product is important. As portable systems are increasing becoming smaller and smaller in size, those antennas are preferred which are able to be integrated with the printed circuit board (PCB) of the portable systems.

2.3 Small Antenna Fundamentals

Antennas on small portable devices are often classified as electrically small antennas. There are various rules of thumb for considering an antenna to be electrically small. The most common definition is that the largest dimension of the antenna is no more than one-tenth of a wavelength. Thus, a dipole with a length of $\lambda/10$, a loop with a diameter of $\lambda/10$, or a patch with a diagonal dimension of $\lambda/10$ would be considered electrically small [2]. This definition makes no distinction among the various methods used to construct electrically small antennas. In fact, most work on these antennas involves selecting topologies suitable for specific applications, and the development of integral or external matching networks. [1]. There is a body of literature which highlights the performance trade-offs inherent in such antennas. In particular there is basic trade-off between size, bandwidth and directivity. Small antennas, with small aperture size, cannot achieve directivity. Similarly, the bandwidth and directivity cannot both be increased if the antenna is to be kept small [3]. As the size decreases, the radiation resistance decreases relative to the ohmic losses, thus decreasing efficiency. Increasing the bandwidth tends to decrease efficiency, although dielectric or ferrite loading can decrease the minimum size. This is best illustrated by examining the relationship between the quality factor, Q of the antenna and

the size. Assuming a resistive match load, for a first-order mode, whether electrical or magnetic, the Q is related to the electrical size of the antenna by [3].

$$Q_{01} = \frac{1}{(Kr)^3} + \frac{1}{Kr} \tag{2.1}$$

where K is wave number and r is radius of the antenna.

If both the electrical and magnetic first-order modes are excited together, then the combined Q is somewhat lower.

$$Q_{E,M01} = \frac{1}{2(Kr)^3} + \frac{1}{Kr} \tag{2.2}$$

2.4 Development of Small Antennas on Small Terminals

One of the trends in small mobile terminal technology in the past few years is the reduction in sizes and weights of mobile terminals driven by the development of modern integrated circuit technology and the preference of the users. This remarkable reduction in the terminal's size has initiated a rapid evolution of the embedded antennas design for mobile terminals. The antennas are required to be small, and yet their optimum performances need to be maintained.

Several reviews of antennas for small mobile terminals have been reported in the past few years [4-8]. Over the past two decades, the size, price and weight of the small mobile terminal have been reduced, as shown in Fig. 2.1, from the single frequency band voice service only portable cellular phone in the late 1980s (about 600cc in volume and approximately 1000g in weight) to the current multi-band multi-functional small handheld mobile terminal (less than 60cc in volume and a weight of less than 100g). The antennas used for small mobile terminals have evolved from monopole to PIFA, and also other types of antennas such as helical antennas, microstrip

patch, meander line and dielectric resonator (DR) antennas also play important roles in small mobile terminals [4, 5, 9-11].

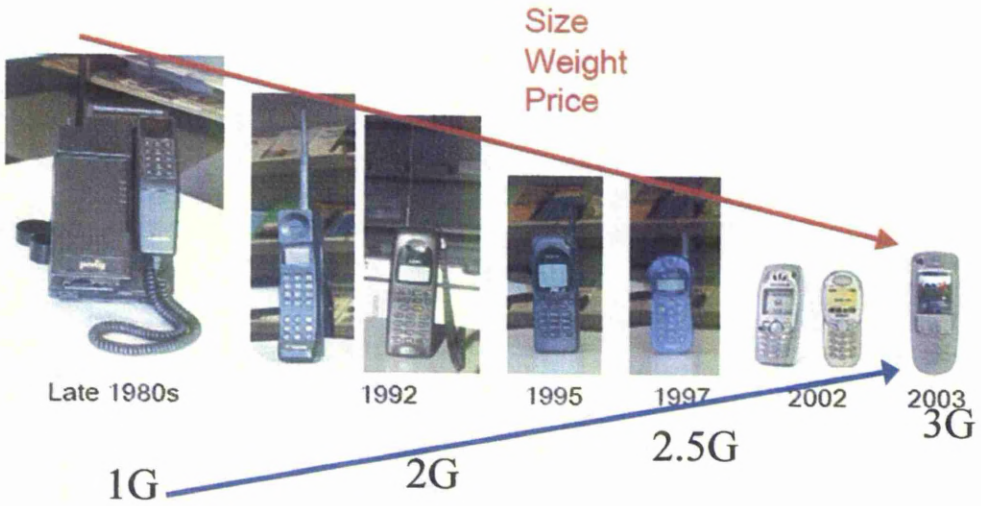

Fig. 2.1 Reduction in size and weight of mobile phones with the passage of time [Internal report]

There has always has been a customer demand to make more compact mobiles, therefore GSM (Global System for Mobile Communications) mobile terminals industry prefers to use built-in (or internal) antennas, instead of using a monopole that remains outside of the main mobile structure as shown in Fig. 2.1. Therefore, PIFA has been widely used now as a built-in (internal) antenna as it can be easily integrated with Printed Circuit Board (PCB) of the antenna. In this section, the commonly used antennas on mobile terminals such as monopole, planar monopole, helical antenna and meander line antennas are discussed in detail and Planar Inverted-F antenna (PIFA) is discussed in the next chapter.

2.4.1 Monopoles

The quarter-wavelength monopole antenna was invented by Marconi by using the image theory in 1896. It is a fundamental mobile antenna and has as a simple structure as shown in Fig. 2.2. The quarter-

wavelength monopole antenna became popular in 1980's for mobile terminals due to its simple structure and short length as it is half of the corresponding dipole. Also its directivity is double whereas the input impedance is half to that of the corresponding dipole antenna. Like half-wavelength dipole antenna, the monopole antenna is a resonant antenna as its input impedance is about 37 Ω which matches well with the 50 Ω transmission line [12]. All these good reasons have made the quarter-wavelength monopole antenna as one of the most popular antennas. Therefore we can find the use of this antenna in many applications such as radio broadcasting towers and mobile phone base stations etc. There are many derivatives of monopole antennas developed to make it suitable for different applications as shown in Fig. 2.3, some of which will be discussed later in this chapter. Fujimoto et al has shown that a quarter-wavelength monopole antenna caused large leakage currents to the terminal case compared to the half-wavelength dipole antenna [4]. Also the monopole antenna is based on image theory which assumes that there is an infinite ground plane connected with the monopole antenna. But in real applications, we do not have an infinite ground plane or the ground plane is not a perfect conductor (like the earth). If the conducting ground plane is of limited size, the radiated power will leak to the lower half of the space, which changes the radiation pattern. There may be side or even back lobes. The edge of the ground plane will diffract the waves which results in many side lobes and the directivity will also reduce and also the input impedance may be changed. If the ground plane is not large enough, it can act as a radiator rather than a ground plane. If the ground plane is very large but not made of a good conductor, all the antenna properties are affected, especially the directivity and gain (reduced); the angle to the maximum radiation is also tilted towards the sky although there are still no lobes in the lower half space.

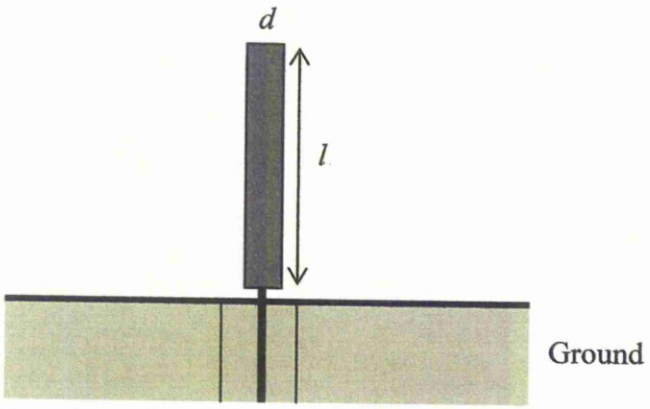

Fig. 2.2 A monopole antenna with a coaxial feed

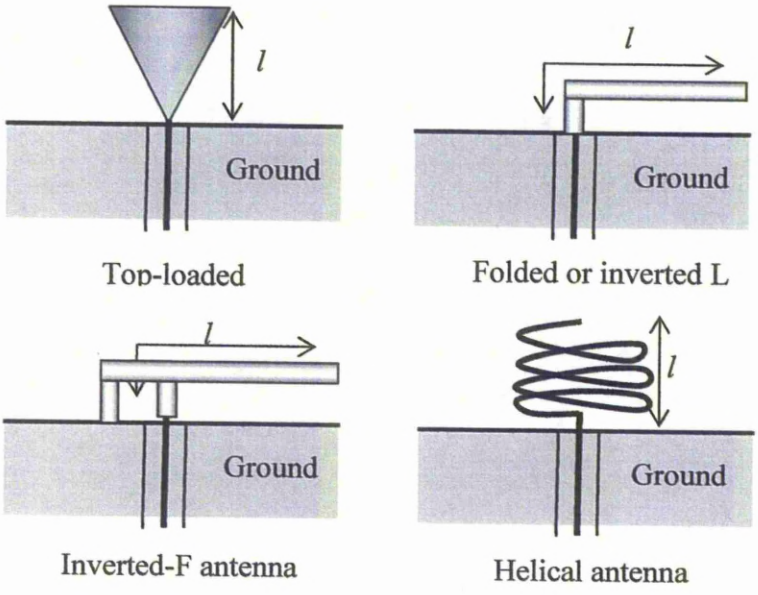

Fig. 2.3 Some popular forms of monopole antenna [12]

2.4.2 Low-Profile and Planar Monopole Antennas

Conventional monopoles for applications in mobile phones are usually protruded from mobile phone housing. Such a protruded monopole tends to break off easily and also greatly increases the total length of the mobile phone. To overcome this problem, several novel monopole designs with a much reduced height have been developed recently. These kind of

low-profile monopoles are very suitable for integration within the mobile phone housing and operation as a built-in antenna [13]. These designs include branch line planar monopole [14-16], branch patch planar monopole in a wrapped structure [17], planar monopole with slits [18], rectangular spiral planar monopole, monopole chip antenna [19] and folded planar monopole [20-21]. The planar monopole antennas have attracted a considerable attention as they offer excellent frequency bandwidth, omni-directional pattern in the azimuth plane, compact size, ease of fabrication and most importantly the planar structure makes them easily integratable with printed circuit boards [22-23]. Owing to their ability of huge bandwidth, a lot of UWB planar monopole antennas have been developed [24-27]. Planar UWB monopoles have been realized by either a coplanar waveguide (CPW) feed [28-30] or a microstrip-line feed [31] as shown in Fig. 2.4, which has eased its fabrication on printed circuit boards.

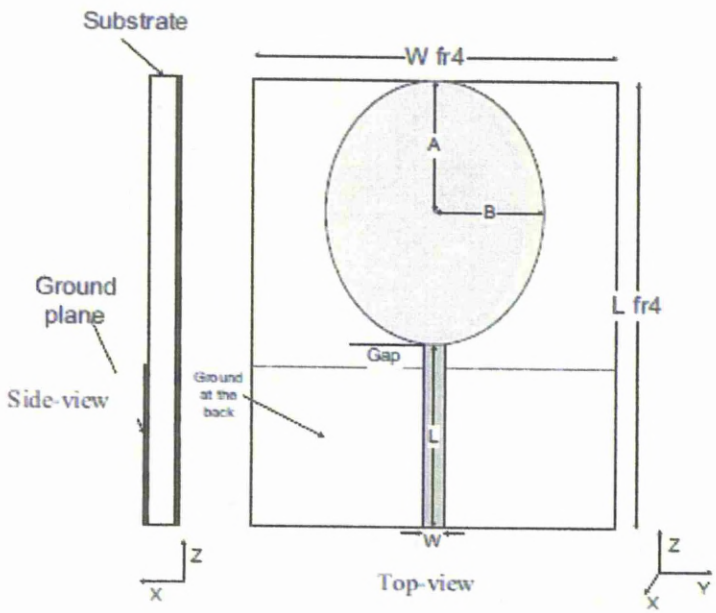

Fig. 2.4 Geometry of the microstrip feed elliptical monopole antenna [31]

2.4.3 Helix / Helical Antennas

The monopole antenna can be reduced in length from quarter wavelength to 4-15% wavelength by introducing a distributed inductive loading, conventionally named helical antenna [4, 12]. A helical consists of a conductor wound into a helical or spiral shape and enclosed in plastic or rubber. It is a circularly / elliptically polarized antenna. The helical antenna is a hybrid of two simple radiating elements, the dipole and loop antennas. A helix can radiate in many modes, the axial (end-fire) and the normal (broadside) mode are the ones of most interest. It consists of a wire wound N turns around a cylinder in diameter D with spacing S between the turns, and it is fed against a ground plane at one end of the structure by a coaxial cable, as shown in Fig. 2.5. The total length of the helix is $L = NS$ while the total length of the wire is $L_w = NL_0 = N\sqrt{S^2 + C^2}$ where $L_0 = \sqrt{S^2 + C^2}$ is the length of the wire between each turn, and $C = \pi D$ is the circumference of the helix. Another important parameter is the pitch angle α (i.e. the angle formed by a line tangent to the helix wire and a plane perpendicular to the helix axis) is defined by [32].

$$\alpha = \tan^{-1}\left(\frac{S}{\pi D}\right) = \tan^{-1}\left(\frac{S}{C}\right) \tag{2.3}$$

A helix becomes a linear antenna (like monopole) when its diameter approaches zero or pitch angle goes to 90°. It is then known as the Normal Mode Helical Antenna (NMHA). In this case, the diameter of the helix is much smaller than the wavelength ($D \ll \lambda$) and the total length is also smaller than the wavelength. A helix of fixed diameter can be seen as a loop antenna when the spacing between the turns vanishes (α=0). The NMHA was widely used in the commercial mobile phones in the middle of 1990s due to its short length, ease of fabrication and low cost. Fig. 2.6 shows a prototype of a dual band non-uniform NMHA. But it is having a deficiency that it cannot be

integrated with the printed circuit board. That is why these antennas are not used now a day in cellular handsets.

The axial mode (end-fire) occurs when the circumference of the helix is comparable with wavelength ($C = \pi D \approx \lambda$) and the total length is much greater than the wavelength. The axial mode helix antennas are mostly used for satellite communication and GPS due to their high gain and end-fire radiation patterns [33].

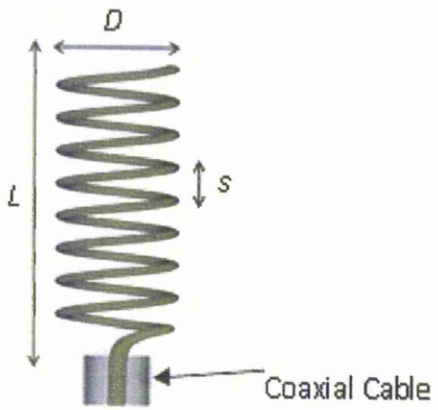

Fig. 2.5 Geometrical configuration of Helix [12]

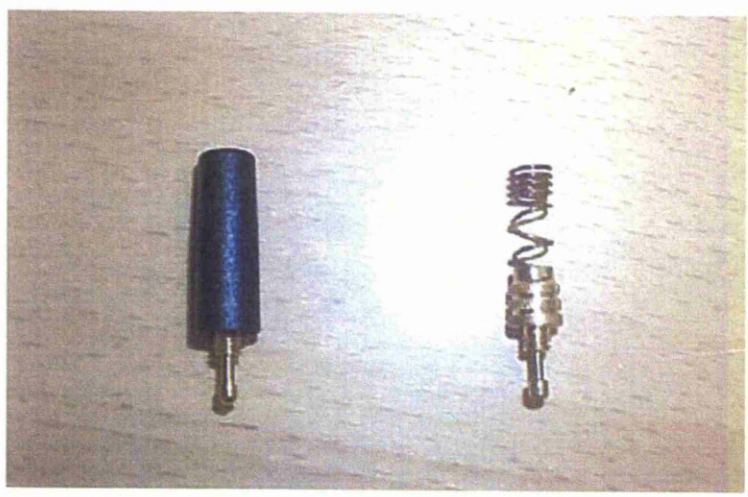

Fig. 2.6 A dual band non-uniform helix invented in 1996 by Z. Ying (Ericsson) [7]

2.4.4 Meander Line Antennas

A monopole antenna can also be shortened by the use of a printed meander line pattern instead of helical wire in case of NMHA. Meander line antennas are physically small but electrically large antennas [4, 34-36]. The meander pattern can be printed on a small piece of flexible board rolled on a core like NMHA as shown in Fig. 2.7. Multi-band characteristics can be accomplished by connecting two or more λ/4 meanders in parallel with each other or on the opposite sides of a substrate as shown in Fig. 2.8.

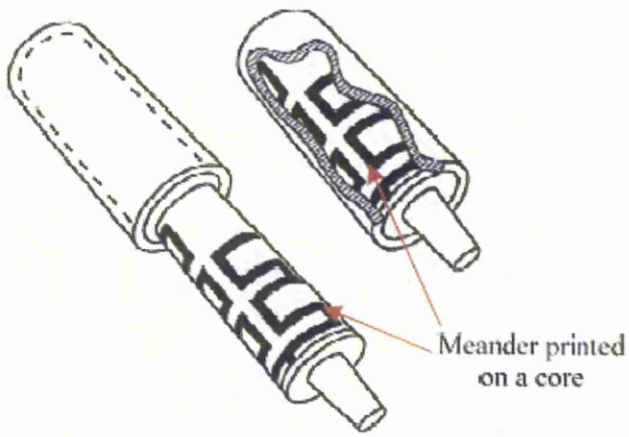

Fig. 2.7 Meander printed antenna on a core [4]

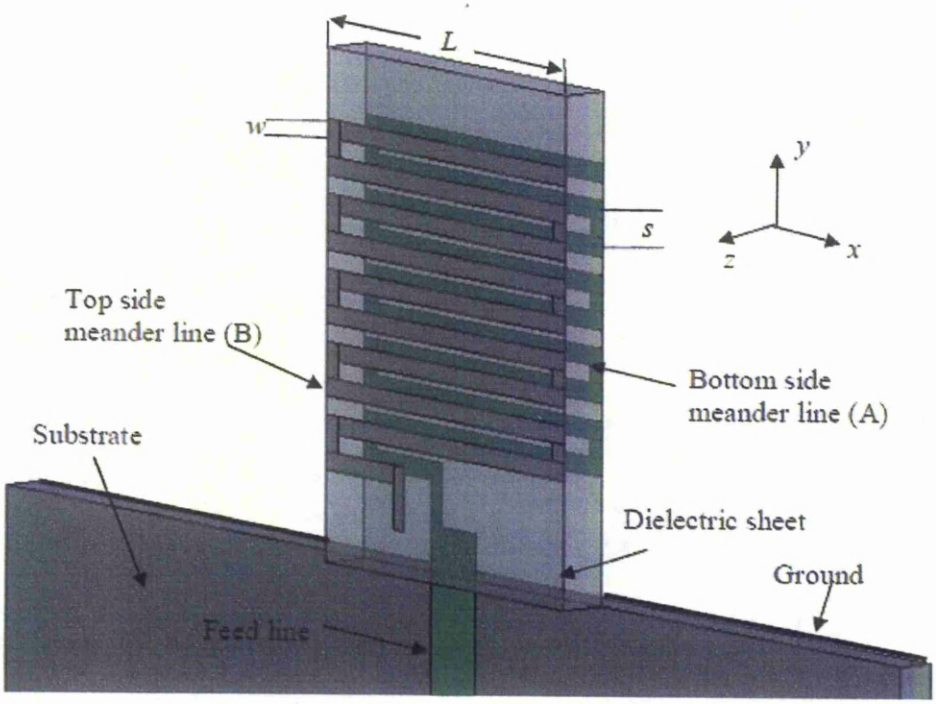

Fig. 2.8 Geometry structure of a dual-band meander-line antenna [25]

References

[1] S. R. Saunder, A. A. Zavala, *Antennas and propagation for wireless communication systems*, 2nd Edition, John Wiley & Sons Ltd, 2007.

[2] D. Miron, *Small antenna design*, Newnes 2006.

[3] J. S. Mclean, "A re-examination of the fundamental limits on the radiation Q of electrically small antennas", *IEEE Transaction on Antennas and propagation*, vol. 44, no. 5, May 1996.

[4] K. Fujimoto and J. R. James, *Mobile antenna systems handbook*, Norwood USA, Artech House, 2nd Edition, 2001.

[5] H. Morishita, Y. Kim, and K. Fujimoto, "Design concept of antennas for small mobile terminals and the future perspective", *IEEE Antennas and Propagation Magazine*, vol. 44, no. 5, pp. 30-43, October 2002.

[6] S. Sekine, H. Shoki, and H. Morishita, "Antennas for wireless terminals," *Institute of Electronics, Information and Communication Engineers (IEICE) Tran.*, vol. E86-B, no. 3, pp. 1005-1015, March 2003.

[7] Z. Ying, "Some important antenna innovations in the mobile terminal industry in the last decade", *Nordic antenna symposium*, Sweden, June 2006.

[8] R. Serrano, S. Blanch, and L. Jofre, "Small antenna fundamentals and technologies: Futrue trends", *European Conference on Antennas and Propagation (EuCap)*, France, November 2006.

[9] J. R. James and P. S. Hall, *Handbook of microstrip antennas*, London: Peter Pereginus Ltd, 1998.

[10] T. Taga and K. Tsunekawa, "Performance analysis of a built-in planar inverted f antenna for 800 MHz band portable radio units," *IEEE Journal on selected areas in communications*, vol. 5, pp. 921-929, March 1987.

[11] Z. Wu, "Application studies of dielectric resonator antennas", *IEEE International Symposium on Microwave, Antenna, Propagation and EMC Technologies for Wireless Communications*, vol. 2, page(s): 1435-1438, August 2005.

[12] Y. Huang and K. Boyle, *Antennas: from theory to practice*, John Wiley & Sons, 2008.

[13] Kin-Lu Wong, *Planar antennas for wireless communications*, John Wiley & Sons, 2003.

[14] Y. Zing, "Multiple band, multiple branch antenna for mobile phone", World Intellectual Property Organization, International Publication No. WO 99/22420, May 6, 1999.

[15] P. L. Teng and K. L. Wong, "Planar monopole folded into a compact structure for very-low-profile multi-band mobile phone antenna", Microwave Opt. Technology Letters, vol. 33, page(s): 22-25, April 5, 2002.

[16] K. Rutkowski and G. J. Hayes, "Multiple frequency band branch antennas for wireless communications", U. S. Patent No. 6198442, March 6, 2001.

[17] F. S. Chang, S. H. Yeh and K. L.Wong, "Planar monopole in wrapped structure for low-profile GSM/DCS mobile phone antenna", *Electronics Letters*, vol. 38, page(s): 499-500, May 23, 2002.

[18] G. Y. Lee and K. L. Wong, "Very-Low-profile bent planar monopole antenna for GSM/DCS dual-band mobile phones", *Microwave and Optical Technology Letters*, vol. 34, page(s): 406-409, September 20, 2002.

[19] K. L. Wong, S. W. Su, T. W. Chiou and Y. C. Lin, "Dual-band plastic chip antenna for GSM/DCS mobile phones", *Microwave and Optical Technology Letters*, vol. 33, page(s): 330-332, June 5, 2002.

[20] G. Y. Lee, S. H. Yeh and K. L. Wong, "A broadband folded planar monopole antenna for mobile phones", *Microwave and Optical Technology Letters*, vol. 33, page(s): 165-167, May 5, 2002.

[21] F. S. Chang and K. L. Wong, "Folded meandered patch monopole antenna for low-profile GSM/DCS dual-band mobile phone", *Microwave and Optical Technology Letters*, vol. 34, page(s): 84-86, July 20, 2002.

[22] N. P. Agrawall, G. Kumar and K. P. Ray, "Wide-band planar monopole antennas", *IEEE Trans. on Antennas Propagation*, vol. 46, no. 2, page(s): 294–295. 1998.

[23] Z. N. Chen, et.al, "Planar antennas" *IEEE Microwave Magazine*, vol. 7, Issue 6, pp. 63 – 73, December 2006.

[24] K. C. L. Chan; Y. Huang, X. Zhu, "A planar elliptical monopole antenna for UWB applications", *IEEE/ACES International Conference on Wireless Communications and Applied Computational Electromagnetics*, pp. 182 – 185, April 2005.

[25] S. Y. Suh, W. L. Stutzman, and W. Davis, "A new ultra wide band printed monopole antenna: the planar inverted cone antenna (PICA)", *IEEE Trans. on Antennas Propagation*, vol. 52, pp.1361-1365, May 2004.

[26] X. Chen, J. Liang, P. Li, L. Guo, C. C. Chiau and C. G. Parini, "Planar UWB monopole antennas". *Asia-Pacific Microwave Conference Proceedings* Vol. 1, pp. 4, December 2005.

[27] J. Liang, C. C. Chiau, X. Chen, and C. G. Parini, "Analysis and design of UWB disc monopole antennas", *IEE Seminar on Ultra Wideband Communications Technologies and Syst. Design*, Queen Mary, University of London, pp. 103–106, July 8, 2004,

[28] Y. Kim and D. H. Kwon, "CPW-fed planar ultra wideband antenna having a frequency band notch functions", *Electronics Letters*, vol. 40, page(s): 403–405, 2004.

[29] W. Wang, S. S. Zhong and S. B. Chen, "A novel wideband coplanar-fed monopole antenna", *Microwave and Optical Technology Letters*, vol. 43, page(s): 50–52, 2004.

[30] S. Y. Suh, W. Shutzman, W. Davis, A. Waltho, and J. Schiffer, "A novel CPW-fed disc antenna". *IEEE Antennas Propagation Soc. Symp.*, vol. 3, 20–25, page(s): 2919–2922, June 2004.

[31] Y. Lu, Y. Huang, Y. C. Shen and H. T. Chattha, "A further study of planar UWB monopole antennas", *Loughborough Antennas and Propagation Conference (LAPC)*, page(s): 353-356, 2009.

[32] C. Balanis, *Advanced engineering electromagnetics*, John Wiley & Sons, 1989.

[33] J. D. Kraus and R. J. Marhefka, *Antennas*, McGraw-Hill Science, 3rd Edition, 2001.

[34] J. P. Lee and S. O. Park, "The meander line antenna for bluetooth", *Microwave and optical Technology Letters*, vol. 34, page(s): 149 – 151, June 2002.

[35] L. J. Jing, Y. Y. Kyi and G. Y. Beng, "Analysis of dual-band meander-line antenna", *IEEE International Symposium Antenna and Propagation Society*, page(s): 2033-2036, 2006.

[36] H. Liu, S. Ishikawa, S. Kurachi and T. Yoshimasu, "Miniaturized microstrip meander-line antenna with very high-permittivity substrate for sensor applications", *Microwave and Optical Technology Letters*, vol. 49, page(s): 2438 – 2440, July 2007.

CHAPTER

3

Planar Inverted-F Antenna

3.1 Introduction

Compact antennas have been the centre of research interests due to the rapid progress in wireless communication in the last two decades. The low profile, light weight and low fabrication cost make microstrip antennas very attractive for wireless communication [1]. However, the size of microstrip antennas cause inconvenience for wireless applications such as handset mobiles at the lower microwave frequencies. To reduce the size of microstrip antenna, a potential candidate is the inverted-F antenna, which is a modified form of the microstrip antenna. The inverted-F antenna typically consists of a rectangular planar element located above a ground plane, a short circuiting pin/plate, and a feeding mechanism for the planar radiating element. The inverted-F Antenna is evolved from monopole antenna as can be seen from Fig. 3.1, where the top section has been folded down which

makes this section parallel to the ground plane. This is done to decrease the height, while maintaining a resonant trace length. This parallel section introduces capacitance to the input impedance of the antenna, which is compensated by the adding a short-circuiting stub. The end of this short-circuit stub is connected to the ground plane. The inverted F antenna is now widely used in mobile and portable applications due to its simple design, lightweight, low-cost, conformal nature and reliable performance [2-7]. Many antenna types for portable applications are extensions of the inverted-F antenna; and many dual band or even tri-band antennas have the inverted- F antenna as the basic antenna element [8-10]. Due to these excellent features, the IFA is one of the strongest candidates for MIMO systems having an array of Inverted-F type of antennas [11-12].

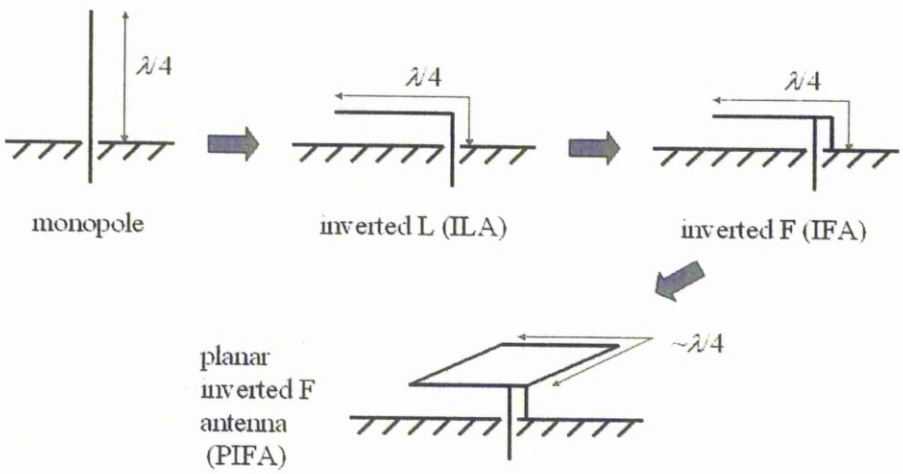

Fig. 3.1 Evolution of PIFA from monopole antenna [6]

The planar inverted-F antenna (PIFA) is an extension of the wire inverted-F antenna in which the wire is replaced with a plate in order to increase the bandwidth. Some of the advantages of the PIFA antenna are as follows.

- PIFA can hide into the housing of the mobile as compared to the whip, rod and helix antennas.

- PIFA has reduced backward radiation towards the user's head, minimizing the electromagnetic wave power absorption (SAR) and enhance antenna performance.
- PIFA exhibits moderate to high gain in both vertical and horizontal states of polarization. This feature is very beneficial in certain wireless communications where the antenna orientation is not fixed and the reflections are present from different corners of the environment. In these cases, the important parameter to be considered is the total field that is vector sum of the horizontal and vertical states of polarizations.

Due to these advantages, PIFA is very suitable for MIMO antenna systems. A comprehensive study is carried out to get an in depth of this PIFA antenna which is discussed next.

3.2 Comprehensive Parametric Study of Planar Inverted-F Antenna

In the case of a wire Inverted-F Antenna (IFA), design curves are available for a given resonant frequency and impedance bandwidth through which IFA can be easily designed [13]. However, no such design curves exist for the PIFA. If similar design curves could be made available, it would be a very useful guideline for people to design the PIFA antenna at a given resonant frequency. There are many papers which describe the variations in the characteristics of PIFA due to changes of its parameters [14-24]. More specifically, the effects of the ground plane and the height of the top plate are discussed in [19-23] and [24] respectively. However, there has not been presented a comprehensive study involving all the parameters of PIFA.

Therefore, a comprehensive simulated and experimental study of planar inverted-F antenna (PIFA) is carried out involving all the parameters

which may affect the characteristics of PIFA including resonant frequency, impedance bandwidth and radiation pattern. The effects on the characteristics of PIFA due to changes in the dimensions of ground plane, position of the PIFA on the ground plane, length, width and height of the top radiating plate, and the distance of shorting plate from the edge of top plate are presented. Similarly the effects of changing the widths of the feed plate and the shorting plate and the feeding positions under the top plate are also discussed.

3.2.1 Antenna Configuration

The configuration of the PIFA used for simulated and experimental study is shown in Figs. 3.2 and 3.3. The radiating top plate has dimensions $L \times W$ and ground plane dimensions are $L_g \times W_g$. The dielectric material used above the rectangular ground plane is FR-4 having a thickness t = 1.5 mm and a relative permittivity ε_r = 4.4. The antenna height h is filled with free space. The shorting plate has dimension $W_s \times (h+t)$ and feed plate has dimensions $W_f \times h$. The horizontal distance between shorting and feeding plates is L_b and vertical distance of feeding plate from upper edge of top plate is L_u. The distance between the shorting plate and the edge of top plate is L_s. The vertical and horizontal distances of the PIFA structure from the ground plane edges are L_z and X respectively, as shown in Fig. 3.3. The ground plane is placed in x-y plane and the height of antenna is along z-axis.

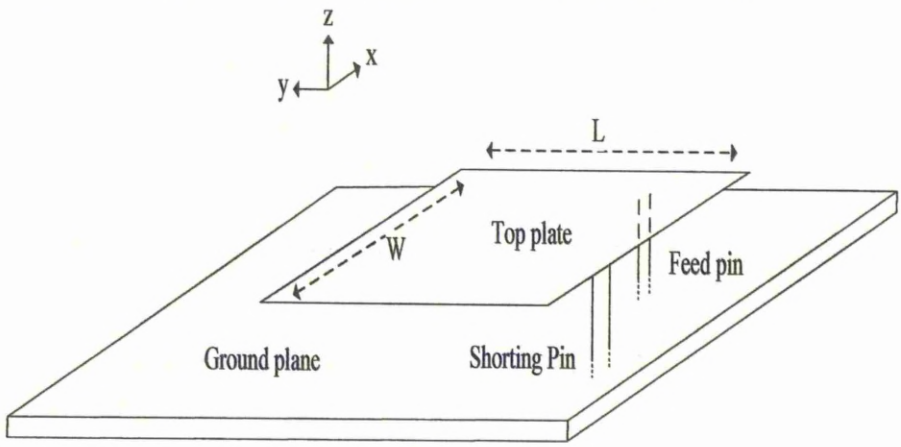

Figure 3.2 Planar inverted-F antenna under study

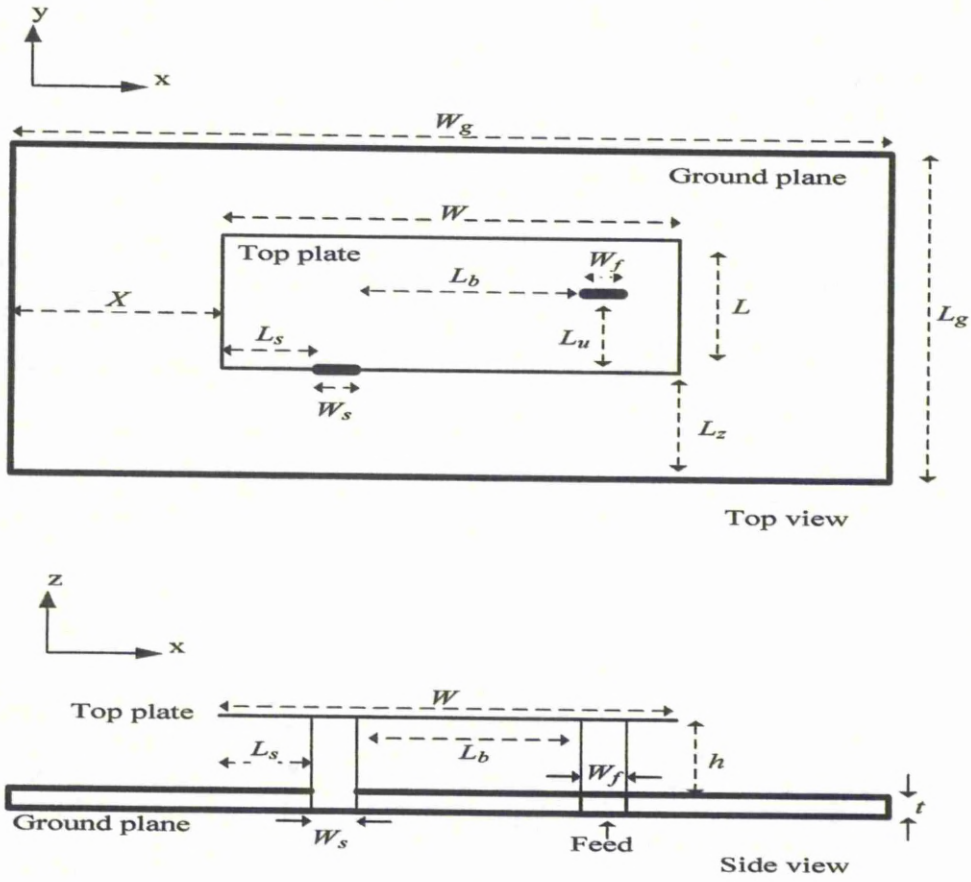

Fig. 3.3 Geometry of PIFA structure

3.2.2 Simulated and Experimental Study

The procedure adopted for this study is that only one parameter is changed at a time to observe its effects on the PIFA characteristics while all other parameters are held constant. Different sets of parameters are taken for study to cover a wide range of values and also at different resonant frequencies. The operational frequency ranges from 0.5 GHz to 3 GHz. The software used for simulations is High Frequency Structure Simulator (HFSS) based on the Finite Element Method.

3.2.2.1 Ground Plane Effects

The width of ground plane W_g is varied from *45 mm* to *85 mm* and

all other parameters are constant at $L_g = 75\ mm$, $W = 37.5\ mm$, $L = 18\ mm$, $h = 12\ mm$, $W_f = 10\ mm$, $W_s = 5\ mm$, $L_b = 15\ mm$, $L_z = 0\ mm$, $X = 0\ mm$, $L_s = 0\ mm$ and $L_u = 0\ mm$. The simulated and experimental results are shown in Fig. 3.4 which shows that changes in width of ground plane as functions of the resonant frequency, fractional bandwidth and radiation pattern. Generally the greater the value of W_g, the lower is the resonant frequency.

Similarly, the length of ground plane L_g is varied from $45\ mm$ to $105\ mm$ while all other parameters are held constant at $W_g = 75\ mm$, $W = 75\ mm$, $L = 30\ mm$, $h = 30\ mm$, $W_f = 24\ mm$, $W_s = 1\ mm$, $L_b = 21\ mm$, $L_z = 0\ mm$, $X = 0\ mm$, $L_s = 0\ mm$ and $L_u = 0\ mm$. The measured and simulated results are shown in Fig. 3.5. It is evident that the variation of length of ground plane changes the resonant frequency, fractional bandwidth and radiation pattern. The increase in L_g decreases the resonant frequency and increases the fractional bandwidth. It is evident from the figures that the resonant frequency is not very sensitive to the dimensions of the ground plane – this could be due to the fact that the antenna dimension is the dominant factor for radiation. After extensive simulations, it is also observed that minimum ground plane dimensions of length plus width required for maximum impedance bandwidth is $\lambda/2$.

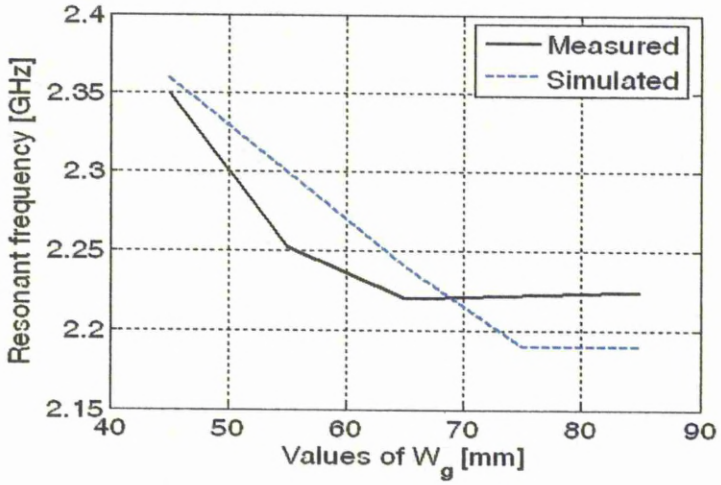

(a)

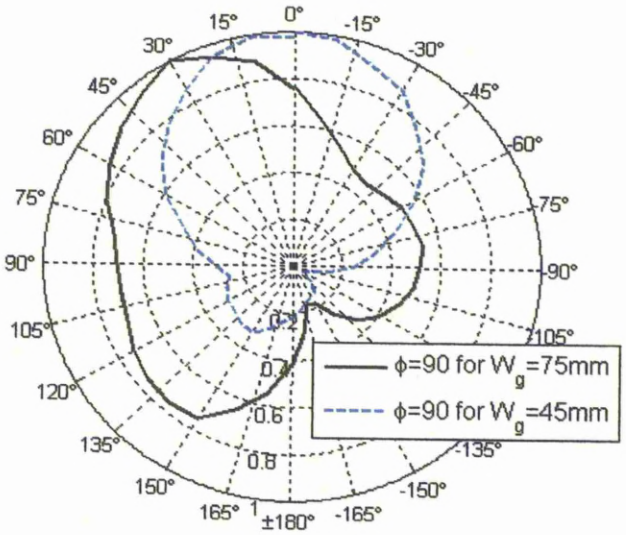

(b)

Figure 3.4 Effect of changes in W_g on (a) Resonant Frequency (b) Rad. pattern in elevation ($\Phi = 90^{\circ}$) plane

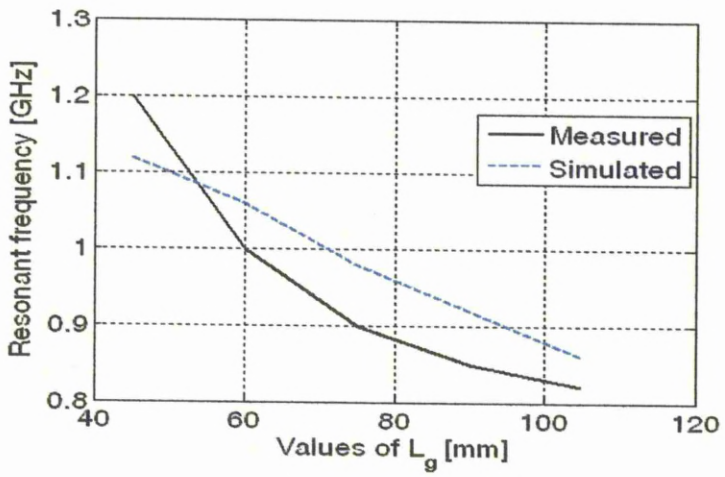

(a)

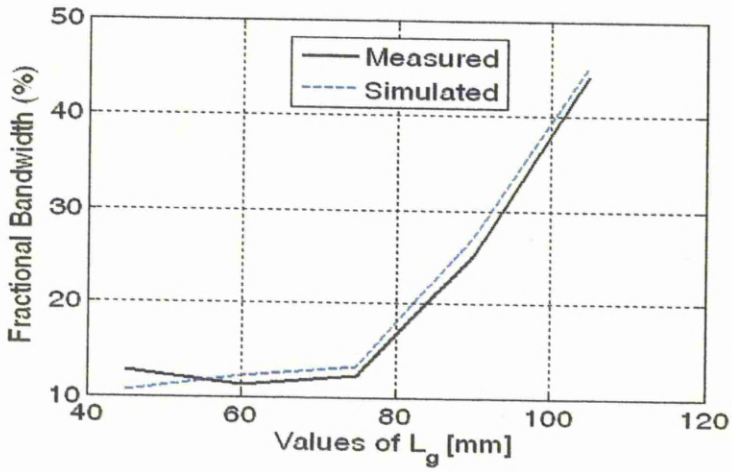

(b)

Fig. 3.5 Effect of variations in ground plane lengths *Lg* on (a) Resonant frequency (b) Fractional bandwidth

3.2.2.2 Position of the PIFA on the Ground Plane

The changes are made in the horizontal distance X and vertical distance L_z of the PIFA from edges of ground plane to observe their effects on the characteristics of PIFA. The value of X is changed from *0 mm* to *20 mm* and the value of L_z is changed from *0 mm* to *50mm* while all other parameters are constant at $L_g = 75$ *mm*, $W_g = 65$ *mm*, $W = 37.5$ *mm*, $L = 18$ *mm*, $h = 12$ *mm*, $W_f = 10$ *mm*, $W_s = 5$ *mm*, $L_b = 10$ *mm*, $L_z = 0$ *mm*, $L_s = 0$ *mm* and $L_u = 0$ *mm*. The simulated and experimental results are shown in Figs. 3.6 and 3.7. The results show that variations in X and L_z change the resonant frequency and impedance bandwidth and have significant effects on radiation pattern, and increase in either X or L_z increases the resonant frequency and decreases the fractional bandwidth.

It is concluded that the placement of PIFA on ground plane significantly affects the characteristics of the PIFA and PIFA needs to be placed at upper edge ($Lz = 0$ *mm*) and side edge ($X = 0$ *mm)* of ground plane for maximum impedance bandwidth.

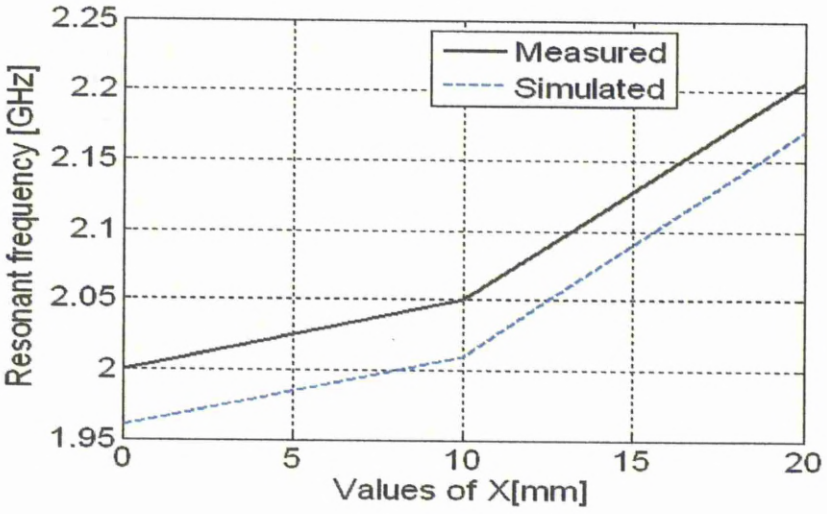
Measured
Simulated
Resonant frequency [GHz]
2.25
2.2
2.15
2.1
2.05
2
1.95
0
5
10
15
20
Values of X[mm]

(a)

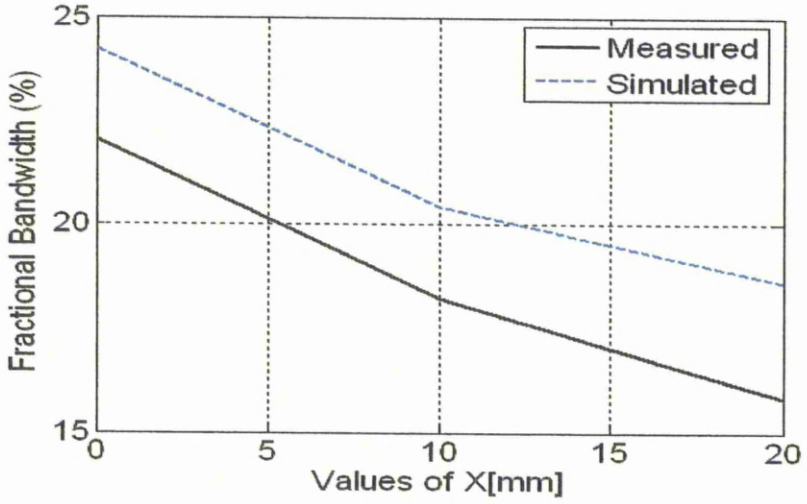
Measured
Simulated
Fractional Bandwidth (%)
25
20
15
0
5
10
15
20
Values of X[mm]

(b)

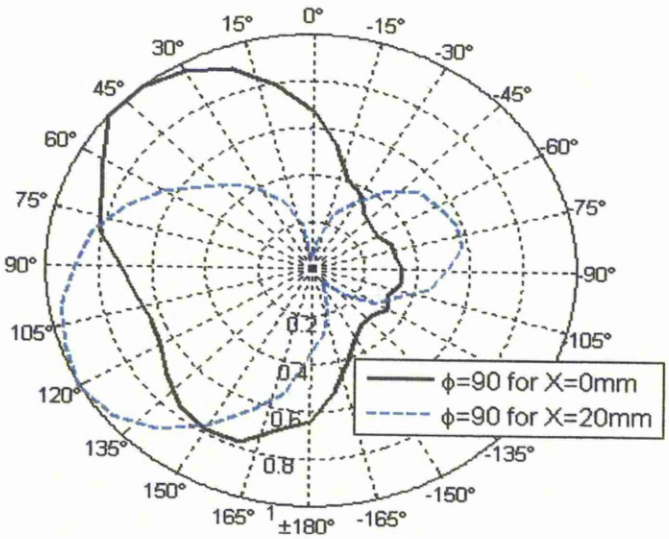

Fig. 3.6 Effect of changes in values of X on (a) Resonant frequency (b) Fractional bandwidth (c) Rad. pattern in elevation ($\Phi = 90^{\circ}$) plane

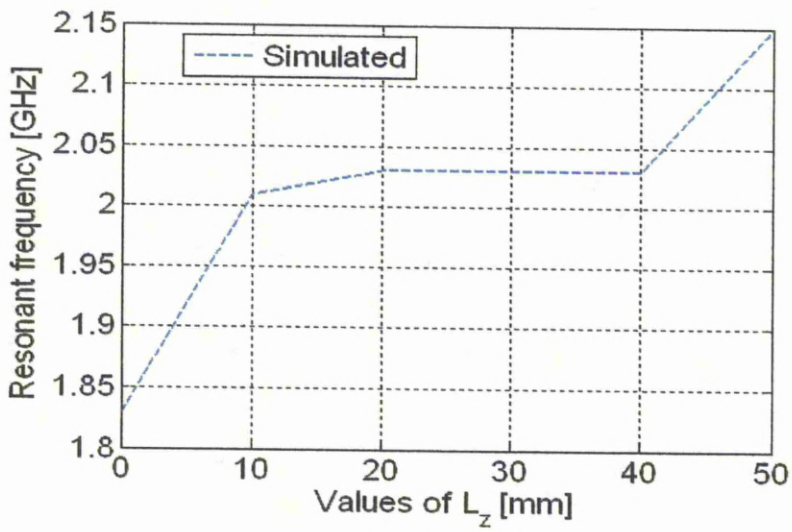

(a)

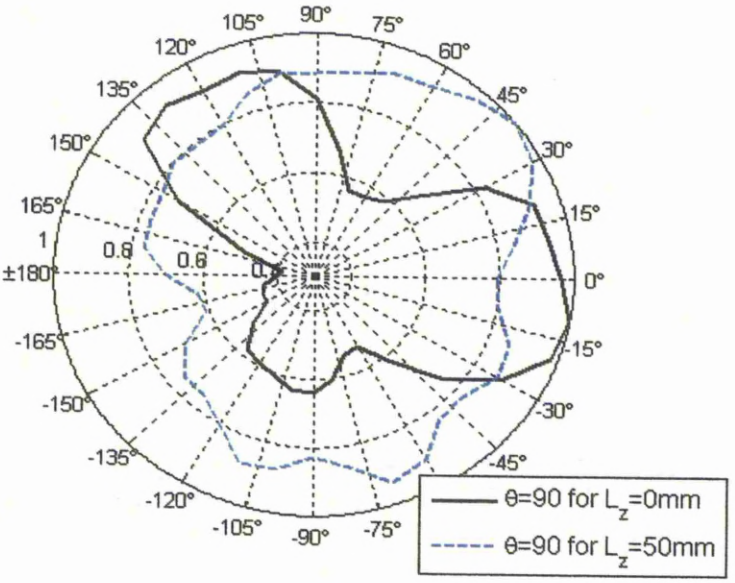

(b)

Fig. 3.7 Effect of variations in the values of *Lz* on (a) Resonant frequency (b) Rad. pattern in azimuth ($\theta = 90°$) plane

3.2.2.3 Dimensions of Top Plate

The changes are made in the length and the width of rectangular top plate and its effects are observed on the characteristics of PIFA. The width of top plate is varied from *38 mm* to *50 mm* and length of top plate is varied from *05 mm* to *25 mm* while all other parameters are constant at $L_g = 60$ *mm*, $W_g = 50$ *mm*, $X = 0$ *mm*, $L_z = 0$ *mm*, $h = 14$ *mm*, $W_f = 15$ *mm*, $W_s = 2$ *mm*, $L_s = 0$ *mm*, $L_b = 10$ *mm* and $L_u = 0$ *mm*. The simulated and experimental results are shown in Figs. 3.8 and 3.9 respectively. The results show that the increase in the length or width of top plate decreases the resonant frequency and affects the impedance bandwidth. As PIFA is a quarter-wavelength antenna so by the increase of either length or width of top plate, the wavelength increases and resonant frequency decreases. The small changes in length and width do not have a significant effect on the radiation pattern but as we know from theory of characteristic modes, the radiation pattern is basically dependent on size and shape of top plate [25]. If the shape of the element is varied, the resonant frequency and the radiating properties of the modes will

change.

It is also concluded that the greater the size of the top plate of PIFA, the more directed the radiation pattern i.e. the directivity will be higher as shown in Fig. 3.9(b).

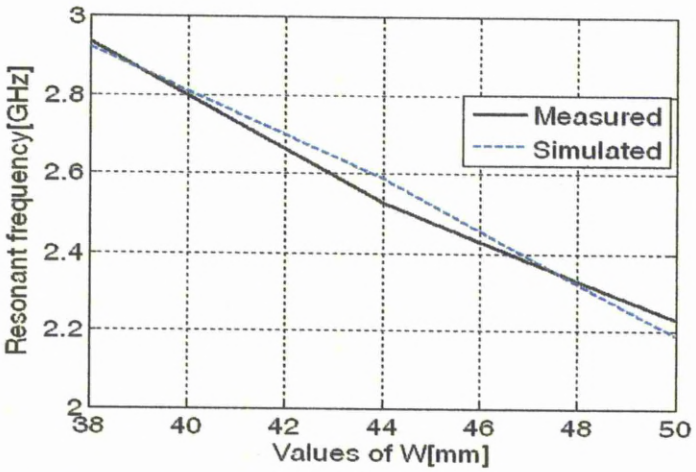

Fig. 3.8 Values of W (mm) vs. resonant frequency (GHz)

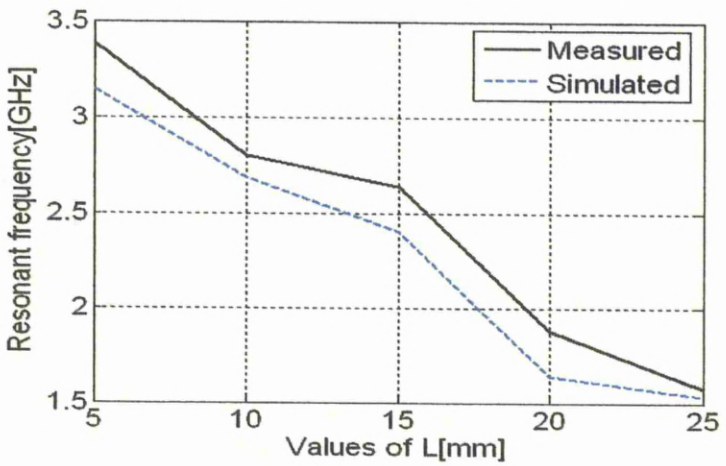

(a)

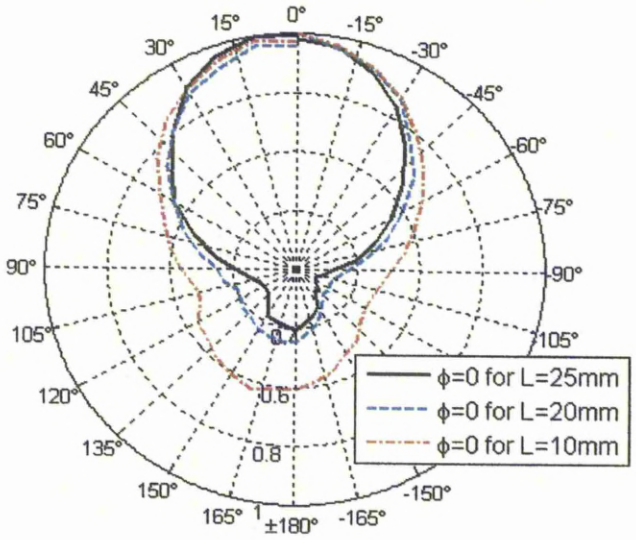

(b)

Fig. 3.9 Effect of altering the values of L on (a) Resonant frequency (b) Radiation pattern in elevation ($\Phi = 0^{\circ}$) plane

3.2.2.4 Height of Top Plate

The height of top plate h is varied from *12 mm* to *20 mm* to observe its effect while all other parameters are constant at $L_g = 75$ *mm*, $W_g = 65$ *mm*, $X = 0$ *mm*, $L_z = 0$ *mm*, $W = 37.5$ *mm*, $L = 18$ *mm*, $W_f = 10$ *mm*, $W_s = 5$ *mm*, $L_s = 0$ *mm*, $L_b = 15$ *mm* and $L_u = 0$ *mm*. The simulated and experimental results are shown in Fig. 3.10. The results show that the increase in height decreases the resonant frequency and increases the fractional impedance bandwidth, but does not have any significant effect on the radiation pattern. The decrease in the resonant frequency is obvious, as h increases the wavelength increases. The height of the PIFA can be increased to enhance the impedance bandwidth but a small height of the top plate is preferred in practice as the antenna has to be small enough to fit it in the chassis of small terminal devices. So the height of antenna cannot normally be used to enhance the impedance bandwidth in applications.

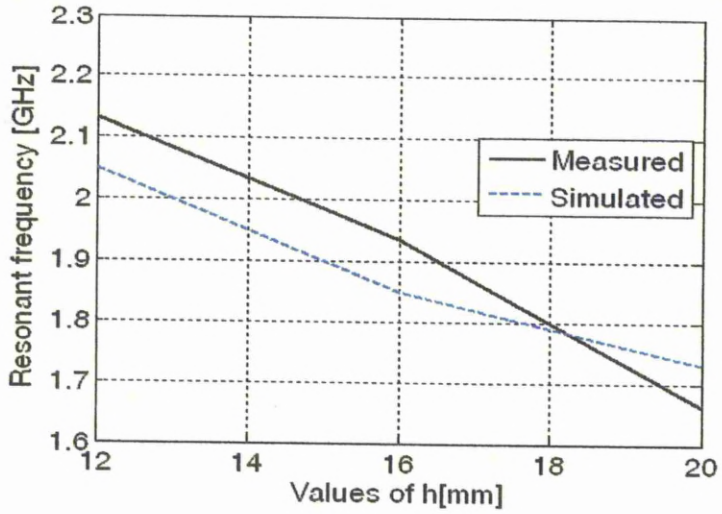
Resonant frequency [GHz]
2.3
2.2
2.1
2
1.9
1.8
1.7
1.6
12
14
16
18
20
Values of h[mm]
Measured
Simulated

(a)

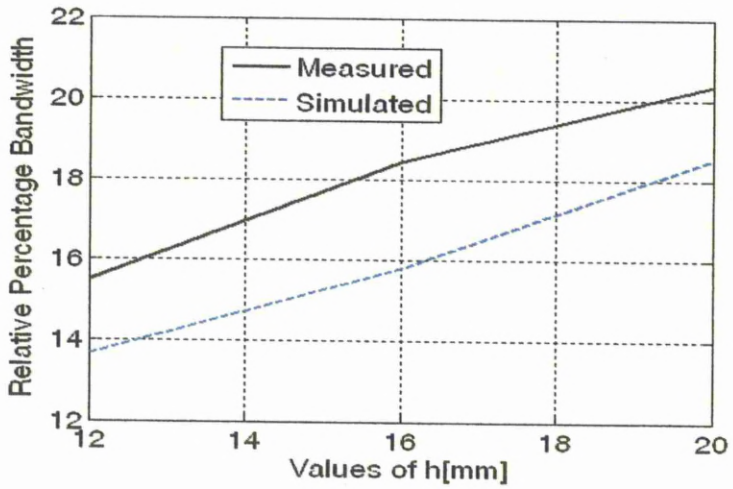
Relative Percentage Bandwidth
22
20
18
16
14
12
12
14
16
18
20
Values of h[mm]
Measured
Simulated

(b)

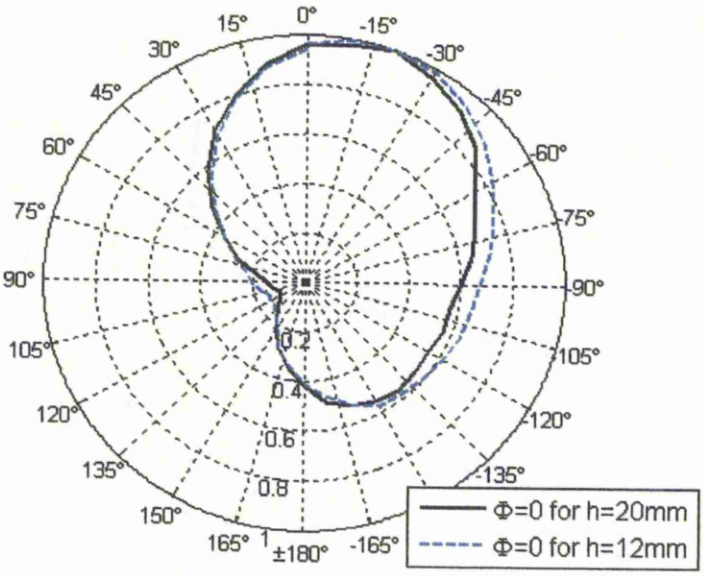

(c)

Fig. 3.10 Effect of changes in the values of h on (a) Resonant frequency (b) Fractional bandwidth (c) Radiation pattern in elevation ($\Phi = 0^{\circ}$) plane

3.2.2.5 Distance of Shorting Plate from the Top Plate Edge

The distance of shorting plate from edge of top plate L_s is varied from *0 mm* to *15 mm* to observe its effect on the characteristics of PIFA while other are constant at $W_g = 75$ *mm*, $L_g = 75$ *mm*, $L = 20$ *mm*, $W = 50$ *mm*, $L_b = 10$ *mm*, $h = 12$ *mm*, $W_s = 5$ *mm*, $W_f = 10$ *mm*, $X = 0$ *mm*, $L_z = 0$ *mm* and $L_u = 0$ *mm*. The simulated and experimental results are shown in the Fig. 3.11. The results show that the increase in L_s increases the resonant frequency and changes the fractional impedance bandwidth but has little effect on the radiation pattern.

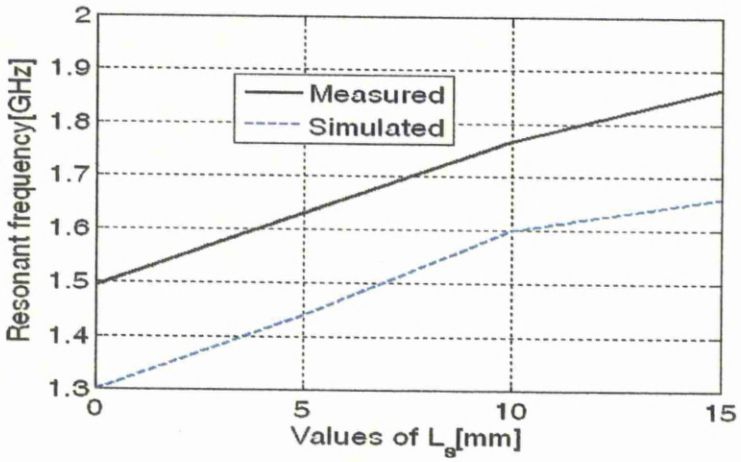

(a)

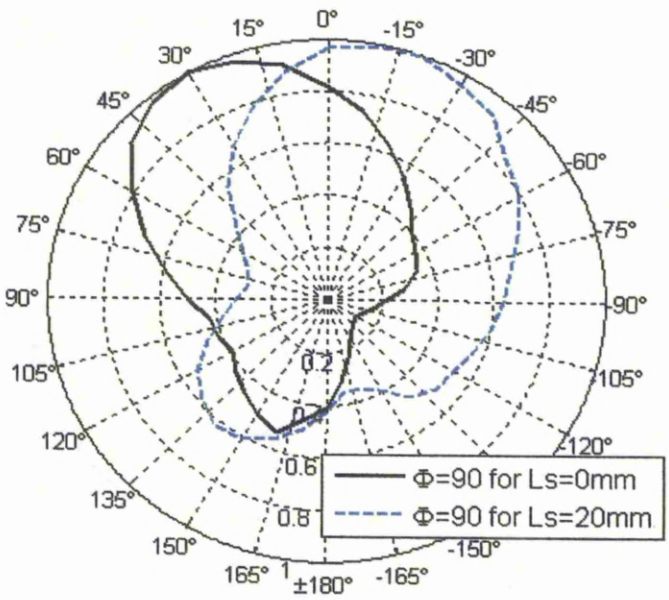

(b)

Fig. 3.11 Effect of variations in the values of L_s on (a) Resonant frequency (b) Radiation pattern in elevation ($\Phi = 90^{\circ}$) plane

3.2.2.6 Position of Feeding Configuration Under the Top Plate

The position of feeding configuration is changed by altering the values of horizontal distance L_b from *5 mm* to *15 mm* and vertical distance L_u from *0 mm* to *18 mm* to observe their effects on the PIFA characteristics while other parameters are constant at $L_g = 75$ *mm*, $W_g = 65$ *mm*, $W = 37.5$

mm, L = 18 mm, h = 12 mm, W_f = 10 mm, W_s = 5 mm, L_z = 0 mm, X = 0 mm and L_s = *0 mm.* The obtained simulated and experimental results are shown in Fig. 3.12. The results show that the changes of feeding position under the top plate significantly affect the resonant frequency, impedance bandwidth and radiation pattern. The increase in horizontal distance between the feeding and shorting plates increases the resonant frequency. Similarly the increase in the distance between the feed and the upper edge of top plate increases the resonant frequency. As we know from the theory of characteristics modes that any conducting surface has a number of modes which can be excited by selecting suitable positions of the feeding configuration; therefore when the feeding position is changed under the top plate, a different mode or a number of modes together are excited which change the resonant frequency, impedance bandwidth and radiation pattern [25]. It implies therefore that the position of feed with respect to the shorting plate is very decisive in order to get the desired resonant frequency and high impedance bandwidth.

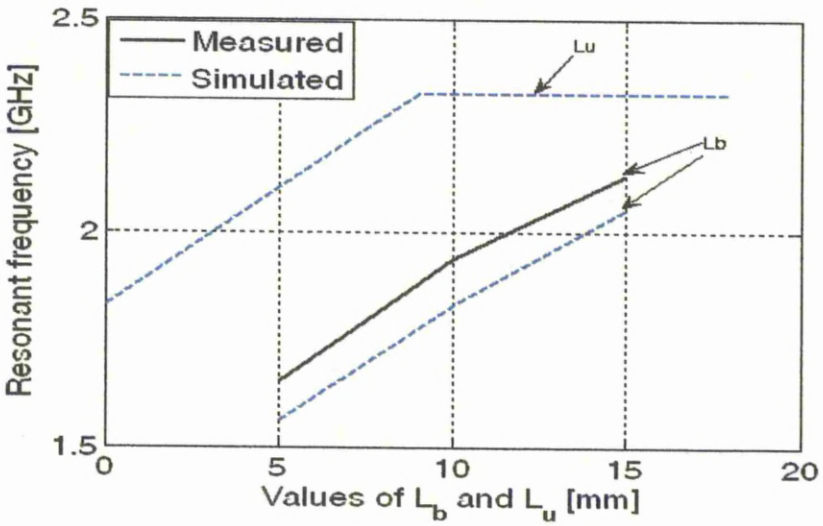

(a)

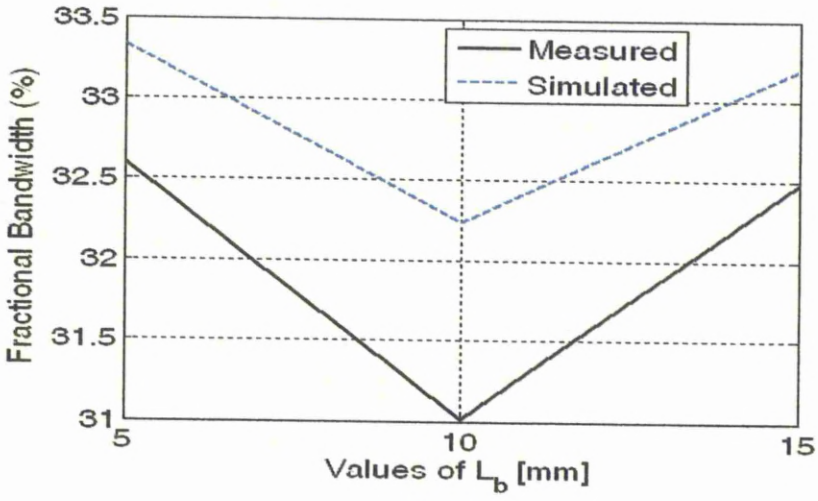
Measured
Simulated
Fractional Bandwidth (%)
33.5
33
32.5
32
31.5
31
5
10
15
Values of L_b [mm]

(b)

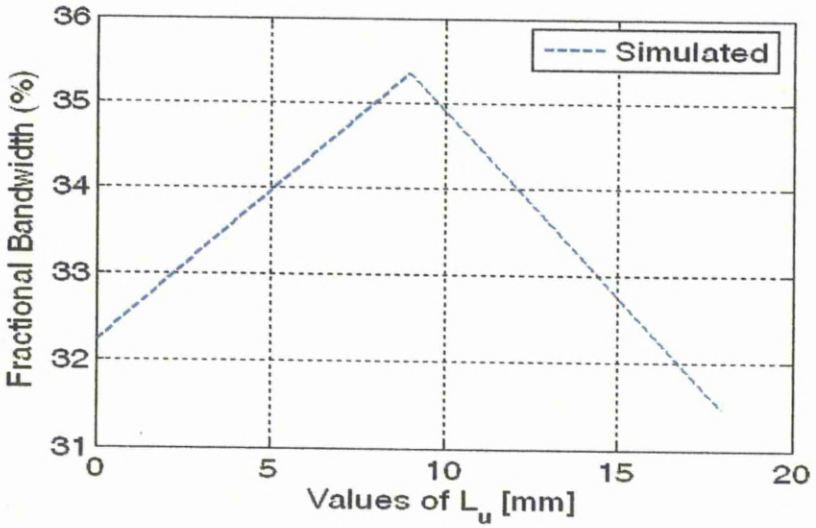
Simulated
Fractional Bandwidth (%)
36
35
34
33
32
31
0
5
10
15
20
Values of L_u [mm]

(c)

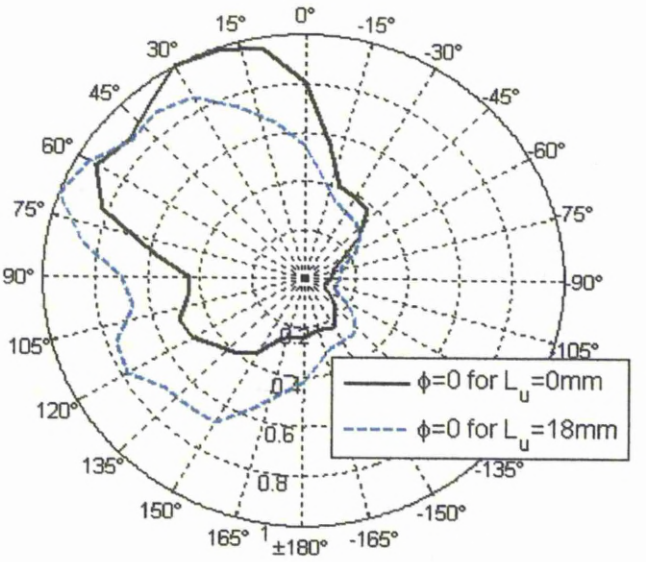

(d)

Fig. 3.12 Effect of variations in the values of L_b and L_u on (a) Resonant frequency (b) & (c) Fractional bandwidth (d) Radiation pattern in elevation ($\Phi = 0°$) plane

3.2.2.7 Width of Shorting Plate

The width of shorting plate is varied from *1 mm* to *20 mm* while other parameters are constant at $L_g = 75\ mm$, $W_g = 65\ mm$, $W = 37.5\ mm$, $L = 18\ mm$, $h = 12\ mm$, $W_f = 10\ mm$, $L_b = 10\ mm$, $L_z = 0\ mm$, $X = 0\ mm$, $L_s = 0\ mm$ and $L_u = 0\ mm$ and simulated and experimental results are shown in Fig. 3.13. It can be concluded that variation in the width of shorting plate changes the resonant frequency and impedance bandwidth and does not have any significant effect on the radiation pattern. The increase in width of shorting plate increases the resonant frequency and it can increase the percentage impedance bandwidth, but as we increase the width of shorting plate, it causes an impedance mismatch that is why bandwidth becomes very narrow when $W_s = 20\ mm$ as shown in Fig. 3.13(b). Therefore if we want to increase the width of shorting plate, the feed position needs to be adjusted every time to obtain a sufficient level of impedance matching [15].

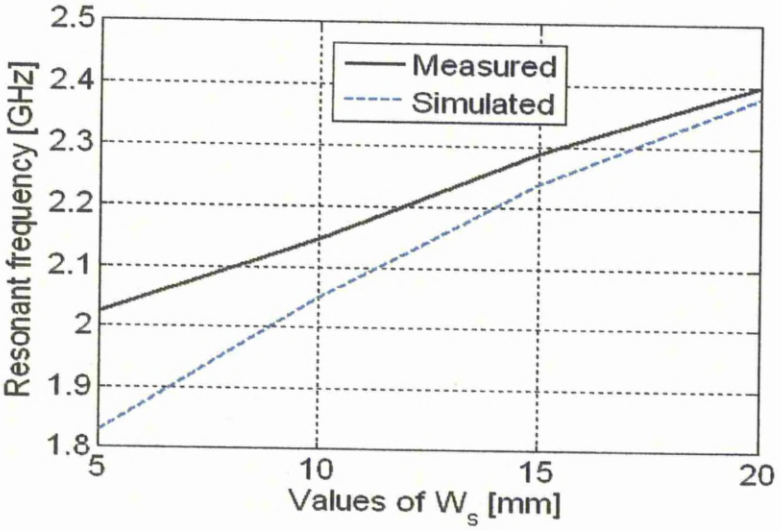
Measured
Simulated
Resonant frequency [GHz]
2.5
2.4
2.3
2.2
2.1
2
1.9
1.8
5
10
15
20
Values of W_s [mm]

(a)

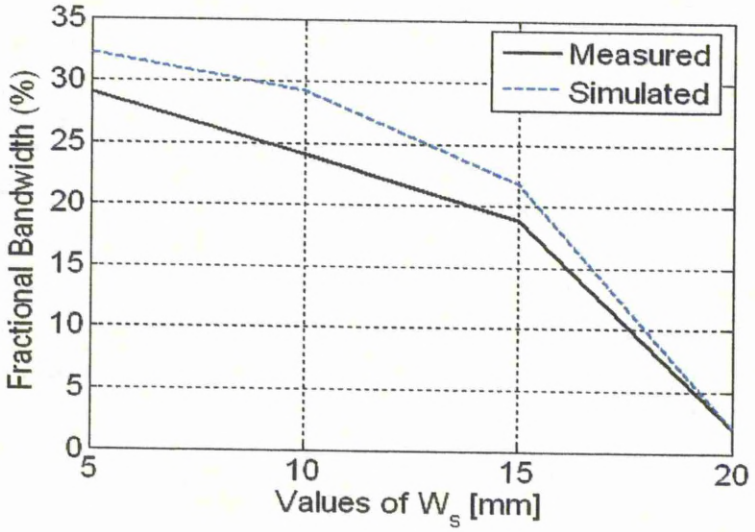
Measured
Simulated
Fractional Bandwidth (%)
35
30
25
20
15
10
5
0
5
10
15
20
Values of W_s [mm]

(b)

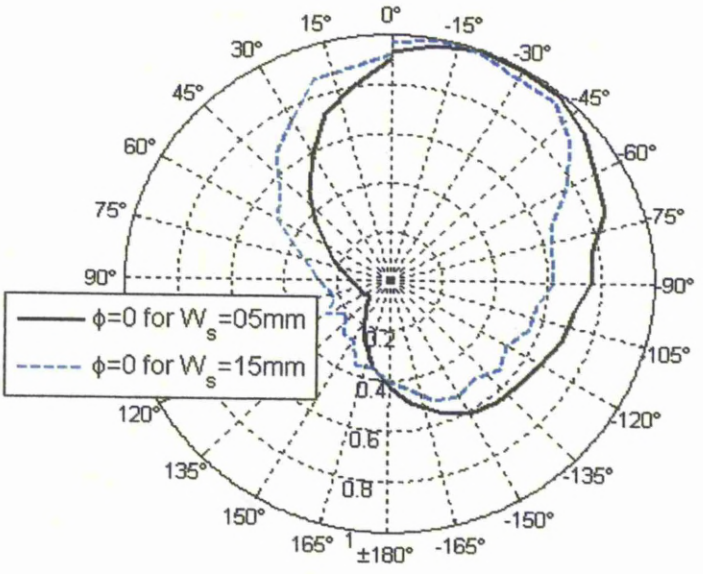

(c)

Fig. 3.13 Effect of changes in the values of W_s on (a) Resonant frequency (b) Fractional bandwidth (c) Radiation pattern in elevation ($\Phi = 0^{\circ}$) plane

3.2.2.8 Width of Feed Plate

The feed plate width is changed from *6 mm* to *14 mm* while other are constant at $L_g = 60$ *mm*, $W_g = 50$ *mm*, $W = 50$ *mm*, $L = 24$ *mm*, $h = 14$ *mm*, $W_f = 10$ *mm*, $W_s = 2$ *mm*, $L_b = 24$ *mm*, $L_z = 0$ *mm*, $X = 0$ *mm*, $L_s = 0$ *mm* and $L_u = 0$ *mm*, and simulated and experimental results are shown in Fig. 3.14. It is concluded that like the width of shorting plate, the width of feed plate changes the resonant frequency and impedance bandwidth and does not have any significant effect on the radiation pattern. The increase in the width of feed plate increases the resonant frequency and significantly increases the fractional impedance bandwidth by 40%. Hence the width of feeding plate can be used to increase the impedance bandwidth of PIFA but it is limited by the increase of resonant frequency which needs to be adjusted by increasing other parameters like the length or width of top plate which will decrease the resonant frequency.

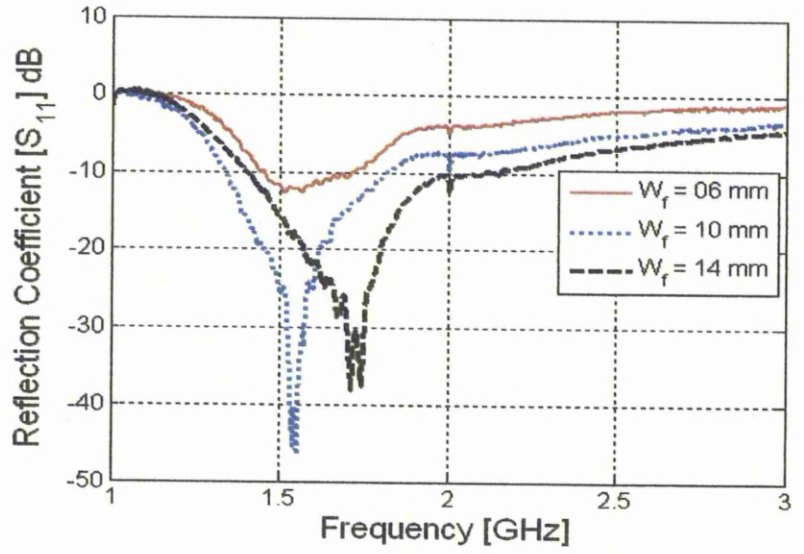
Reflection Coefficient [S11] dB
Frequency [GHz]
Wf = 06 mm
Wf = 10 mm
Wf = 14 mm
10
0
-10
-20
-30
-40
-50
1
1.5
2
2.5
3

(a)

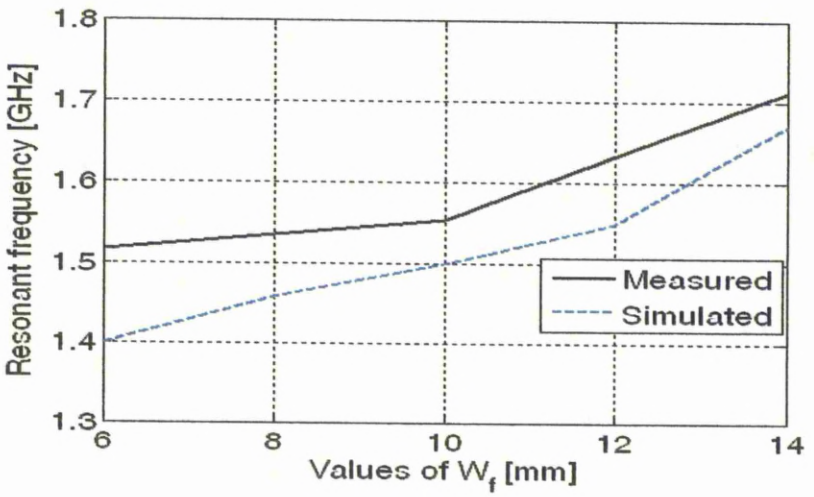
Resonant frequency [GHz]
Values of Wf [mm]
Measured
Simulated
1.8
1.7
1.6
1.5
1.4
1.3
6
8
10
12
14

(b)

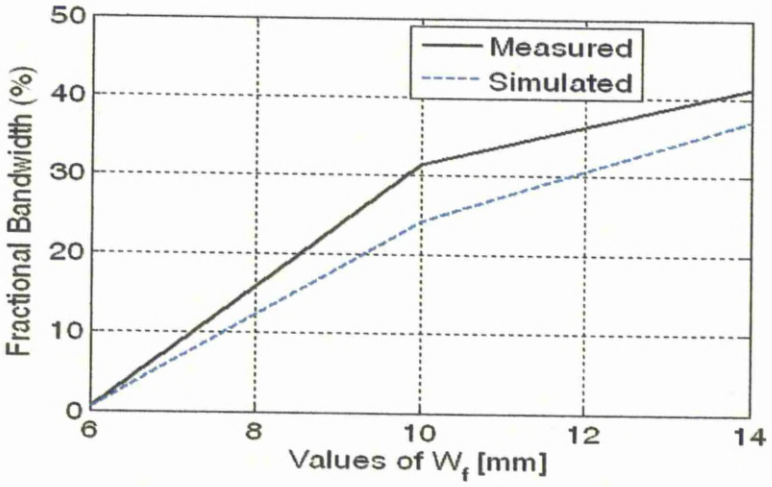

(c)

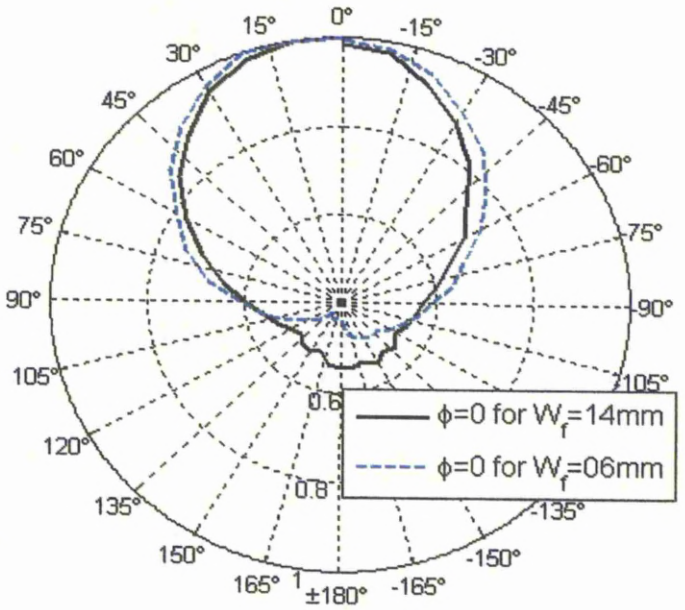

(d)

Fig. 3.14 Effect of variations in the values of W_f on (a) Reflection coefficient (b) Resonant frequency (c) Fractional bandwidth (d) Radiation pattern in elevation ($\Phi = 0^\circ$) plane

3.3 Empirical Equation of PIFA

It is well-known that for a monopole antenna, the desired length is quarter-wavelength since it is resonant in this case. Using the same analogy, the following empirical equation was proposed for finding the resonant frequency of PIFA [7, 26-27].

$$f_0 = \frac{c}{4\,(W + L)} \tag{3.1}$$

where c is the speed of light, L and W are the length and width of the top plate of PIFA and f_0 is the resonant/operating frequency. This equation means that the sum of the length and width of the top plate should be quarter-wavelength. However, it is actually a very rough approximation and does not cover all the parameters which significantly affect the resonant frequency of PIFA as it will be shown later. It can hardly be used to guide the design in practice, thus a more accurate, robust and comprehensive design equation is required. In [17], an effort was made to incorporate some parameters of the antenna (other than W and L) in the evaluation of resonant frequency. In particular, the width of the shorting plate (Ws) was incorporated with two degrees of freedom. The formula is given as follows for $W_s \geq 20$ mm:

$$f_c = \frac{c}{4\left(L + \Delta L + K_1(W - W_s)^2 + K_2(W - W_s)\right)} \tag{3.2}$$

where $\Delta L = 2.741$, $k_1 = 0.0188$ and $k_2 = 0.0767$. Note that this equation has a restricted application due to the condition on W_s. This equation also does not cover all the significant parameters of PIFA which affect the resonant frequency.

Based on our comprehensive parametric study, a large database of different set of parameters using different ground plane dimensions is created and a new empirical equation is derived to find the centre frequency by using

the function 'nlinfit' (Nonlinear least-squares data fitting by the Gauss-Newton method) of MATLAB, taking into account all those parameters which significantly affect the value of the resonant frequency as seen in Figs. 3.4-3.14. These parameters are length, width and height of the top plate, widths of shorting and feed plates, and locations of shorting plate and feeding configuration under the top plate. Only horizontal distances of locations of shorting and feed plates are chosen. The vertical distances of feed and shorting plates from the edge of top plate are neglected to make the equation simple and also because their role is found not as significant as compared to the horizontal distances. The new proposed equation is therefore obtained as follows.

$$f_0 = \frac{c}{3W + 5.6L + 3.7h - 3W_f - 3.7W_s - 4.3L_b - 2.5L_s} \tag{3.3}$$

where W, L and h are the width, length and height of the top plate respectively. W_f and W_s are the widths of feed and shorting plates whereas L_b is the horizontal distance between these plates and L_s is the distance of shorting plate from side edge of the top plate.

Fig. 3.15 shows the comparisons for predicting the operational frequency of PIFA among equation (3.1), equation (3.2) and the new empirical equation (3.3) for the changes in the values of length, width and height of the top plate of PIFA, with the feed at the top edge of top plate and the simulated resonant frequencies are taken as the actual operational frequencies. The comparisons show that the equations (3.1) and (3.2) give poor prediction of the operational frequency of the PIFA and the predictions are the poorest when changes are made in the parameters other than the length, width of the top plate and width of the shorting plate. It is evident that the new empirical equation gives a much better prediction of the resonant frequency than the previous two equations. There is no significant effect on the resonant frequency even if we replace the thin FR4 substrate with air as shown in Fig. 3.15. In some configurations of PIFA, the shorting plate is used

at edge of the top plate and the feeding configuration is vertically downward under the top plate [15-18, 28]. In this case, the horizontal distance L_b should be taken between the feed plate and one side edge of the top plate and the equation still holds. Fig. 3.16 shows the comparisons for prediction of the operational frequency of PIFA for changes in the widths of feed [28] and shorting plates [16,18] when the feed is provided in the middle of the top plate. On average, as compared to the old empirical equation, the new proposed equation provides 35% more accuracy in predicting the operational frequency of the PIFA. This new equation can provide much more accurate prediction of the resonant frequency when the whole PIFA structure is placed on the edge of ground plane and the feed is provided at the upper edge of the top plate i.e. $X = L_z = L_u = 0\ mm$. We can have even better prediction of the resonant frequency by adding the dimensions of ground plane in above equation but these dimensions are ignored due to the fact that the resonant frequency is less affected by the variations of these dimensions and also it will make the equation complex. This new equation gives the prediction of the first resonant frequency of the antenna. It has been tested that the new equation can be applied for normal applications where the antenna size is smaller than one wavelength, i.e., $h+W+L< \lambda$.

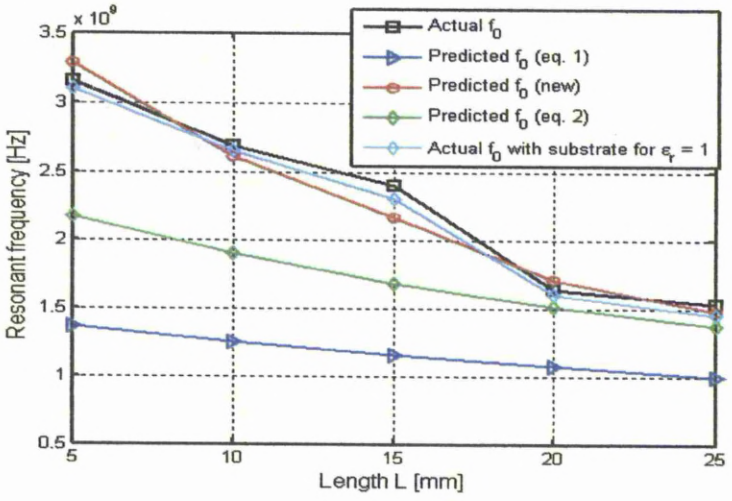

(a)

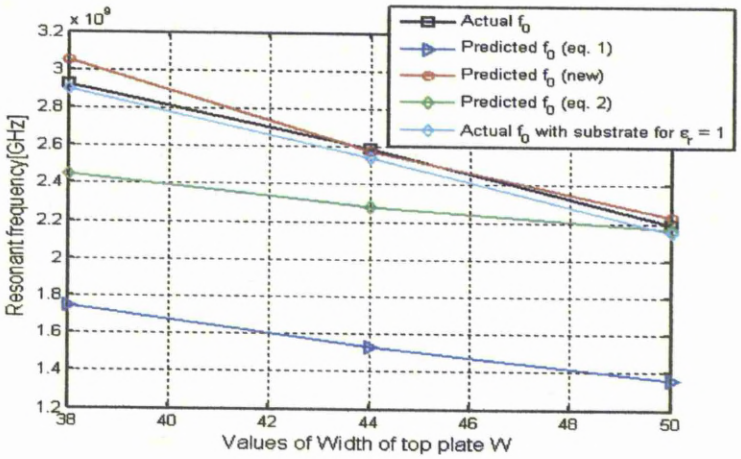

(b)

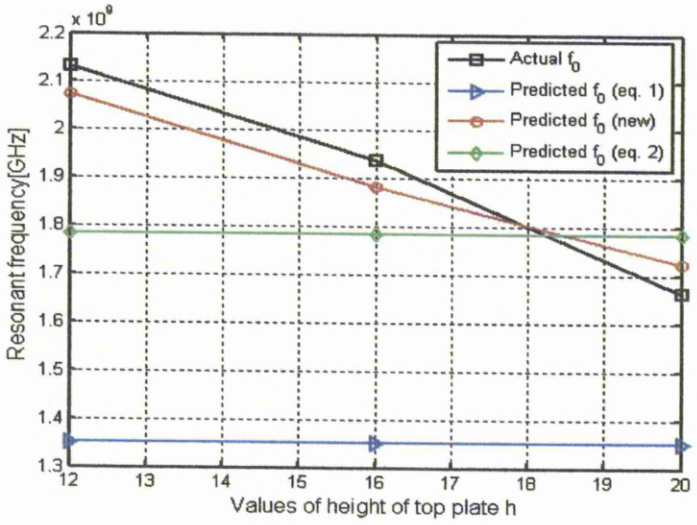

(c)

Fig. 3.15 Comparisons among equations 1 and 2 and new equation for different values of (a) length of top plate L (b) width of top plate W (c) height of top plate h

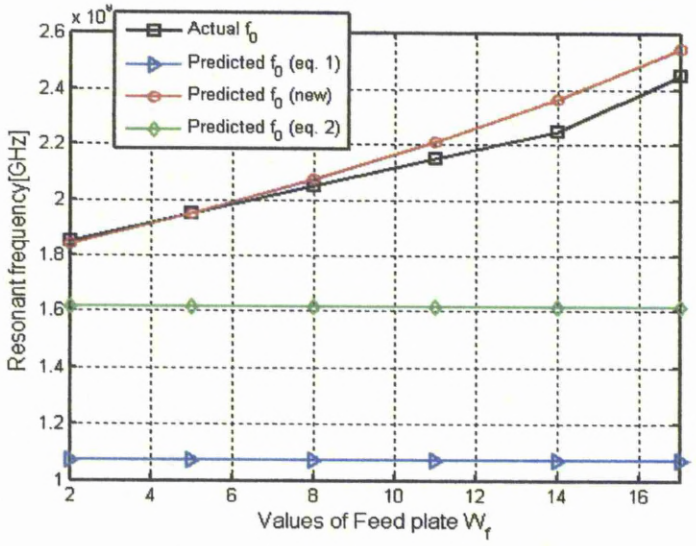

(a)

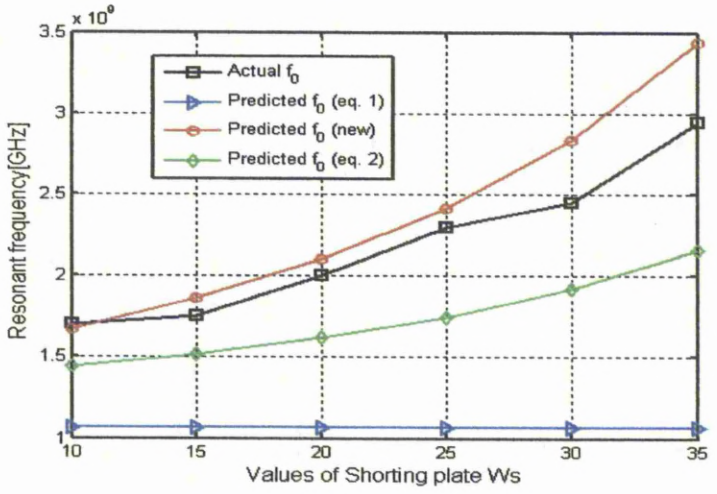

(b)

Fig. 3.16 Comparisons among equations 1 and 2 and new equation for different values of (a) width of feed plate W_f (b) width of shorting plate W_s

3.4 Summary

In this chapter, it is shown that the PIFA characteristics are affected by a number of parameters. The conclusions of this parametric study are summarized as follows.

1. The radiation pattern of PIFA is basically dependent on the size and shape of top plate and is affected by the dimensions of ground plane and the position of PIFA on the ground plane.

2. By increasing the length, width or height of top plate, the resonant frequency decreases.

3. By increasing the height of top plate, fractional impedance bandwidth increases but as PIFA needs to be low profile so it limits the height to be used for increasing the impedance bandwidth.

4. The greater the size of top plate, the radiation pattern will be more directive which means that it will have a higher gain and directivity as well. If we decrease the size of length or width of top plate, then directivity of antenna decreases and intensity of radiation pattern behind the ground plane increases.

5. By increasing the widths of shorting plate or feed plate, the distance of shorting plate from edge of top plate and the horizontal distance of feeding position from shorting plate, the resonant frequency increases.

6. The width of feeding plate is very effective in achieving the broadband PIFA. As increase in feeding and shorting plates increase the resonant frequency, so the size of shorting plate should be narrow and size of feeding plate should be larger to get the maximum impedance bandwidth.

7. The resonant frequency is also affected by the ground plane dimensions and position of PIFA on the ground plane.

8. The minimum total ground dimensions for maximum impedance bandwidth should be equal or greater than $\lambda/2$ i-e length + width of ground plane $\geq \lambda/2$.

9. A new empirical equation is presented for predicting the resonant frequency of PIFA. The average percentage error found between the predicted and the actual operational frequencies is less than 3%.

References

[1] D. M. Pozar and D. H. Schaubert, *Microstrip Antennas: The analysis and design of microstrip antennas and arrays*, New York, IEEE Press, 1995.

[2] H. Haruki and A. Kobayashi, "The inverted-F antenna for portable radio units," Digest *of IECE Japan*, p. 613, 1982.

[3] K. Hirasawa and M. Haneishi, *Analysis, design, and measurement of small and low-profile antennas*, Artech House, 1992.

[4] T. Taga and K. Tsunekawa, "Performance analysis of a built-in planar inverted-F antenna for 800 MHz hand portable radio units," *IEEE J. Selected Areas in Communication*, SAC-5, page(s): 921-929, 1987.

[5] P. Salonen, L. Sydanheimo, M. Keskilammi and M. Kivikoshi, "Planar inverted-F antenna for wearable applications," *3rd International Symposium on Wearable Computers*, San Francisco, page(s): 95-98, October 1999.

[6] Y. Huang and K. Boyle, *Antennas: from theory to practice*, John Wiley & Sons, 2008.

[7] P. S. Hall, E. Lee, C. T. P. Song, *Planar inverted-F antennas, Chapter 7, printed antennas for wireless communications*, Edited by R. Waterhouse, John Wiley & Sons, 2007.

[8] Z. Li, Y. Rahmat-Samii and T. Kaiponen, "Bandwidth study of a dual band PIFA on a fixed substrate for wireless communication", *IEEE Transactions on antennas and Propagation*, page(s): 22-27, January 2003.

[9] P. Song, P. S. Hall, H. G. Shiraz and D. Wake, "Triple band planar inverted F antenna", *IEEE APS International Symposium*, vol. 2. pp. 908-911, July 1999.

[10] D. Liu and B. Gaueher, "A triband antenna for WLAN applications", *IEEE APS International Symposium and USNC/URSI National Radio Science Meeting*, vol. 2. pp. 18-21, June 2003.

[11] M. Manteghi, Y. Rahmat-Samii, "Novel compact tri-band two-element and four-element MIMO antenna designs", *IEEE APS International Symposium,* page(s): 4443-4446, 2006.

[12] Y. Gao, C. C. Chiau, X. Chen and C. G. Parini, "A compact dual-

element PIFA array for MIMO terminals", *Loughborough Antennas & Propagation Conference (LAPC), U.K.*, April 2005.

[13] http://www.supernec.com/ifa.htm.

[14] K. L. Virga and Y. R. Samii, "Low-profile enhanced-bandwidth PIFA antennas for wireless communication packaging", *IEEE transaction on microwave theory and techniques*, vol. 45, no. 10, October 1997.

[15] N. A. Saidatul, A. A. H Azremi and S. R. Norra, "A parametric study of broadband planar inverted-F antenna for WLAN application", *International Conference on Electronic Design*, pp. 1 – 6, December 2008

[16] H. M. Chen and Y. F. Lin, "Experimental and simulated studies of planar inverted-F antenna", *IEEE International Workshop on antenna technology (iWAT)*, 2005.

[17] P. S. Hall, C. T. P. Song, H. M. Chen, Y. F. Lin and P. S. Cheng, "Parametric study on the characteristics of planar inverted-F antenna", *IEE Proc.-Microw. Antennas Propagation*, vol. 152, no. 6, December 2005.

[18] T. Y. Wu, K. L. Wong, "On the impedance bandwidth of a planar inverted- F antenna for Mobile handsets", *Microwave and optical technology letters*, vol. 32, no. 4, February 2002.

[19] M. C. Huynh and W. Stutzman, "Ground plane effects on planar inverted-F antenna (PIFA) performance", *IEE Proc. Microwave Propagation*, vol. 150, no. 4, August 2003.

[20] A. T. Arkko, "Effects of ground plane size on the free-space performance of mobile handset PIFA antenna", *Nokia Corporation, Nokia Mobile phones*, Finland.

[21] A. T. Arkko and E. A. Lehtola, "Simulated impedance bandwidths, gains, radiation patterns and SAR values of a helical and a PIFA antenna on top of different ground planes", *IEE 11th International Conf. on antennas and Prop.*, April 2001.

[22] A. K. Bhattacharya, "Effects of ground plane and dielectric truncations on the efficiency of a printed structure", *IEEE transactions on Antenna and Prop.*, vol. 39, no. 3, March 1991.

[23] S. Fujio, "Effects of ground size on plane inverted-F antenna", *IEEE International Workshop on Antenna Technology (iWAT)*, page(s): 269 – 272, March 2006.

[24] D. Liu and B. Gaucher, "The inverted-F antenna height effects on bandwidth", *IEEE APS International Symposium*, vol. 2A, page(s): 367-370, 2005.

[25] M. C. Fabres, E. A. Daviu, A. V. Nogueira and M. F. Bataller, "The theory of characteristic modes revisited: a contribution to the design of antennas for modern applications", *IEEE Antennas and Propagation Magazine*, vol. 49, no. 5, October 2007.

[26] H. Haruki and A. Kobayashi, "The inverted-F antenna for portable radio units", *in Conv. Rec. IECE Japan (in Japanese)*, pp. 613, March 1982.

[27] K. L. Wang, *Planar antennas for wireless communications*, published by Hoboken, NJ. Wiley-Interscience, 2003.

[28] R. Feick, H. Carrasco, M. Olmos and H. D. Hristov, "PIFA input bandwidth enhancement by changing feed plate silhouette", *Electronics Letters*, July 22, 2007.

CHAPTER

4

Bandwidth Enhancement Techniques of PIFA

4.1 Introduction

The planar inverted-F antenna (PIFA) is widely used in mobile systems due to its excellent performance. However, PIFA is generally considered a narrow band antenna and significant amount of effort has been made to broaden its bandwidth. It was shown that the height [1], shorting plate width [2], meandered shorting strip [3], tapering of top plate and T-shaped ground plane [4-5] and diversely shaped feed plates (of up to about 25% fractional bandwidth) [6] can be used to increase the impedance bandwidth. But they did not investigate the size of the feed plate. This study, as part of a comprehensive study of the PIFA antenna, investigates the effects of changing both the widths of the rectangular feed plate and shorting plate

on the impedance bandwidth of PIFA. It is found that much wider bandwidth than previously reported can be achieved and the PIFA may be regarded as a wide (or even ultra-wide) band antenna if the correct widths of the feed and shorting plates are chosen. The proposed approach seems to be the simplest and the most practical way of getting the maximum impedance bandwidth than the previously reported methods. Furthermore, the impedance bandwidth is increased even further by introducing small parasitic elements at appropriate places on ground plane of PIFA.

4.2 PIFA Bandwidth Enhancement by Changing the Widths of Feed and Shorting Plates

4.2.1 Antenna Configuration

The configuration of a typical PIFA shown in Fig. 4.1 is chosen for this study. The radiating top plate has dimensions $W \times L$ and ground plane dimensions are $W_g \times L_g$. There is a substrate of thickness $t = 1.0\ mm$ between the rectangular ground plane and feed plate. The antenna height h is also filled with air (free space). The shorting plate has dimensions $W_s \times (h+t)$ and feed plate has dimensions $W_f \times h$. The horizontal distance between shorting and feed plates is L_b. The software package used for simulation is Ansoft's High Frequency Structure Simulator (HFSS) based on the Finite Element Method.

4.2.2 Simulated and Experimental Results

The effect of changing the width of feed plate on the fractional bandwidth is shown in Fig. 4.2. It is evident that increasing the width of the feed plate increases the fractional bandwidth up to a certain value and then further increase in feed plate width decreases the fractional bandwidth. So an optimum value for the width of feed plate should be selected for achieving the maximum impedance bandwidth. Similarly the effect of changing the

width of shorting plate on the fractional bandwidth is investigated and the result is shown in Fig. 4.3 for $W_f = 5mm$. Simulated and measured results are in good agreement. It is obvious that increasing the width of shorting plate increases the fractional bandwidth up to 25% only and then further increase decreases the fractional bandwidth for a given feed plate. Thus there should also be an optimum width of shorting plate.

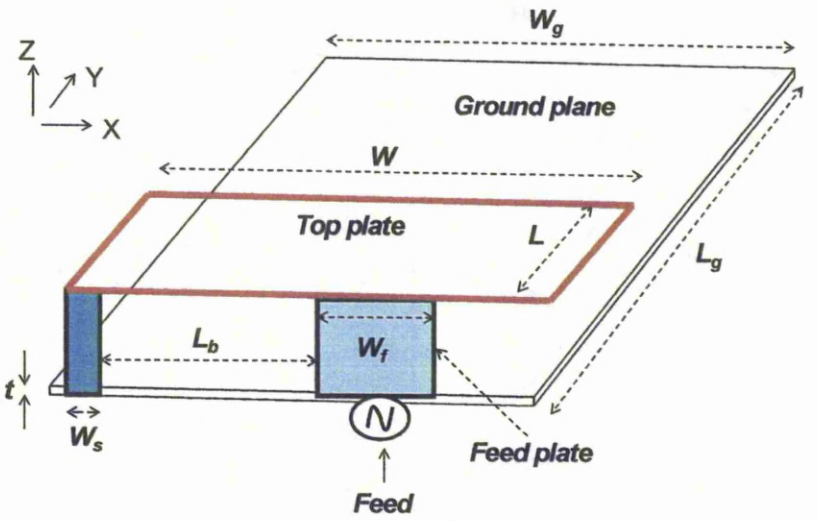

Fig. 4.1 Geometry of PIFA

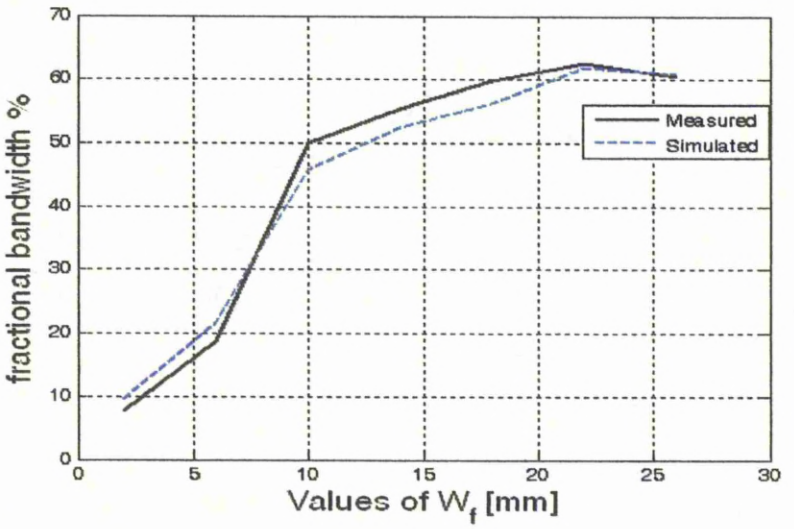

Fig. 4.2 Values of feed plate width vs. fractional bandwidth

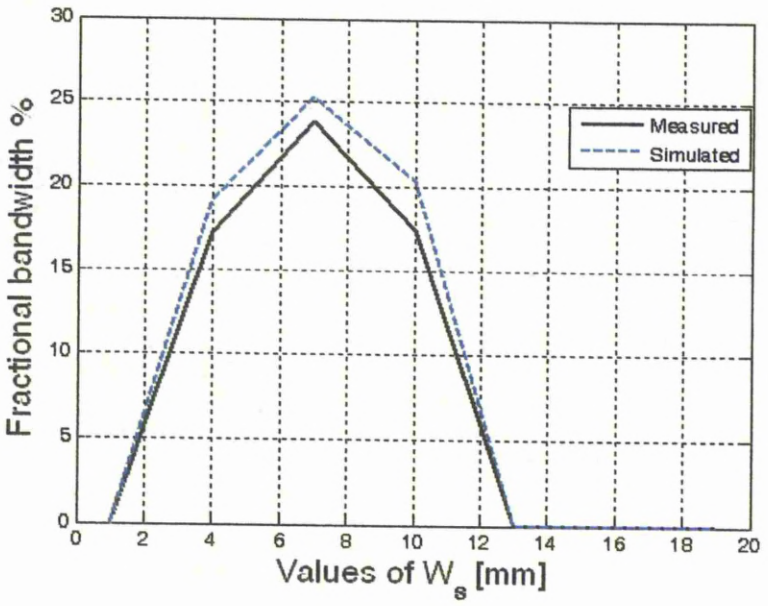

Fig. 4.3 Values of shorting plate width vs. fractional bandwidth for $W_f = 5$ mm

All the parameters of PIFA should be optimized in order to get the maximum impedance bandwidth. For example, if the center frequency is around 2.2 GHz, the optimized values of all the parameters are found as follows: $W_f = 18$ *mm*, $W_g = 40$ *mm*, $L_g = 60$ *mm*, $W = 40$ *mm*, $L = 20$ *mm*, $h = 10$ *mm*, $W_s = 2$ *mm* and $L_b = 15$ *mm*. It is found that ground plane dimensions are very decisive in achieving the maximum bandwidth. Furthermore the PIFA structure is placed at the edge of ground plane which will result in lower value of Q (Quality factor) and high impedance bandwidth.

The simulated and experimental results of the reflection coefficient are shown in Fig. 4.4. It is evident that the bandwidth achieved by this technique for $S_{11} < -10$ dB is extremely broad with a fractional bandwidth of 65%, from about 1.6 GHz to 3 GHz which covers the frequencies of most of the current mobile applications (GSM, PCS, DCS, UMTS, WLAN, WiMax and Bluetooth).

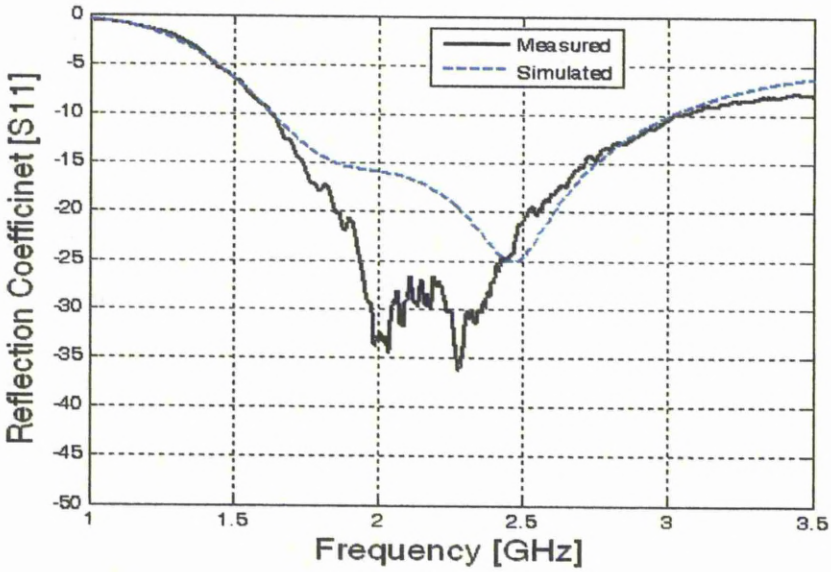

Fig. 4.4 Reflection coefficient (S11) in dB vs. frequency in GHz

To understand how the antenna works, an approximate equivalent circuit of the proposed PIFA antenna is developed and shown in Fig. 4.5. The feed plate and top radiating plate is replaced by a series resistor R_1 and a series inductor L_1 and a capacitor C_1 in parallel with series combination of R_1 and L_1. The shorting plate is replaced by a series combination of a resistor R_2 and an inductor L_2. This series combination of R_2 and L_2 is in parallel to a capacitor C_2 which is due to the coupling between the top plate and the ground plane and space (air) between these two acts as a dielectric. As lumped elements cannot fully describe the behavior of distributed elements, so it cannot predict the behavior of this PIFA antenna over the whole frequency range. However, the values of the lumped elements can be approximated for a certain frequency. For example, if $f = 2.5\ GHz$ then the values of the lumped elements are as follows: $R_1 = 25\ \Omega$, $L_1 = 0.1\ nH$, $C_1 = 0.1\ fF$, $R_2 = 15\ \Omega$, $L_2 = 0.5\ nH$ and $C_2 = 1.87\ pF$. For these values, the equivalent impedance of this equivalent circuit ($Z_{equivalent} = 44.1 + i\ 0.8483$) is almost same as the simulated values of input impedance ($Z_{in} = 44 + i\ 0.84$) of the PIFA antenna.

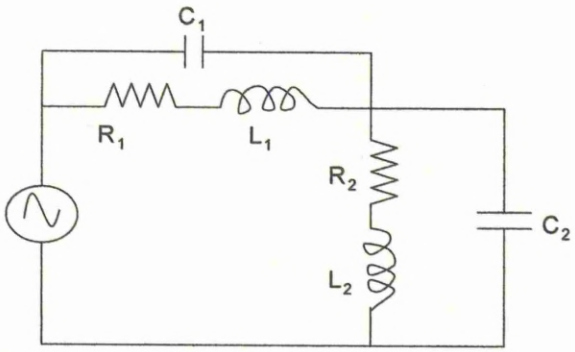

Fig. 4.5 Equivalent circuit of the proposed PIFA antenna

The 3D simulated polar plot of radiation pattern of this PIFA antenna at 2.5 GHz is shown in Fig. 4.6 and the measured radiation patterns of this antenna as shown in Fig. 4.7 are similar to that of a conventional PIFA as changing the widths of feed and shorting plates do not have significant effects on the gain and radiation pattern of the antenna. It is evident that the resultant PIFA antenna has a directional radiation pattern. The average simulated radiation efficiency of this PIFA antenna is about 85% with the peak efficiency of 95%. It can be concluded that a properly configured PIFA antenna can be made as a broadband antenna.

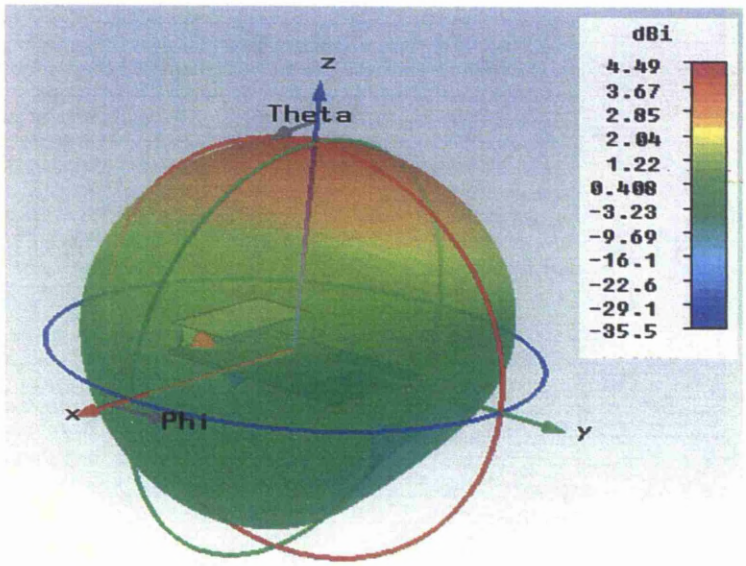

Fig. 4.6 3D simulated polar plot of radiation pattern of PIFA at 2.5 GHz

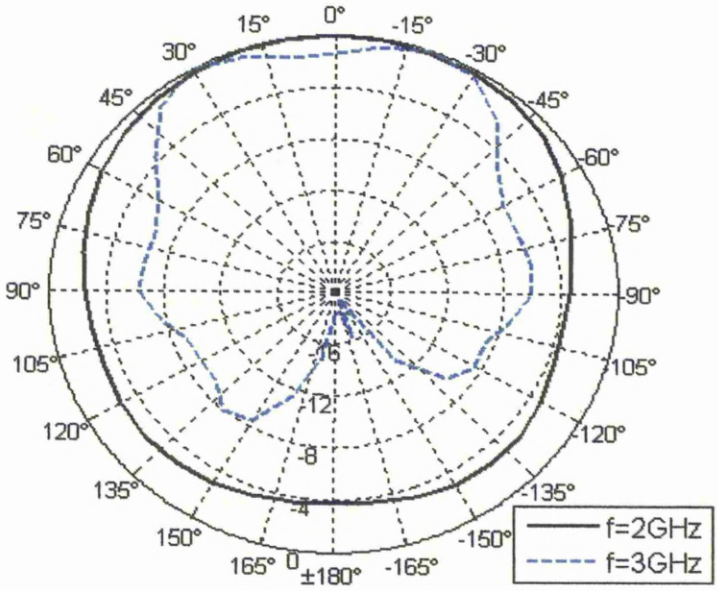

(a) XZ plane ($\Phi = 0°$)

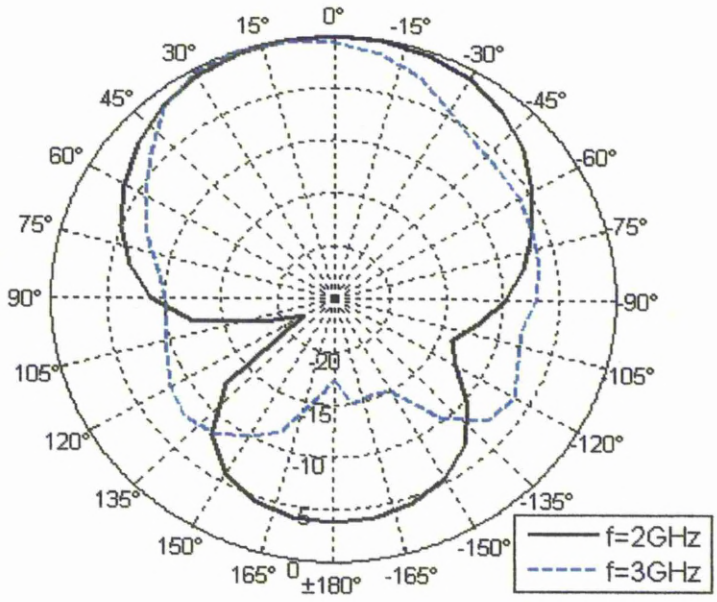

(b) XY plane ($\Phi = 90°$)

Fig. 4.7 2D measured radiation patterns in dB scale for different planes and different frequencies

The overall antenna size is larger than the radiating plate. The effect of ground plane dimensions is very significant in achieving the maximum bandwidth. Fig. 4.8 shows the effect of changing the length of the ground plane on the reflection coefficient of the antenna. Thus there exists an optimal ground plane dimension for maximum impedance bandwidth. However, it is found by extensive simulations with different ground plane dimensions that the 50% fractional impedance bandwidth can be achieved for any given ground plane dimensions with the given technique by changing and optimizing the other parameters.

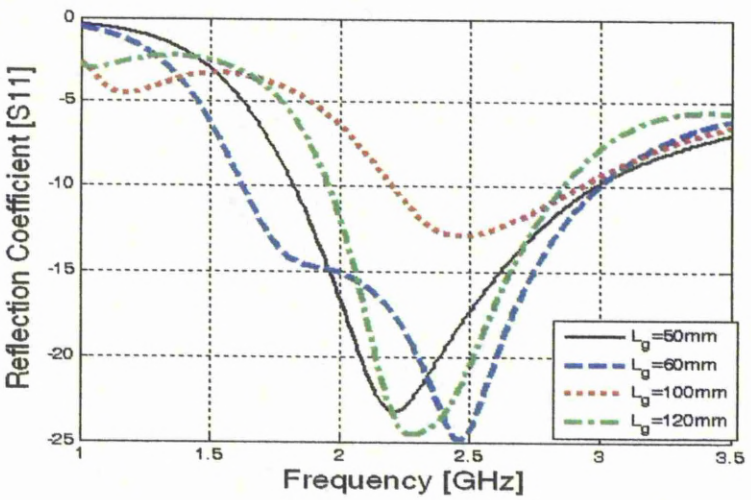

Fig. 4.8 Reflection coefficient [S_{11}] for different values of the length of ground plane

4.2.3 Reason for Bandwidth Enhancement

The question now is: why can the bandwidth of the PIFA be significantly increased using the proposed technique? As we know, the impedance bandwidth of a half-wavelength dipole can be significantly increased by increasing its diameter. We believe for the same reason that the impedance bandwidth of PIFA can also be improved by increasing the size of feed plate. Fig. 4.9 shows the real and imaginary components of impedance Z of PIFA versus frequency. It is evident that by increasing the width of feed

plate, the impedance changes slowly around the resonant frequency which means an increase in the impedance bandwidth of the antenna.

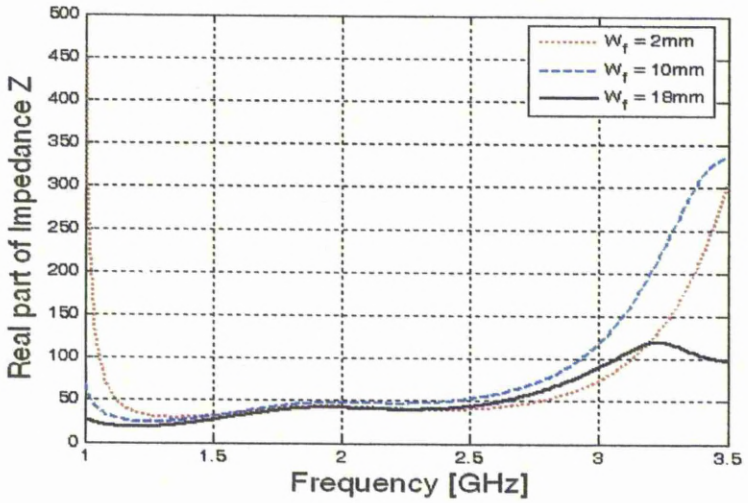

(a) Resistance

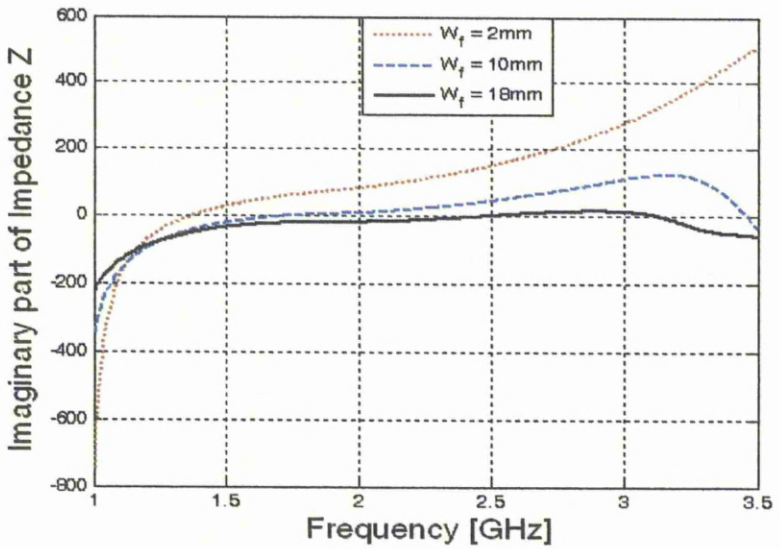

(b) Reactance

Fig. 4.9 Input Impedance Z as a function of the frequency for different widths of feed plate

4.3 Bandwidth Enhancement of PIFA by Adding an Inverted-L Shaped Parasitic Element

The ultra wide band (UWB) transmission system as approved by Federal Communications Commission is defined as a device with a fractional bandwidth in excess of 20% or having an impedance bandwidth greater than 500 MHz with a carrier frequency in the range of 3.1 GHz to 10.6 GHz [7-8].

This study is an extension of our previous study in which 65% impedance bandwidth is achieved by ontaining optimal ground plane dimensions and setting the widths of feeding and shorting plate to the right values. It further enhances the impedance bandwidth by investigating the effect of adding a parasitic element on the impedance bandwidth of PIFA whereas all other parameters are already optimized [9]. The approach of adding a parasitic element was used in the case of wire type of antennas [10-11] but here it is used in a planar antenna. It is found that a very wider bandwidth is achieved by this technique and the PIFA may be used as an ultra-wide band antenna. The proposed technique is also suitable for fabrication of PIFA antennas at a large scale.

4.3.1 Antenna Configuration

The configuration of the PIFA is shown in Fig. 4.10. The radiating top plate has dimensions $W \times L$ and ground plane dimensions are $W_g \times L_g$. There is an air substrate of thickness $t = 1.0\ mm$ between the rectangular ground plane and feed plate. The antenna height h is also filled with air (free space). The shorting plate has dimensions $W_s \times (h+t)$ and feed plate has dimensions $W_f \times h$. The horizontal distance between shorting and feed plates is L_b. The distance between parasitic element and feed plate is D_c. The thicknesses of the parasitic element are t_{c1} and t_{c2} as shown in Fig. 4.10. The height of the parasitic element is (h+t)-d where d is the vertical distance between the top plate and the element.

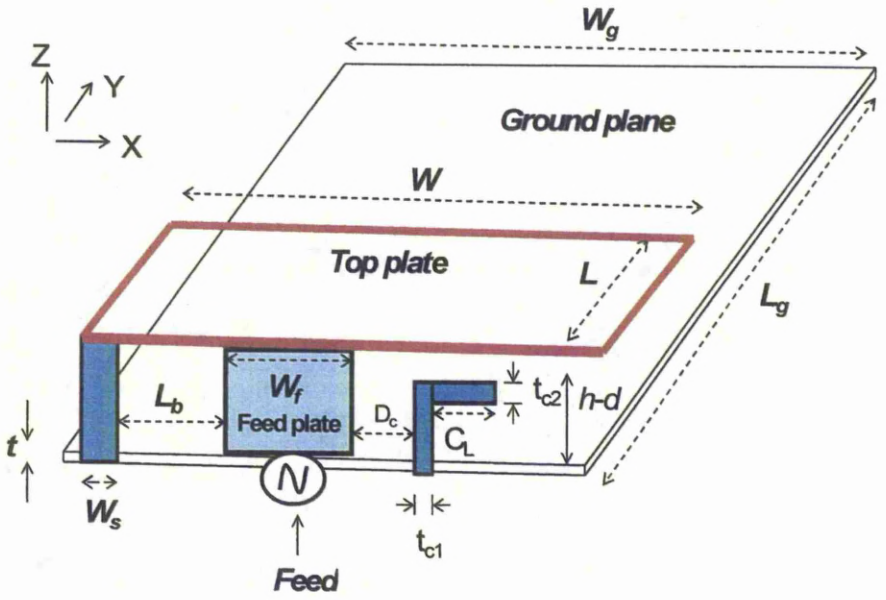

Fig. 4.10 Geometry of PIFA

4.3.2 Simulated and Experimental Results

The parameters of PIFA are optimized first to produce the maximum impedance bandwidth without adding the parasitic element which are as follows: $W_f = 18\ mm$, $W_g = 40\ mm$, $L_g = 60\ mm$, $W = 40\ mm$, $L = 20\ mm$, $h = 10\ mm$, $W_s = 1\ mm$ and $L_b = 12\ mm$.

Now the parasitic element is added at a distance $D_c = 1\ mm$ from feed plate in such a way that it creates a second resonant frequency at such value that the reflection coefficient S_{11} remains below -10 dB level. The thickness of the parasitic element is $t_{c1} = t_{c2} = 1mm$ and the height of this element is $(h+t)-d = 10.5\ mm$ where $d = 0.5\ mm$. The horizontal increase of this element is $C_L = 5\ mm$ and the simulated and measured results are shown in Fig. 4.11. Simulated and measured results are in good agreement. It is evident that the bandwidth achieved by this technique for S11 < -10 dB is extremely broad with a fractional bandwidth of more than 100%, from about 1.6 GHz to 4.45 GHz. The 3D simulated polar plot of radiation pattern of this PIFA antenna at 3 GHZ is shown in Fig. 4.12.

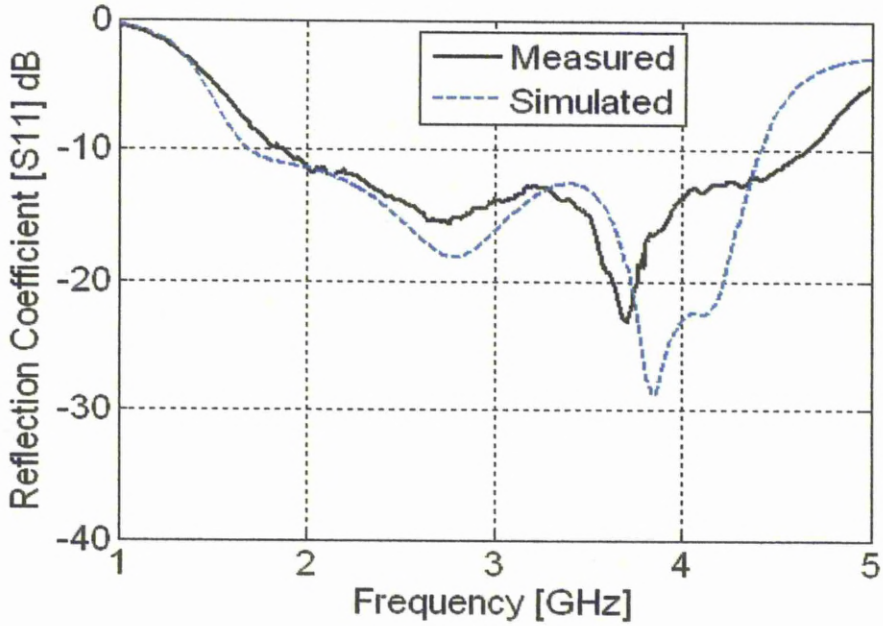

Fig. 4.11 Reflection coefficient (S_{11}) in dB vs. frequency in GHz with the addition of parasitic element

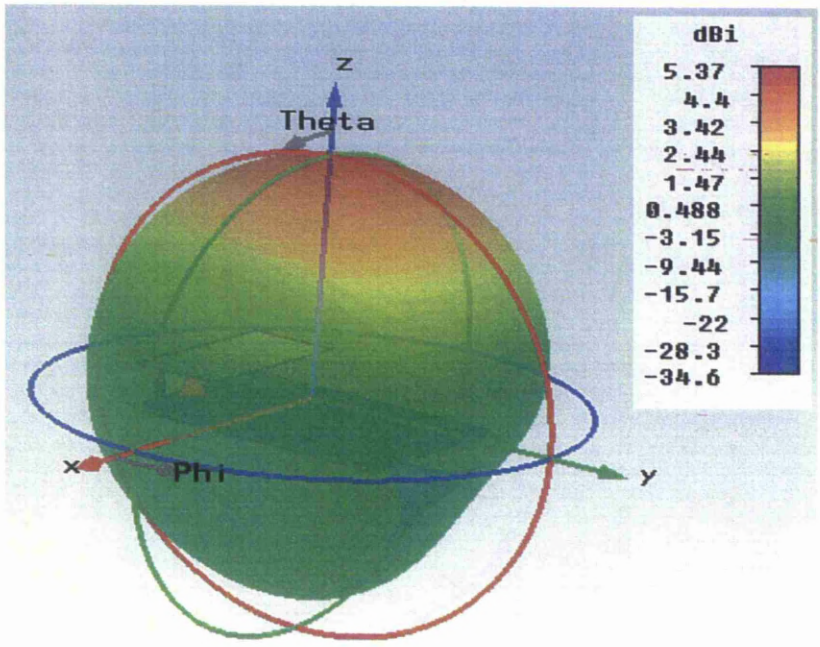

Fig. 4.12 3D simulated polar plot of radiation pattern of PIFA at 3 GHz

The effect of changing the dimensions of ground plane is shown in Fig. 4.13 which shows that the dimensions of ground plane are very critical and by changing the length of ground plane changes the resonant frequency as well as impedance bandwidth. If the value of ground plane is changed then other parameters need to be adjusted to get the maximum impedance bandwidth. For example, if the length of ground plane is changed to *80 mm* which is the worst case in Fig. 4.13, then some other parameters are modified as $W_f = 22\ mm$, $L_b = 9\ mm$, $C_L = 3\ mm$. The fractional bandwidth achieved in this case is about 80%.

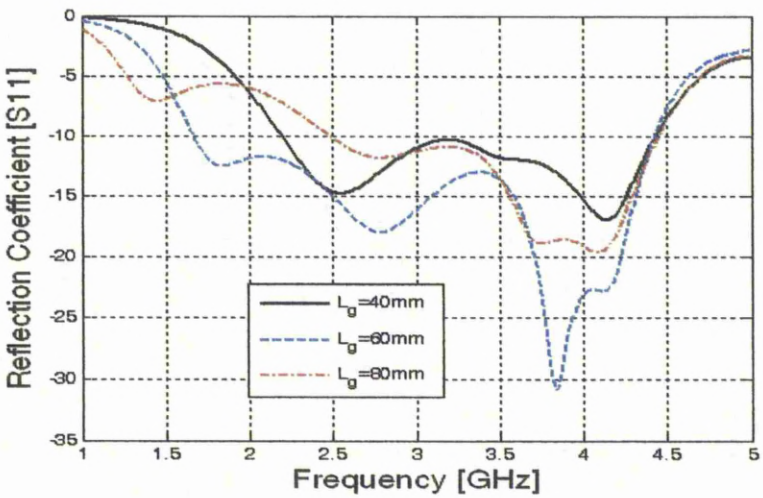

Fig. 4.13 Reflection coefficient S_{11} in dB versus frequency in GHz for different Values of L_g

Now to find the reason of such a wide impedance bandwidth of the PIFA using the proposed techniques, the Smith chart of the PIFA antenna without (Fig. 4.1) and with the parasitic element (Fig. 4.10) are shown in Figs. 4.14 and 4.15(a) respectively. It is evident that by the addition of the parasitic element, multiple resonances are created (Fig. 4.15(a)) and imaginary component of input impedance does not change significantly and remain around zero due to which impedance bandwidth of the antenna increases (Fig. 4.15(b)).

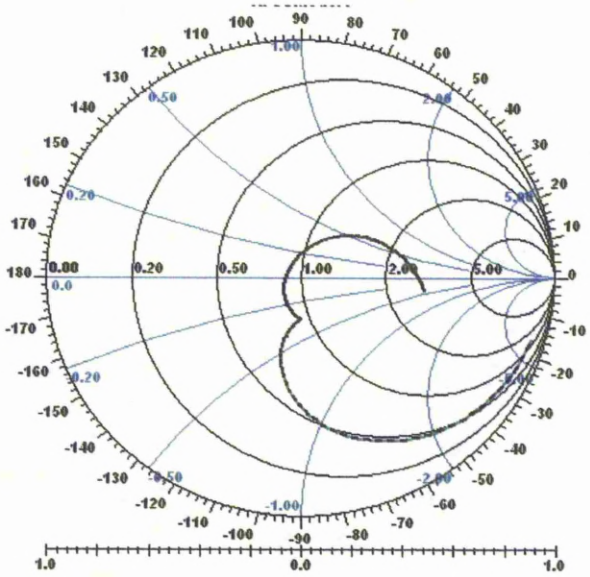

Fig. 4.14 Simulated Smith chart for impedance bandwidth of PIFA antenna without adding the parasitic element

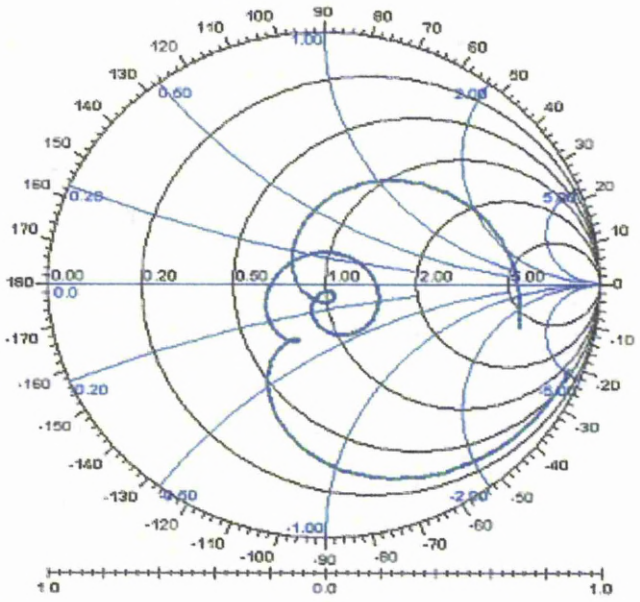

(a)

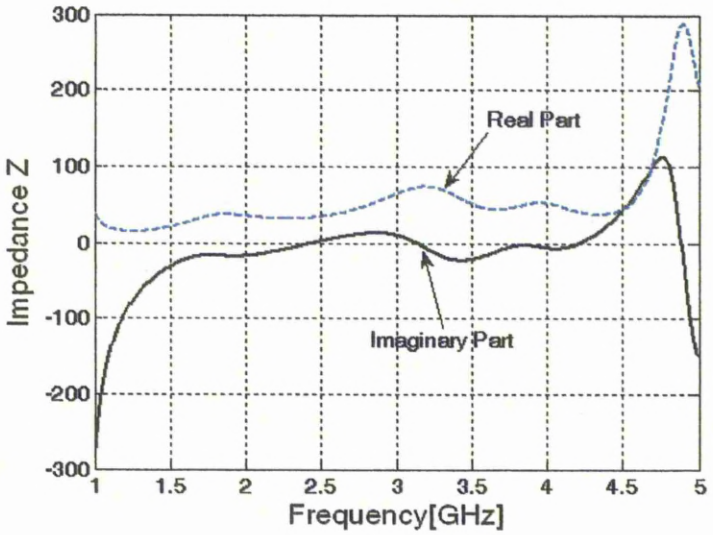

(b)

Fig. 4.15 Impedance Z of PIFA antenna with the parasitic element on (a) Smith chart (b) Linear Graph versus frequency in GHz

4.3.3 Ultra Wideband Planar Inverted-F Antenna with One Parasitic Element

Using this technique, a PIFA antenna is made and tested for ultra wide band applications. The parameters for this PIFA antenna are as follows: $W_g = 18.5$ *mm*, $L_g = 28$ *mm*, $W = 18.5$ *mm*, $L = 9.5$ *mm*, $h = 4.5$ *mm*, $W_f = 8.5$ *mm*, $W_s = 0.5$ *mm*, $L_b = 5.5$ *mm*, $D_c = 0.5$ *mm*, $t_{c1} = t_{c2} = 0.5$ *mm*, $(h+t)-d = 5$ *mm* and $C_L = 2.5$ *mm*. The simulated and measured results are shown in Fig. 4.16 which are in good agreement and the difference is due to the reasons described above.

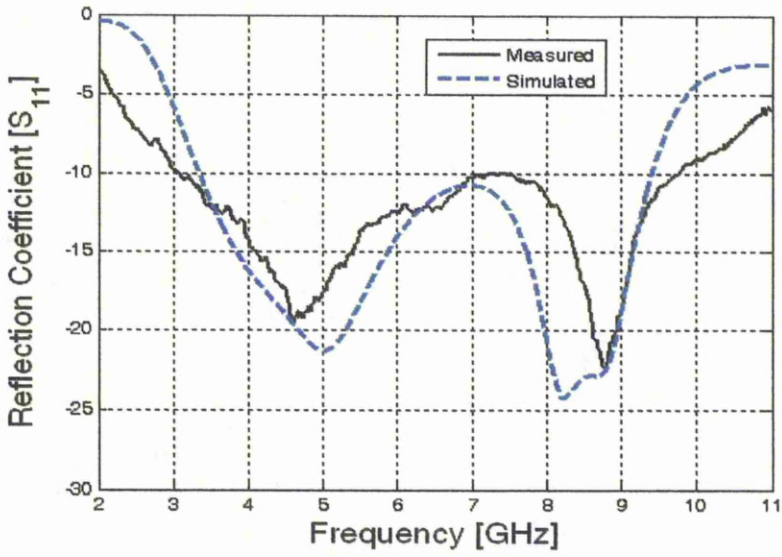

Fig. 4.16 Reflection coefficient S_{11} in dB versus frequency in GHz

It is evident that the bandwidth achieved by these techniques for $S_{11} < -10$ dB is extremely broad with a **fractional bandwidth of more than 102%,** from about 3.35 GHz to 9.4 GHz for simulated and from about 3.1 GHz to 9.7 GHz for measured.

In addition to the equivalent circuit shown in Fig. 4.5, a capacitor C_3, an inductor L_3 and a resistor R_3 are added in parallel due the addition of a parasitic element as shown in Fig. 4.17. The capacitor C_3 is due to the coupling between the top plate and the parasitic element and the parasitic element itself is replaced with a series combination of a resistor R_3 and an inductor L_3. If $f = 5$ *GHz* then the values of the lumped elements are as follows: $R_1 = 42\ \Omega$, $L_1 = 0.1$ *nH*, $C_1 = 0.1$ *fF*, $R_2 = 20\ \Omega$, $L_2 = 0.5$ *nH*, $C_2 = 30$ *pF*, $R_3 = 5\ \Omega$, $L_3 = 0.5$ *pH*, $C_3 = 15$ *pF*. For these values, the equivalent impedance of this equivalent circuit ($Z_{equivalent} = 40.9\text{-}i1.99$) is almost same as the simulated values of input impedance ($Z_{in} = 39.82\text{-}i1.91$) of the PIFA antenna.

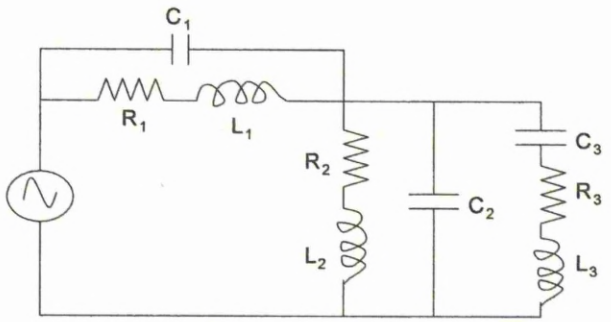

Fig. 4.17 Equivalent circuit of the proposed UWB PIFA antenna with a parasitic element

The 3D simulated polar plot of radiation pattern of UWB PIFA at 6 GHZ is shown in Fig. 4.18 and the 2D polar plots of the measured radiation patterns of this antenna at different frequencies in dB scale are shown in Fig. 4.19 for different planes.

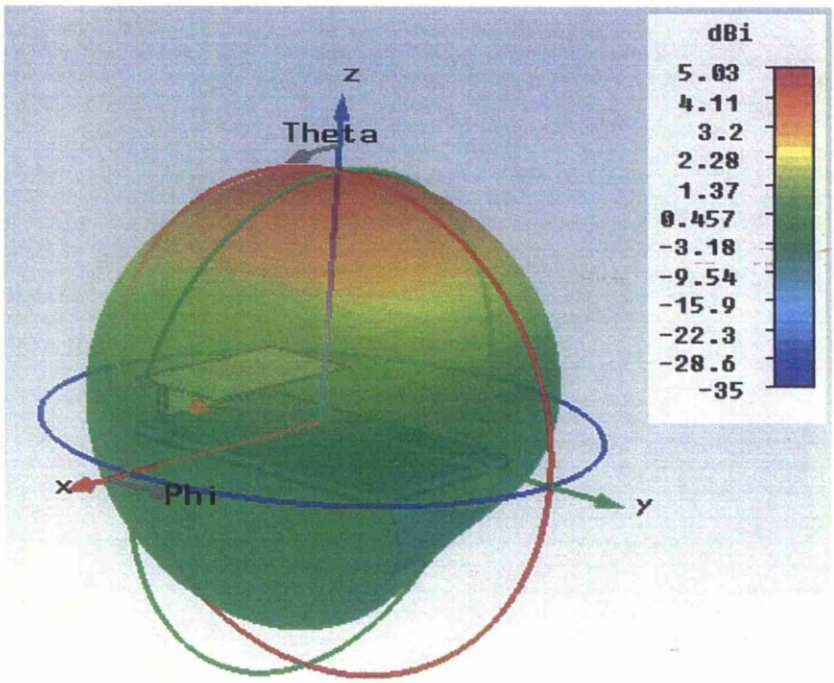

Fig. 4.18 3D simulated polar plot of radiation pattern of UWB PIFA at 6 GHz

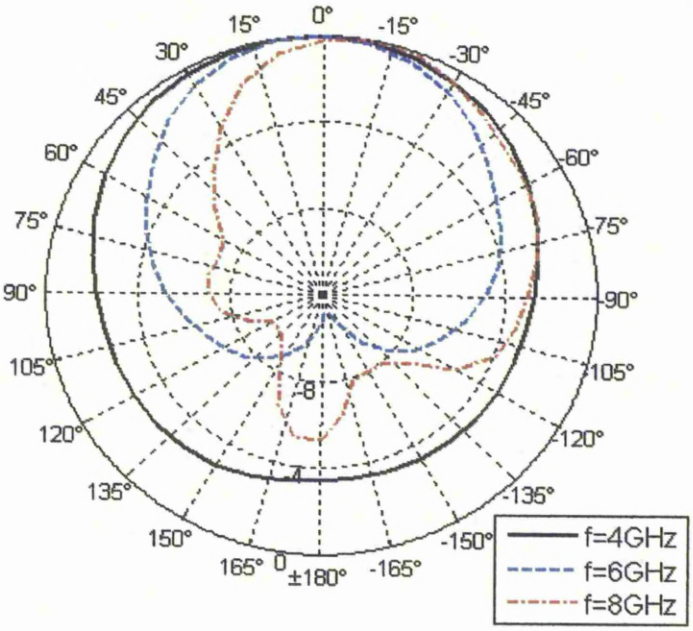

(a) XZ ($\Phi = 0°$) plane

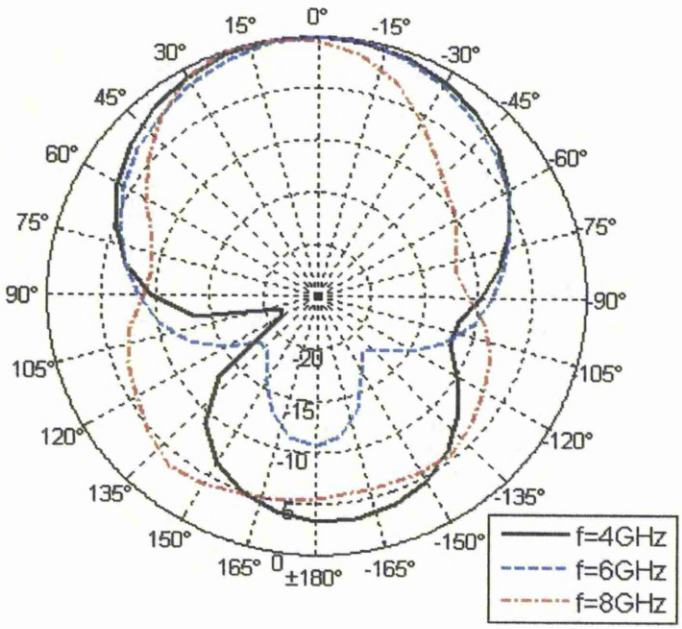

(b) ZY ($\Phi = 90°$) plane

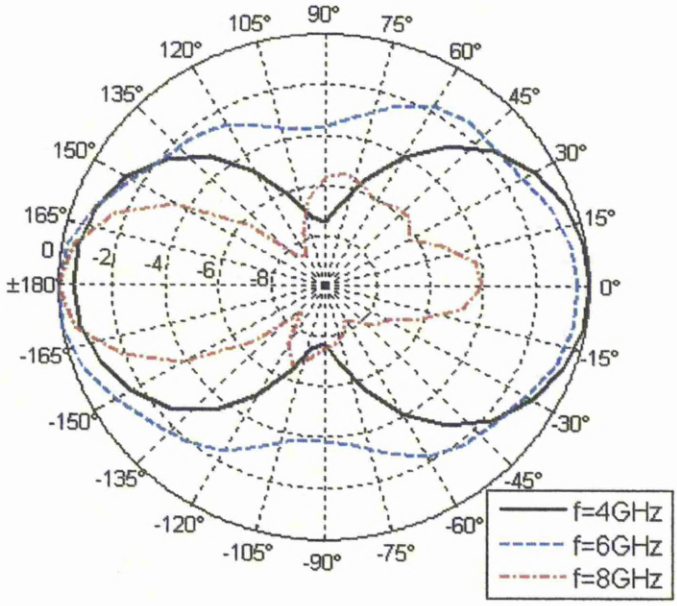

(c) XY ($\theta = 90°$) plane

Fig. 4.19 2D measured radiation patterns in dB scale for different planes and different frequencies

4.4 Addition of a Rectangular Shaped Parasitic Element

Just like an inverted-L shaped parasitic element, further bandwidth enhancement of PIFA shown in Fig. 4.10 can be achieved by adding a rectangular shaped parasitic element between the shorting plate and the feed plate as shown in Fig. 4.20. This rectangular parasitic element is inserted at the edge of the ground plane at a distance $D_{c1} = 6\ mm$ from the shorting plate. The width of this element is $t_{c3} = 3\ mm$. The height of this rectangular element is the same as that of inverted-L parasitic element, i.e. $(h+t)-d = 10.5\ mm$.

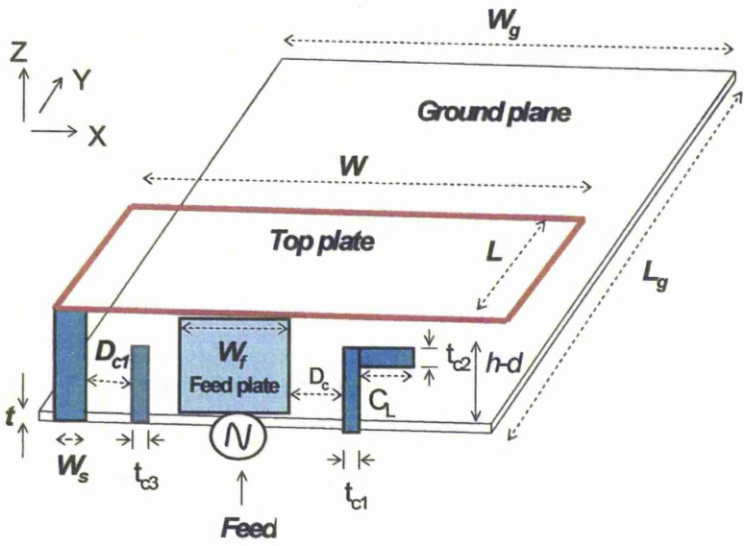

Fig. 4.20 Geometry of PIFA with the two parasitic elements

The simulated and measured results are shown in Fig. 4.21. The simulated and experimental results are quite similar. It is evident that the measured bandwidth achieved by this technique for S_{11} < -10 dB is extremely broad with a measured fractional bandwidth of about 110%, from about 1.6 GHz to 5.3 GHz while the simulated is about 120%.

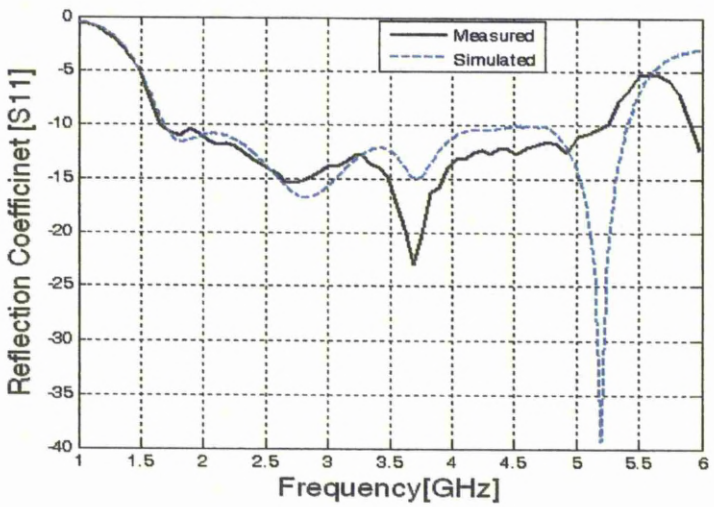

Fig. 4.21 Reflection coefficient (S11) in dB versus frequency in GHz with the addition of two parasitic elements

The equivalent circuit for the PIFA antenna with two parasitic elements is shown in Fig. 4.22. Similar to the equivalent circuit shown in Fig. 4.19, a capacitor C_4, an inductor L_4, and a resistor R_4 are added due the addition of the rectangular shaped parasitic element.

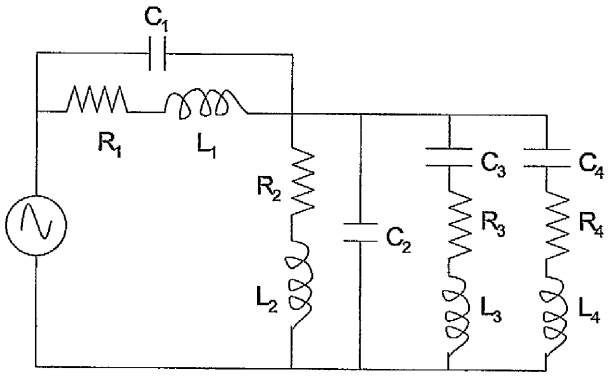

Fig. 4.22 Equivalent circuit of the PIFA antenna with two parasitic elements

It can be concluded that a properly configured PIFA antenna with the additions of two parasitic elements can be made as a very broadband antenna. The 3D simulated polar plot of radiation pattern of PIFA antenna at 3.5 GHZ is shown in Fig. 4.23 and the 2D polar plots of the measured radiation patterns of this antenna at different frequencies are shown in Fig. 4.24 for different planes in dB scale.

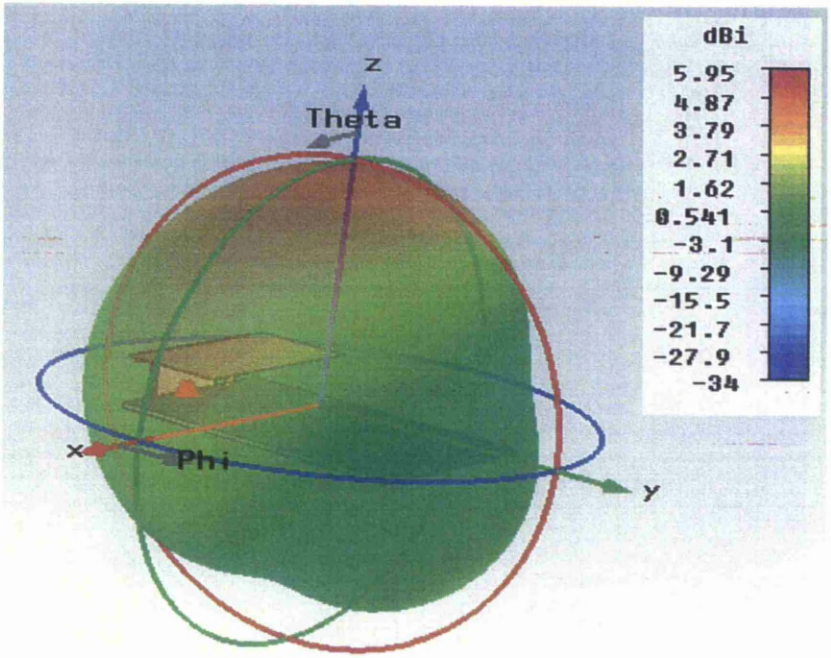

Fig. 4.23 3D simulated polar plot of radiation pattern of PIFA at 3.5 GHz

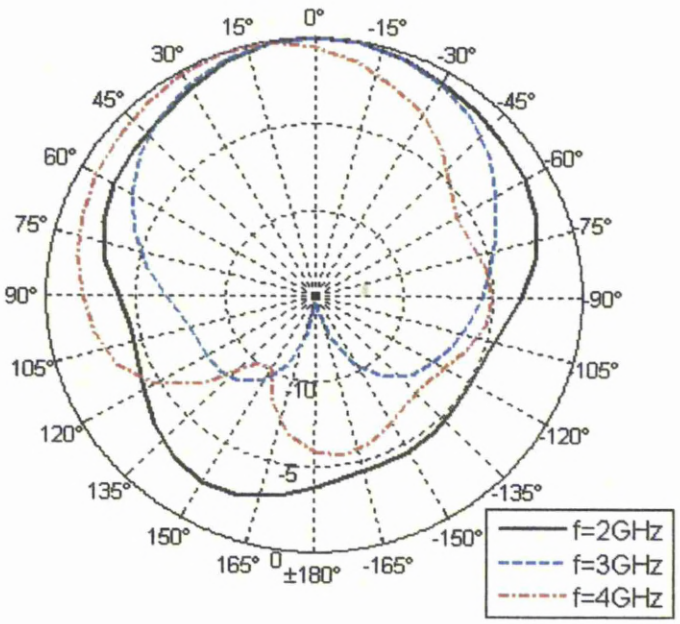

(a) XZ ($\Phi = 0^{\circ}$) plane

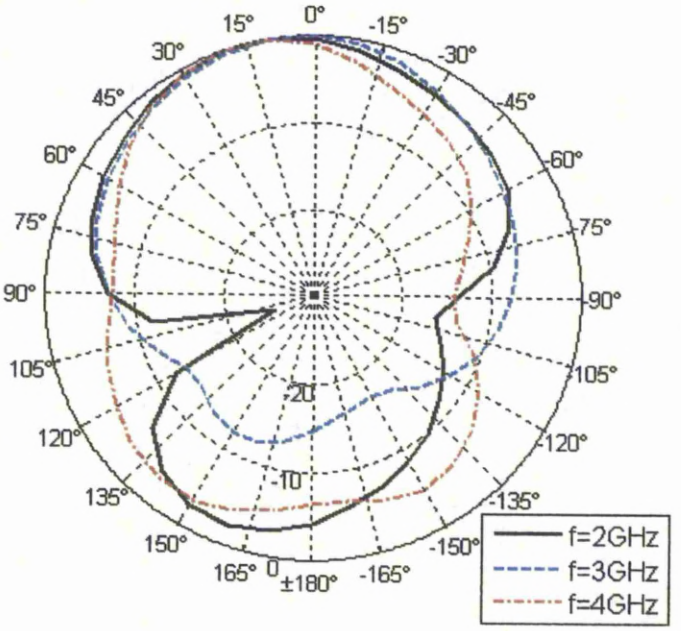

(b) YZ ($\Phi = 90^{\circ}$) plane

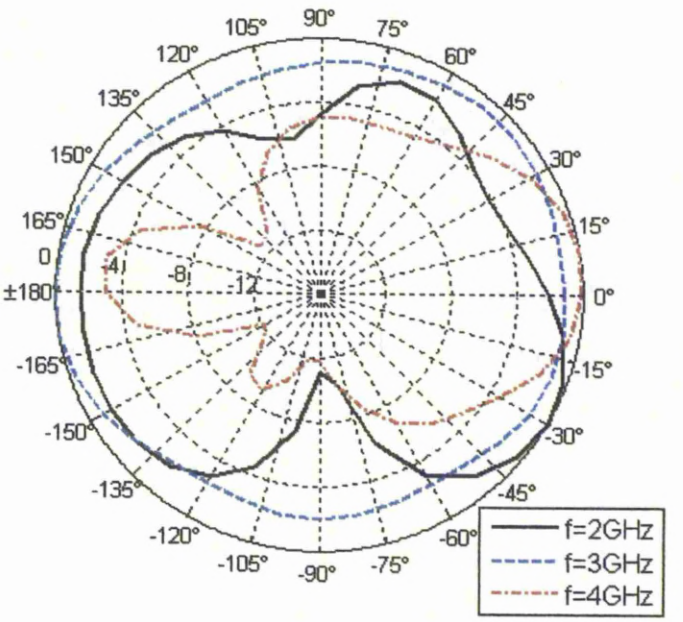

(c) XY ($\theta = 90^{\circ}$) plane

Fig. 4.24 2D measured radiation patterns in dB scale for different planes and different frequencies

The Smith chart of the PIFA antenna with the inverted-L shaped and rectangular shaped parasitic elements is shown in Fig. 4.25. It is evident that by the addition of these parasitic elements, multiple resonances are created due to which the impedance bandwidth of the antenna increases.

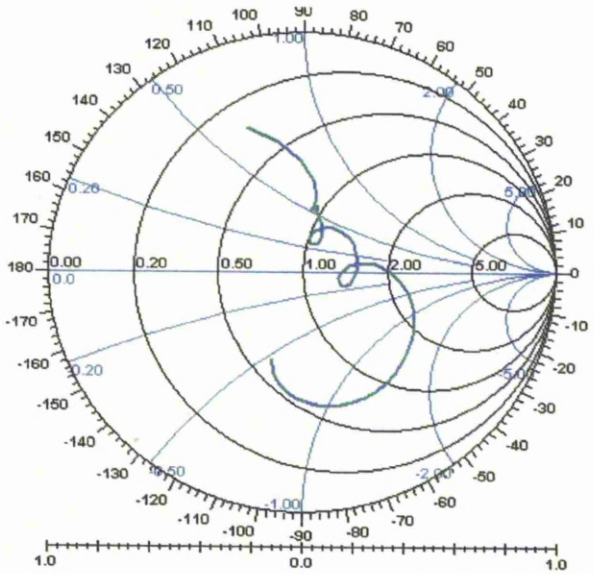

Fig. 4.25 Simulated Smith chart for impedance bandwidth of PIFA antenna with the two parasitic elements

4.4.1 Ultra Wide Band PIFA with the Two Parasitic Elements

The ultra wide band PIFA with one parasitic element discussed in the last article has a deficiency that it does not cover the full ultra wide band from 3.1 GHz to 10.6 GHz. For this reason, an ultra wide band PIFA with two parasitic elements (inverted-L shaped and rectangular shaped) is developed and tested. All the parameters are the same as in the article 4.3.3, now a rectangular shaped parasitic element is inserted at a distance $D_{c1} = 3$ *mm* from the shorting plate. The simulated and measured results of S_{11} are shown in Fig. 4.26. It can be seen that this UWB PIFA covers the ultra wide band from 3.5 GHz to 10.7 GHz.

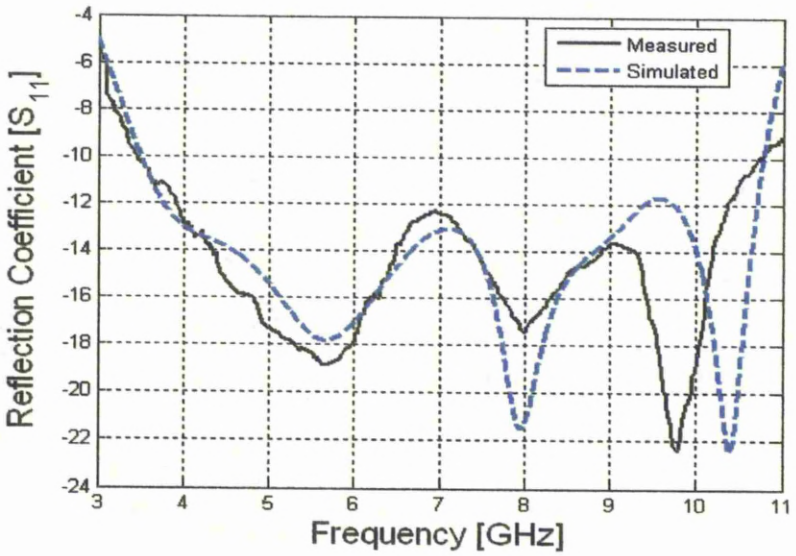

Fig. 4.26 Reflection coefficients S_{11} versus frequency in GHz

The 3D simulated polar plot of UWB PIFA at 6 GHZ is shown in Fig. 4.27 and the 2D polar plots of the measured radiation patterns of this UWB PIFA antenna are shown in Fig. 4.28.

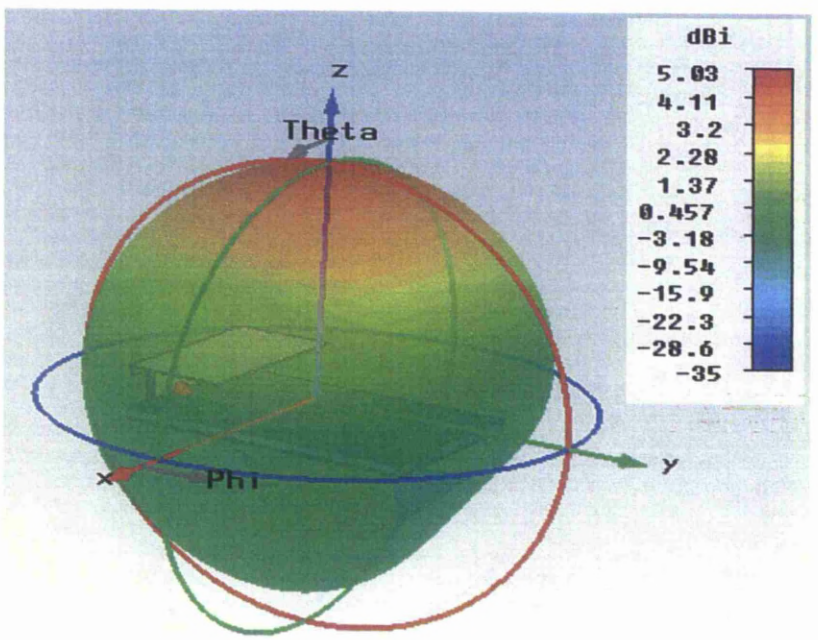

Fig. 4.27 3D simulated polar plot of radiation pattern of UWB PIFA with two parasitic elements at 6 GHz

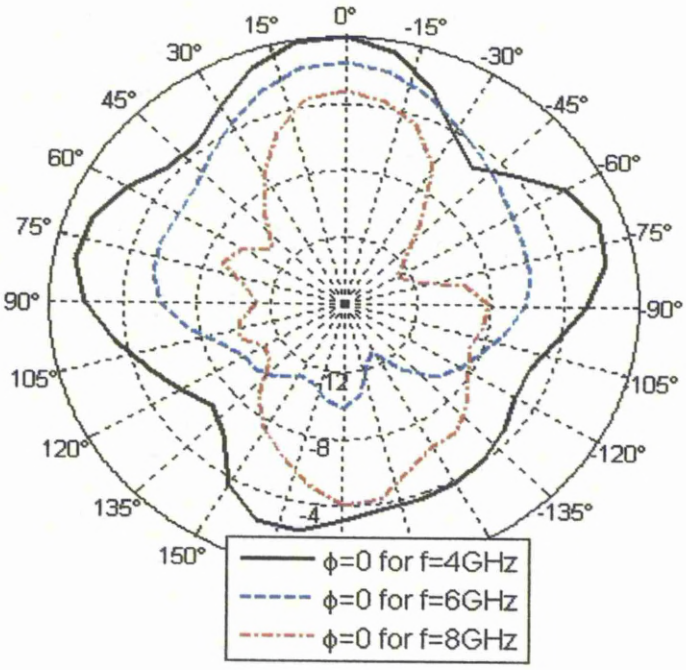

(a) XZ ($\Phi = 0^{\circ}$) plane

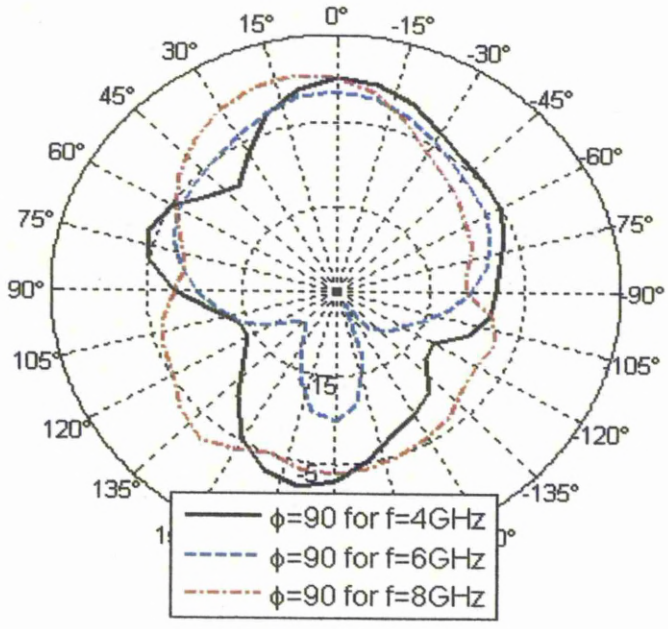

(b)YZ ($\Phi = 90^{\circ}$) plane

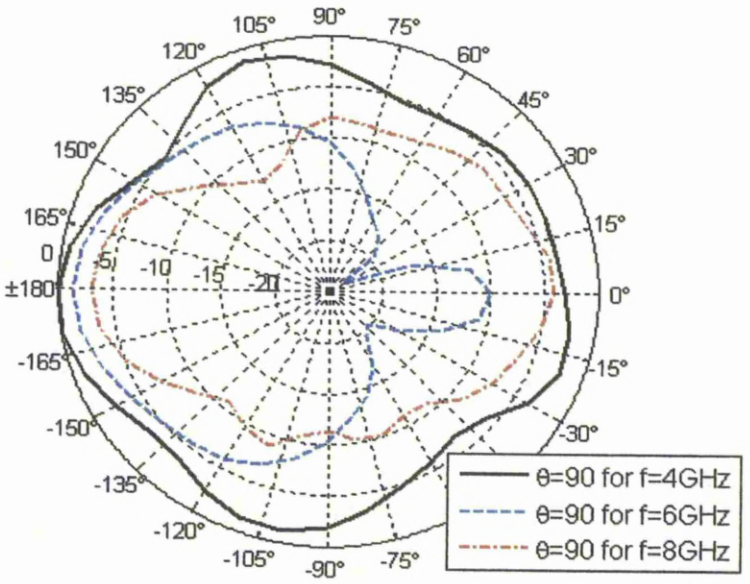

(c) XY ($\theta = 90^{\circ}$) plane

Fig. 4.28 2D measured radiation patterns in dB scale for different planes and different frequencies

4.5 Summary

The PIFA was generally considered a narrowband antenna. This prior fact led to the invention of multiple band PIFAs during the last decade. We have shown that the PIFA can be a broad band antenna and have proved this via three different bandwidth enhancement techniques. The first technique describes that very broadband (up to 65% fractional bandwidth) can be achievable for a PIFA antenna by taking optimal dimensions of ground plane and selecting the right values for the feed and shorting plates. It is shown that shorting plate should be narrowed and feed plate should be broadened in order to increase the bandwidth of PIFA.

The second bandwidth enhancement technique involves the addition of an inverted-L shaped parasitic element at a right place. The concept used is to place the parasitic element at a position to produce a second resonance such that reflection coefficient remains below -10 dB

reference level. It is shown that up to 102% fractional bandwidth can be achieved by the use of this technique. An ultra wide band PIFA antenna is fabricated and measured using this technique which covers the frequency range from 3.35 GHz to 9.4 GHz (simulated). It does not cover the full ultra wide band due to which a third technique is introduced.

The third bandwidth enhancement technique also involves the addition a parasitic element but the shape of this parasitic element is rectangular. It is shown that due to addition of this parasitic element, more than 120% fractional bandwidth is achieved. An ultra wide band PIFA with two parasitic elements is made and tested and it covers almost the full UWB band from 3.5 GHz to 10.7 GHz.

References

[1] D. Liu and B. Gaucher, "The inverted-F antenna height effects on bandwidth", *IEEE APS International Symposium*, vol. 2A, page(s): 367-370, 2005.

[2] P. S. Hall, C. T. P. Song, H. H. Lin, H. M. Chen, Y. F. Lin and P. S. Cheng, "Parametric study on the characteristics of planar inverted-F antenna", *IEE Proc.-Microw. Antennas Propagation*, vol. 152, no. 6, December 2005.

[3] P. W. Chan, H. Wong and E. K. N. Yung, "Wideband planar inverted-F antenna with meandering shorting strip", *Electronic Letters,* vol. 44, no. 6, March 13, 2008

[4] F. Wang, Z. Du, Q. Wang and K. Gong, "Enhanced-bandwidth PIFA with T-shaped ground plane" *Electronics Letters*, vol. 40, no. 23, November 11, 2004.

[5] A. Khoshniat, H. S. Mopidevi and B. A. Cetiner, "Broadband capacitively fed tapered type PIFA with modified ground plane", *Electronics Letters*, vol. 46, no. 7, April 1, 2010.

[6] R. Feick, H. Carrasco, M. Olmos and H. D. Hristov, "PIFA input bandwidth enhancement by changing feed plate silhouette", *Electronics Letters*, July 22, 2007.

[7] D. Porcino and W. Hirt, "Ultra wideband technology: potential and challenges ahead", *IEEE Comm. Magazine,* pp. 66-74, July 2003.

[8] H. Arslan, Z. N. Chen and M. D. Benedetto, *Ultra wideband wireless communication,* Wiley-Interscience, 2006.

[9] H. T. Chattha, Y. Huang, and Y. Lu, "PIFA bandwidth enhancement by changing the widths of feed and shorting plates", *IEEE Antennas and Wireless Propagation Letters,* vol. 8, page(s):637 – 640, 2009.

[10] D. Liu and B. Gaucher, "A new multiband antenna for WLAN/cellular applications", *IEEE Vehicular Technology Conference*, vol. 1, page(s): 243 – 246, September 2004.

[11] k. Wong, L. Chou and C. Su, "Dual-band flat-plate antenna with a shorted parasitic element for laptop applications", *IEEE transactions on Antennas and Propagation*, vol. 53, no. 1, January 2005.

CHAPTER

5

MIMO Systems and Diversity

In this chapter, the stemming of the capacity of wireless channels from the SISO system to MIMO system is discussed. Two popular signaling schemes used to exploit the MIMO systems are described. Then the definition of diversity, diversity combining techniques, the different methods of diversity techniques, the role of correlation and mutual coupling on diversity gain are described.

5.1 SISO System

In a conventional wireless communication system, there is only one antenna at both the transmitter and the receiver, which is called the Single-Input Single-Output (SISO) system. This system suffers a bottleneck in terms of capacity due to the Shannon-Nyquist criterion [1] which describes that either signal power or bandwidth is to be increased in order to increase the capacity. The received channel signal in a multi path environment with no

LOS is normally distributed (complex Gaussian). The amplitudes of that signal are Rayleigh distributed, the phase is uniformly distributed over 2π and the power is exponentially distributed [2-3].

5.2 MIMO System

Recent developments have shown that MIMO system can increase the capacity of wireless channel substantially without increasing the transmitted power and bandwidth [4-6]. Unlike the SISO system, the MIMO exploits the multi-path fading to increase the system capacity. In the MIMO systems, multiple antenna elements are required at both the transmitter and the receiver, as shown in Fig. 5.1.

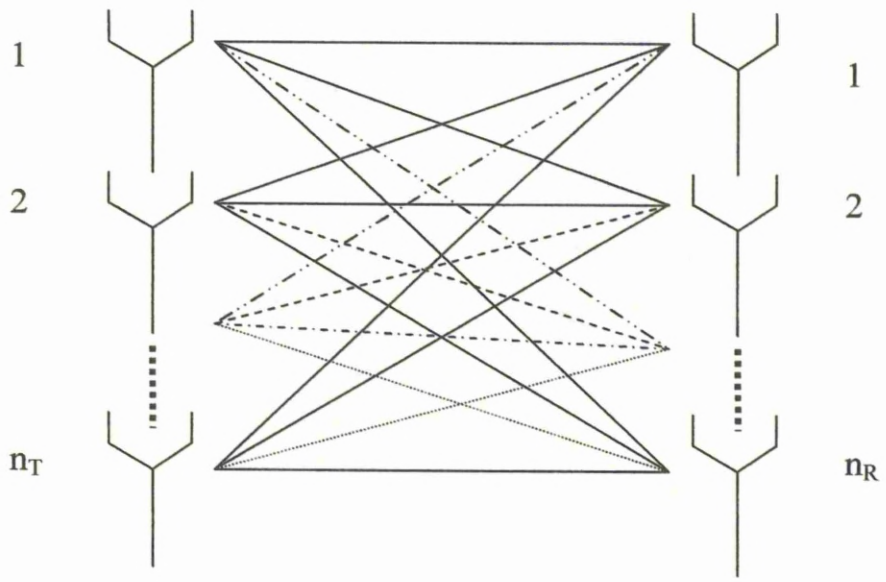

Fig. 5.1 A MIMO system created by two antenna arrays, comprising n_T transmit and n_R receive elements

Fig. 5.1 shows a MIMO system with n_T transmit elements and n_R receive elements. For a narrowband channel, the complex transmission coefficient between element k $\in$ [1,….., n_T] at the transmitter and element j $\in$ [1,….,n_R] at the receiver at time t is represented by $h_{jk}(t)$. A matrix containing all channel coefficients (channel coefficient matrix, H (t)) can be shown as:

$$H(t) = \begin{pmatrix} h_{11}(t) & h_{12}(t) & \cdots & h_{1nT}(t) \\ \vdots & & \ddots & \vdots \\ h_{nR1} & h_{nR2}(t) & \cdots & h_{nRnT}(t) \end{pmatrix} \quad (5.1)$$

Hence, a system transmitting the signal vector x(t) = [x1(t), $x_2(t)$,....,$x_{nI}\{t)]^T$, where xk(t) is the signal transmitted from the k^{th} element would result in signal vector y(t) = $[y_1(t),y_2(t),.....y_{nR}(t)]^T$ being received, where y(t) is the signal received by the j^{th} element, and

$$Y(t) = H(t)\, x(t) + n(t) \quad (5.2)$$

where n(t) is additive white Gaussian noise.

5.2.1 MIMO System Capacity

With the assumption that no channel state information exist at the transmitter and that the transmit power is equally allocated to all *n* antennas; the channel capacity of a narrow band (*n*, *n*) MIMO system is given by Foschini [6].

$$C(\xi) = \log_2 \det\left[I_N + \frac{\rho}{n}.HH^H\right] \text{ bits / s / Hz} \quad (5.3)$$

Where ρ donates the average SNR at each receiver, det denotes the determinant, and I_N denotes the identity matrix and H is the normalized $n \times n$ channel matrix.

The channel matrix H in the MIMO systems capacity of equation (5.3) is the mathematical representation of the physical transmission path, which includes the multipath channel characteristics of the physical environment and the antenna configurations. Therefore the multipath channel characteristics and the antenna configurations play a key role in determining the communication performance in a MIMO

system. For matrix H, its singular value decomposition (SVD) is expressed as

$$H = U\sum V^H \tag{5.4}$$

where $N_R \times N_R$ matrix U and the $N_T \times N_T$ *matrix* V are unitary matrices and $\sum$ is an $N_R \times N_T$ diagonal matrix of the singular values σ_i of H. The rank of H is equal to its number of non-zero singular values. The power gain of the i^{th} sub-channel is $\lambda_i = \sigma_i^2$, where λ_i is also the i^{th} largest eigen value of HH^H, equation (5.3) becomes

$$C(\xi) = \log_2 \det\left[I_N + \frac{\rho}{n}.HH^H\right] = \sum_{i=1}^{n} \log_2\left[1 + \frac{\rho}{n}\lambda_i\right] \text{bits/s/Hz} \tag{5.5}$$

According to the above equation, when the channel exhibits rich scattering, the MIMO system can achieve almost *min* (n_T, n_R) more bits per hertz for every 3 dB increase in SNR. This is a great improvement over the single antenna case which achieves one additional bit per hertz for every 3 dB increase in SNR [10-12].

5.2.2 Spatial Multiplexing

Spatial multiplexing (SM) is a signaling scheme where independent data streams are transmitted simultaneously in parallel channels from each element in an array of antennas. The basic principle of SM is illustrated by examining a system with two elements at the transmitter and two elements at the receiver below.

Firstly, the bit stream of data to be transmitted is de-multiplexed into two sub-streams, then modulated and transmitted simultaneously from each transmit antenna as shown in Fig. 5.2. If the propagation channels are uncorrelated, the signals that arrive at the receive antenna are well separated. Assuming that the receiver has knowledge of the channel, it can differentiate between the co-channel signals and extract both signals. After demodulating

the received signals, the original sub-streams can be combined to yield the original bit stream of data. Therefore, the spatial multiplexing increases the channel capacity with the number of transmit-receiver antenna pairs [5]. This concept can be extended to more general MIMO channels. If the number of elements at the transmitter, n_T and the receiver n_R are not equal, the maximum parallel channels that can be achieved in an ideal MIMO system is min (n_T, n_R). A spatial multiplexing scheme called Bell labs Layered Space–Time (BLAST) proposed by Bells Labs was first widely publicized in 1996 [5]. Considerable research activities have been carried out to show that the spatial multiplexing concept has the potential to significantly increase spectral efficiency [13-14]. Further research has been carried out on creating and evaluating enhancements to the spatial multiplexing concepts, such as combining with other modulation schemes like OFDM (Orthogonal Frequency Division Multiplexing) [15-17]. In general, this technique assumes channel knowledge at the receiver and the performance can be further improved when the knowledge of the channel response is available at the transmitter [18-19].

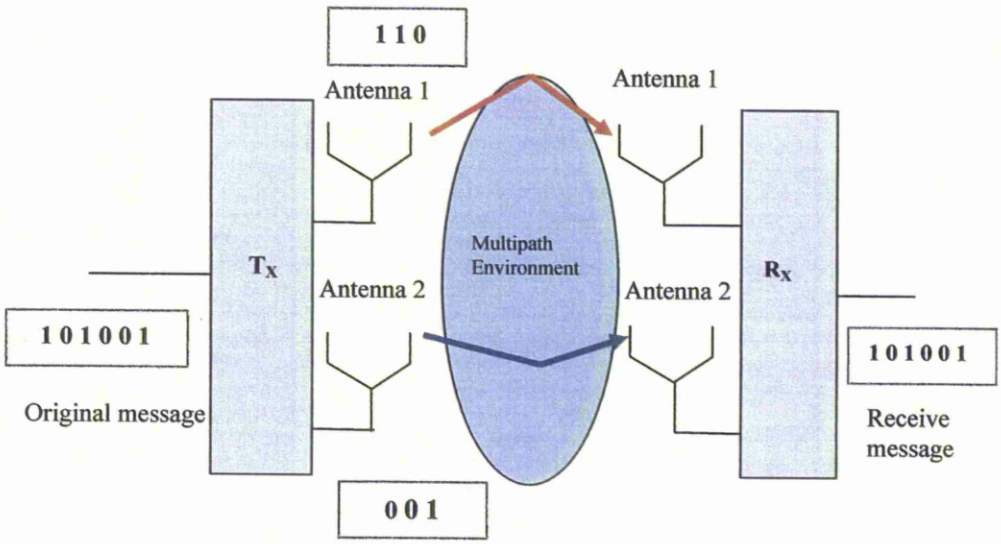

Fig. 5.2 A 2x2 MIMO system with a spatial multiplexing scheme.

5.2.3 Space-Time Coding

An alternative method of exploiting MIMO channels, known as space-time coding, has also recently generated large amounts of research [20-22]. This method aims to improve the system's performance by exploiting the multiple element antennas for diversity gain rather than for the spatial multiplexing gain of parallel data streams. It increases network throughput by selecting quality signal paths such that higher data rates can be achieved and avoiding signal paths that are likely to produce packet errors and retransmissions.

A space-time coded transmitter differs from that of a spatial multiplexing system in that a single data stream is encoded across both time and space to produce the symbol streams for each transmit element as shown in Fig. 5.3. Appropriate decoding at the receiver allows a diversity gain to be achieved. This method is particularly attractive as it does not require channel knowledge in the transmitter. The resulting diversity gain improves the reliability of fading wireless links and hence improves the quality of the transmission.

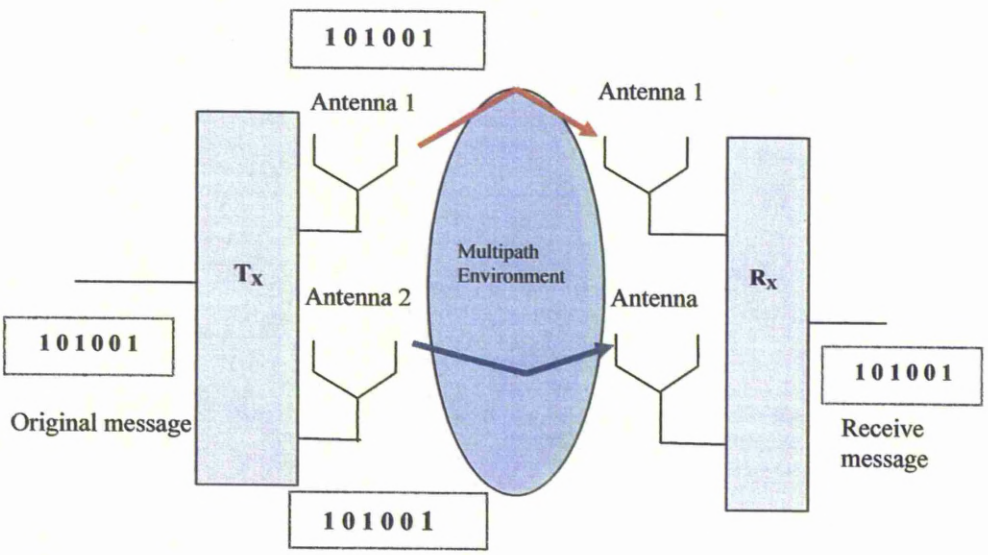

Fig. 5.3 A 2x2 MIMO system with a space-time coding scheme.

5.3 Diversity

One well known method of reducing the effects of fading is the use of diversity reception techniques. The basic concept of diversity is that the receiver should have available more than one version of the transmitted signal, where each version is received through a distinct channel. If the fade in each of these paths is uncorrelated then the occurrence of obtaining simultaneous deep fade in each path is greatly reduced. An N branch diversity system can suppress up to N-1 interfering channels. The diversity performance depends on the number of diversity branches, the correlation between the branches, the difference in the received signal levels of the branches and the diversity increases as correlation and the difference in signal levels decreases [23-24].

Diversity can only be used in the multipath fading environment. In a line-of-sight (LOS) environment, it is impossible to get diversity gain as no multipath waves can be generated. Objects surrounding the transmitter and receiver reflect and scatter the signals causing multipath with the waves arriving at the receiving along different paths. Rayleigh fading or small-scale fading occurs when there are only non-line-of-sight (NLOS) paths and no line-of-sight (LOS) path exists. If a line-of-sight (LOS) signal exists at the receiver along with the various multipath signals, the fading is usually a Rician fading. An example of different paths is shown in Fig. 5.4.

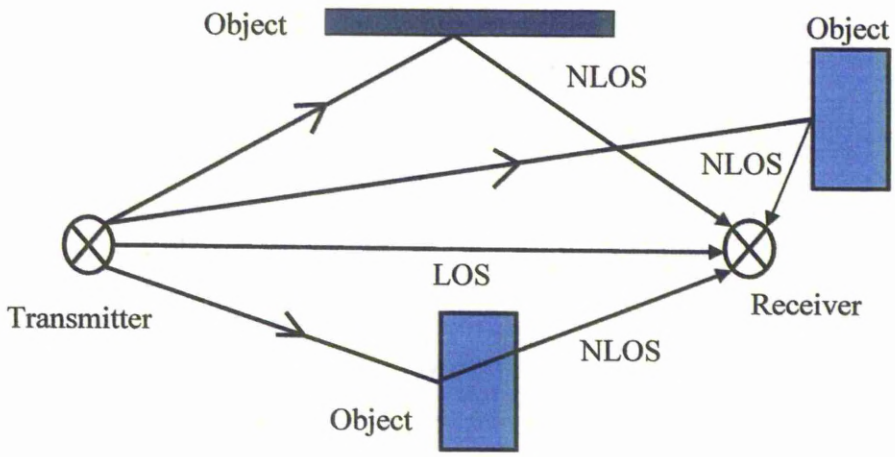

Fig. 5.4 Line-of-sight (LOS) and non-line-of-sight (NLOS) propagation

5.3.1 Diversity Combining Techniques

There are four different types of diversity combining techniques [25].

- Switched combining
- Selection combining
- Equal gain combining (ECG)
- Maximum ratio combining (MRC

5.3.1.1 Switched Combining

The switched combining technique requires only one receiver radio between the N branches as shown in Fig. 5.5. The receiver is switched to other branches only when the SNR on the current branch is lower than a predefined threshold. Whereby, other combining techniques require *N* receivers to monitor the received instantaneous signals level of every branch when there are *N* element antennas. Due to size restrictions, battery life and complexity, the switched combining technique is presently implemented in mobile terminals with diversity antennas [26]. The optimum performance that a switched combiner can achieve is similar to that of a selection combiner.

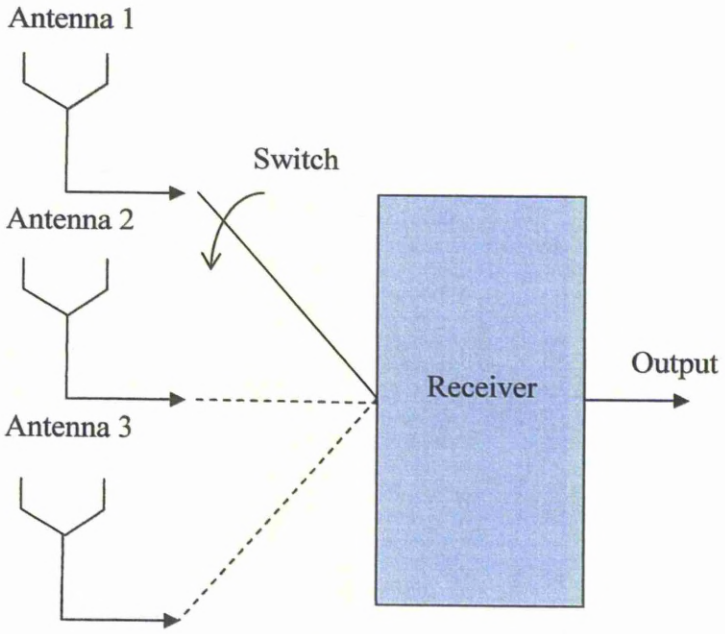

Fig. 5.5 Block diagram of switched combining for N branches/antenna elements with only one receiver.

5.3.1.2 Selection Combining

The selection combining technique is similar to the switched combining technique except that N receivers are required to monitor instantaneous SNR at all branches. The branch with the highest SNR is selected as the output signal.

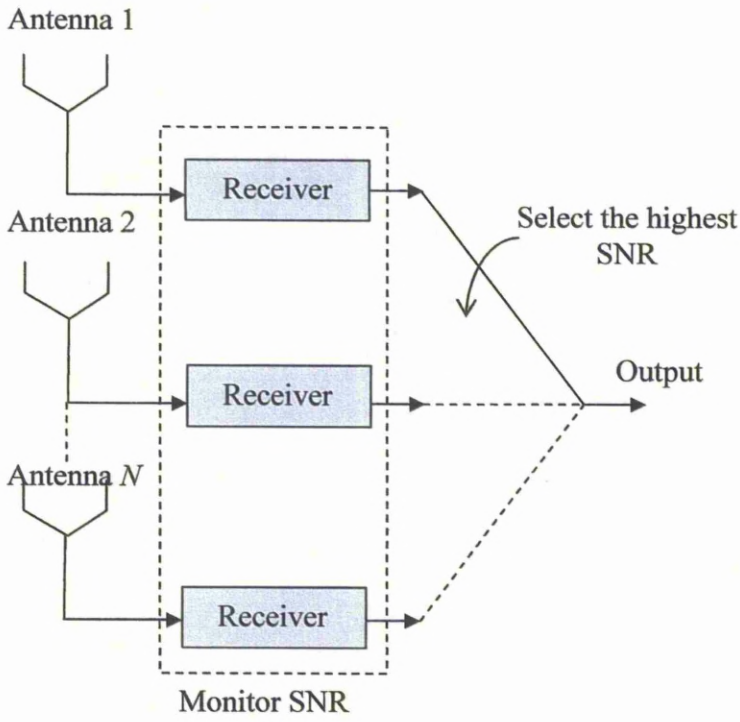

Fig. 5.6 Block diagram of selection combining for N branches/antenna elements.

5.3.1.3 Equal Gain Combining (EGC)

Both switched and selection combining techniques only use the signal from one of the branches as the output signal. In order to improve SNR at the output, the signals from all branches are combined to form the output signal. However, the signal from each branch is not in-phase.

Therefore, each branch must be multiplied by a complex phasor having a phase $-\theta_i$, where θ_i is the phase of the channel corresponding to branch i (i.e. co-phased) as shown in Fig. 5.7. When this is achieved, all signals will have zero phases and are combined coherently.

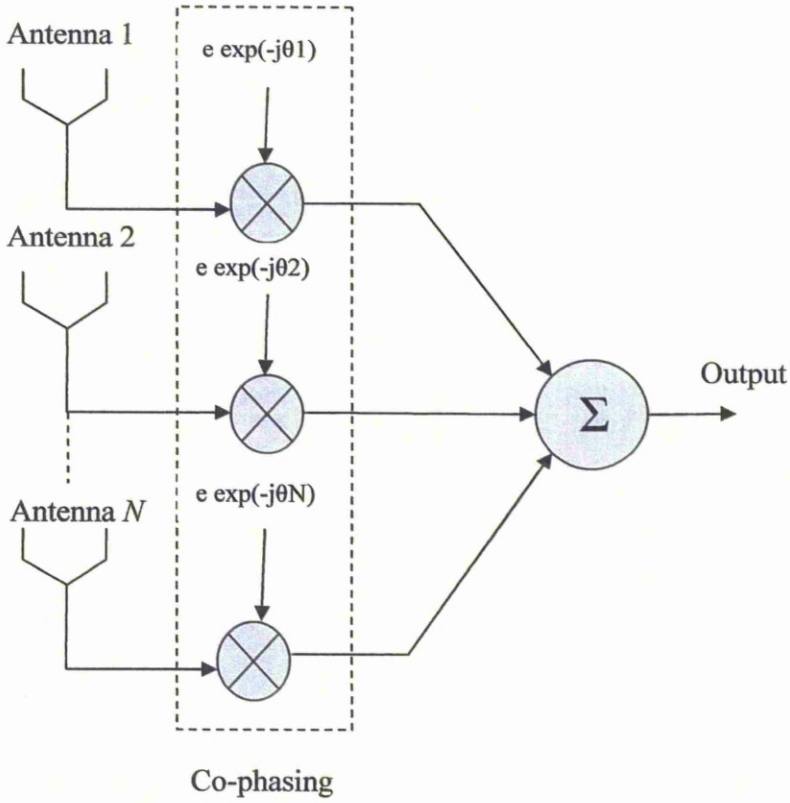

Fig. 5.7 Block diagram of equal gain combining for N branches / antenna

5.3.1.4 Maximum Ratio Combining (MRC)

In the equal gain combining technique, all the branches may have different SNRs. Sometimes one of the branches has a much lower SNR than the other branches and this will reduce the overall SNR to a lower value at the output. In order to maximize the SNR at the output, each branch is applied with a weight, w_i before all the signals are combined coherently as shown in Fig. 5.8. In order to maximize the SNR at the output, a branch with a higher SNR will be given a higher weighting.

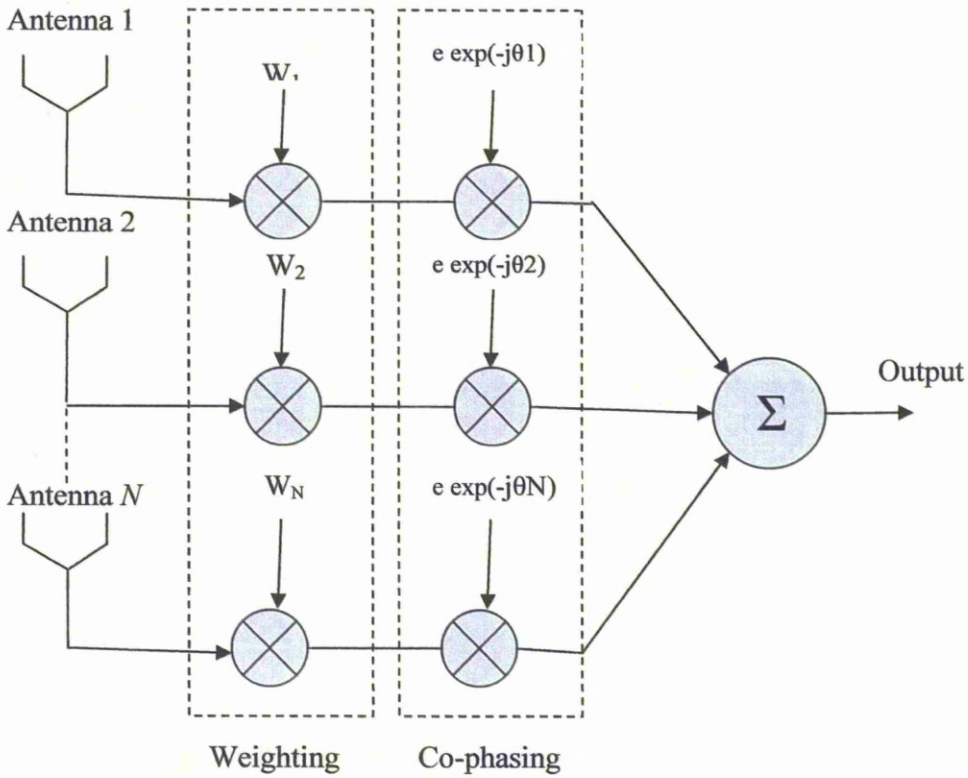

Fig. 5.8 Block diagram of maximum ratio combining for N branches/antenna elements

5.3.2 Diversity Gain

Diversity gain is defined as the improvement in the SNR of the combined signals relative to the SNR from a single antenna element. The cumulative distribution function (cdf) of a Rayleigh channel is given as [25].

$$P(\gamma \angle \gamma_s)_N = \left[1 - e^{-\frac{\gamma_s}{\Gamma}}\right] \tag{5.6}$$

where Γ is the mean SNR, γ is the instantaneous SNR, $P(\gamma < \gamma_s)$ is the probability that the SNR will fall below the given threshold, γ_s. For a selection combiner with N independent branches, assuming that the N branches have

independent signals and equal mean SNRs, the probability of all branches having a SNR below γ_s is equivalent to the probability for a single branch raised to the power N as:

$$P(\gamma \angle \gamma_s)_N = \left[1 - e^{\frac{\gamma_s}{\Gamma}}\right]^N \tag{5.7}$$

where N is the number of antennas / branches.

Equations 5.6 and 5.7 are plotted in Fig. 5.9 to show the reduction of the probability of fading below a given threshold when increasing the number of antenna, N. In this figure, diversity gain is also illustrated in terms of the increase in SNR of a combined output compared to a single antenna. Here, the diversity gain is marked off where $P(\gamma < \gamma_s)$ of 1% (i.e. 99% reliability). The figure shows that there is a 10 dB and 13 dB of diversity gain for the two branches and three branches selection combiner respectively.

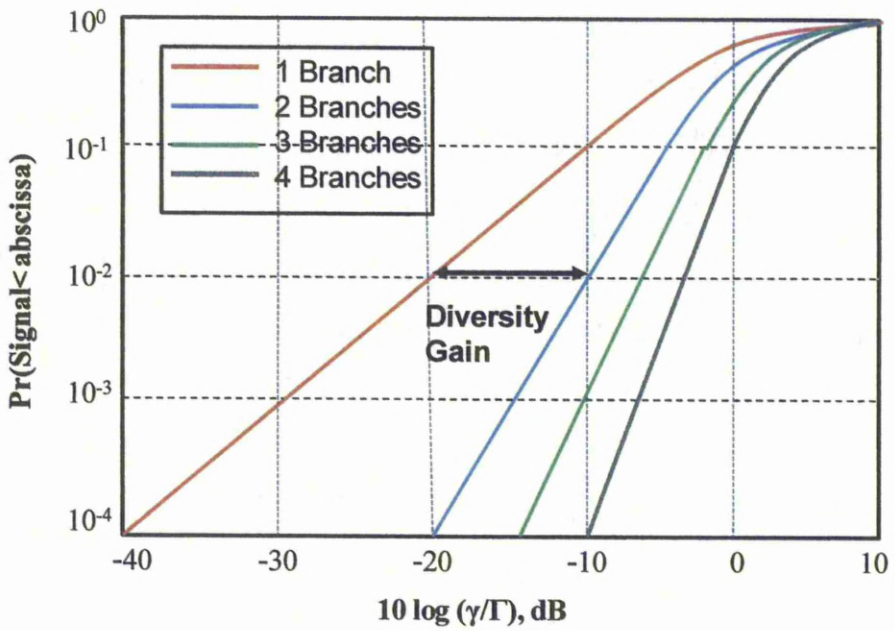

Fig. 5.9 Cumulative distribution functions of Rayleigh fading signals for different diversity branches

5.3.3 Diversity Gain Measurement in a Reverberation Chamber

Traditionally antennas were designed for use in environments where there is a Line Of Sight (LOS) path between the two sides of a communication link. Therefore, these antennas were characterized in terms of their free space equivalents; the measurements typified by use of an anechoic chamber. Modern day mobile telephones for example do not operate in such circumstances. The signal propagation reaching the mobile phone in an urban and indoor environment typically has no LOS path and the waves will encounter reflection, diffraction and scattering after originating from the transmitting antenna. The wave contributions via these 'paths' will add at the receiving side. These waves will have independent complex amplitudes (i.e. amplitudes and phase) and may add up constructively or destructively or anything between these two extremes. The wave path and their complex amplitudes will also change fast with time, due to the movement of the terminal or parts of the environment, which results in variations at the receiver as a function of time; more commonly referred to as fading.

The multipath environment can at the receiving side be characterized by several independent incoming plane waves. If the LOS is absent, the quadrature components of the received complex signal become normally distributed (complex Gaussian); from this their magnitudes become Rayleigh distributed, their phase become uniformly distributed over 2π, and the power becomes exponentially distributed. This is what a reverberation chamber emulates well.

In practice however, the arriving waves reaching a mobile phone will have a certain AoA distribution in the elevation and azimuth planes. Therefore an elevation distribution may be needed to characterize a real multipath environment – as in practice a real environment will have a larger content of vertically polarized waves than horizontal owing to most base stations being vertically polarized. This can prove problematic as then antennas measured will depend on where they are used and measured; and as such, the results will not be directly transferrable.

The reverberation chamber has been proposed to perform the diversity measurements because an isotropic reference environment can exist within the

facility, which means that the results obtained can be statistically repeatable [27-29]. Furthermore, having a uniform angle of arrival can simplify the performance and characterization of an antenna, as the antennas performance is independent from the orientation.

The reverberation chamber is a large metallic enclosure which works in what is termed an 'over mode' condition (i.e. many modes). The signal propagation in this environment constitutes a rich scattered characteristic, which manifests itself as being statistically Rayleigh distributed – a factor which makes it ideal for the measurement of diversity gain as it is very similar to propagation characteristics of the urban and indoor environments. Fig. 5.10 shows the reverberation chamber at the University of Liverpool. The chamber is constructed from aluminium panels and its dimensions are 3.6m x 4m x 5.8m (width x height x length). The chamber is equipped with two principle sets of mechanical stirring paddles; one set configured from the floor to the ceiling for vertically polarized waves, the second set mounted from the front to back wall at ceiling height – used for stirring horizontally polarized waves. Both principle sets of mechanical stirring paddles work simultaneously during the chambers' operation, thus all differing polarizations of the reflected waves will be accurately stirred.

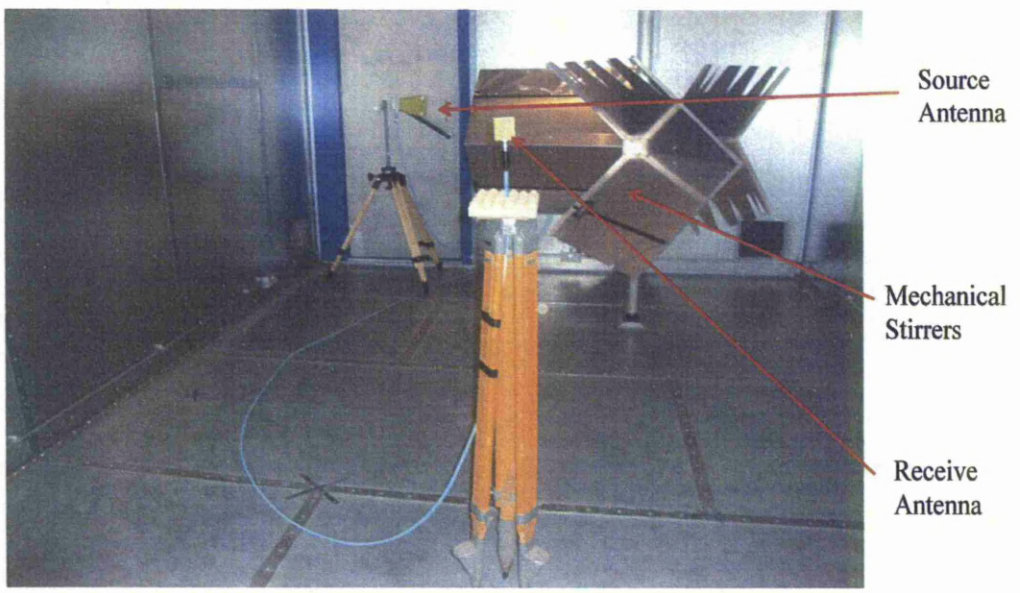

Fig. 5.10 The Reverberation Chamber at University of Liverpool

The exact diversity gain measurement procedure is described here which was utilized to acquire the results presented in the next chapter [30].

The measurement procedure started with a full 2 port calibration from 2 – 3 GHz. An Anritsu 37369A VNA was used for the measurements, of which port 1 was associated with the transmitting side. The measurement procedure utilized an amplifier connected to port 1 to actively boost the power levels of the transmitted signal to levels well above the noise floor of the chamber. The chamber during the measurement was loaded with a model of a human torso. The requirement for this was to increase the average mode bandwidth to accurately excite more of the modes inside the chamber – by doing this the accuracy of the measurement would be increased.

The measurement was performed in conjunction with a reference antenna with known efficiency values; in this case a dual ridge horn antenna (Satimo SH2000). While the reference measurement took place the dual feed PIFA antenna was located inside the chamber, terminated with 50 Ω. To establish the scattering parameters in a precise manner and to give rise to enough channel samples a large amount of data was selected. Thus, all measurements used 1601 frequency data points from 2 – 3 GHz and 1 degree mechanical stirring intervals.

The reference antenna was measured first according to the aforementioned stated parameters. Throughout this measurement the PIFA antenna was placed inside the chamber, terminated on both ports with 50 Ω. This was required because throughout the measurements the loading on the chamber (and thus the subsequent Q factor) needs to remain exactly the same. After the reference measurement, one branch of the PIFA was connected to the VNA while the other branch was terminated with 50 Ω. This was performed such that the mismatch on the opposite branch would be reduced. The reference antenna also remained inside the chamber terminated with 50 Ω. After branch 1 was measured branch 2 was connected to the VNA with branch 1 terminated

The average transmission samples were recorded for each branch such that a total of 359 x 1601 = 574759 total samples existed. Once all samples were

acquired the reference antenna was first to be processed. A transfer function is established for this antenna in accordance with [31]:

$$T_{REF} = \frac{1}{N}\sum_{n=1}^{N}\frac{|S_{21\,(n)}|^2}{(1-|S_{11}|^2)(1-|S_{22}|^2)} \tag{5.8}$$

where N = total number of stirrer positions and S_{11} and S_{22} represent the transmit and receive sides respectively. With respect to [32], where it is stated that maintaining a power balance is important for determining the diversity gain, all the PIFA samples are normalized to the square root of the average power level of the reference antenna, and its known efficiency values. The measured dual feed PIFA channel samples are processed as follows:

$$H_{CHANNEL} = \frac{N_{sample}}{\sqrt{P_{REF}}} \tag{5.9}$$

where $P_{REF} = {}^{T_{REF}}/_{\eta_{RAD}}$ and η_{RAD} = radiation efficiency of the reference antenna.

Once all 574759 channel samples are processed the cumulative distribution is then calculated for each branch and each PIFA antenna respectively. Similar to other investigations undertaken, the two branches for each dual-feed PIFA antenna have been combined using two different diversity combination rules; that is, selection combining (SC) and maximal ratio combining (MRC). The two combination diversity schemes can be characterized as, MRC is the sum of branch 1 and branch 2 for each respective sample and SC is the maximum value of the respective samples of branch 1 and branch 2. In this work, the diversity gain has been read as the difference along the abscissa axis between the maximal ratio and the level of the strongest branch, at a constant 1% cumulative probability level as described in the next chapter.

5.3.4 Correlation

One of the conditions for obtaining diversity gain is low correlation. The correlation can be described by two metrics: complex and envelope correlations [33]. The complex correlation ρ_{12} is described as "the complex correlation between two signal envelopes" [34]. The magnitude and phase are used to calculate correlation. In the time domain, the complex correlation is defined in closed form as follows:

$$\rho_{12} = \frac{\int_0^T \left(v_1(t) - \overline{v_1}\right)\left(v_2(t) - \overline{v_2}\right)^* dt}{\sqrt{\int_0^T \left|v_1(t) - \overline{v_1}\right|^2 dt \int_0^T \left|v_2(t) - \overline{v_2}\right|^2 dt}} \tag{5.10}$$

where t is the instantaneous time point and T is the time period over which the fading signals correlate. The two fading signals $v_1(t)$ and $v_2(t)$ are voltage functions of time and have mean values $\overline{v_1}$ and $\overline{v_2}$ in volts, V.

However, in order to evaluate the correlation between two antennas in an angular domain, the complex correlation is computed as follows [35].

$$\rho_{12} = \frac{\int_0^{\pi}\int_0^{2\pi}\left[XPR.E_{\theta\pi}(\theta,\phi)E^*_{\theta\pi}(\theta,\phi)P_\theta(\theta,\phi) + E_{\phi\pi}(\theta,\phi)E^*_{\phi\pi}(\theta,\phi)P_\phi(\theta,\phi)\right]\sin\theta d\phi d\theta}{\sqrt{\sigma_1^2\sigma_2^2}} \tag{5.11}$$

where the variance, σ_n^2 is the variance of branch n in V^2

$$\rho_R^{12} = \int_0^{\pi}\int_0^{2\pi}\left[XPR.E_{\theta\pi}(\theta,\phi)E^*_{\theta\pi}(\theta,\phi)P_\theta(\theta,\phi) + E_{\phi\pi}(\theta,\phi)E^*_{\phi\pi}(\theta,\phi)P_\phi(\theta,\phi)\right]\sin\theta d\phi d\theta \tag{5.12}$$

where XPR is the ratio of time averaged vertical power to time average horizontal power [36] in the fading environment in linear form:

$$XPR = \frac{P_v}{P_H} \tag{5.13}$$

The second type of correlation metric is the envelope correlation, ρ_e which is the correlation between two signal envelopes without considering the phase [34]. Under the assumption that the received signal have a Rayleigh-distributed enveloped and randomly distributed phase, the cross-correlation and envelope-correlation are related by [36].

$$\rho_e \approx |\rho_{12}|^2 \tag{5.14}$$

A good diversity gain can be obtained when the signals satisfy the following two conditions [37].

$$\rho_e < 0.5 \text{ and } P_1 \cong P_2 \tag{5.15}$$

where P_i is the average received power from each antenna branch. These parameters can be obtained from directly measuring the received signal in a typical wireless environment. They can also be calculated from the radiation pattern or from the mutual coupling between the ports. The complex cross-correlation between the antenna ports can also be estimated from the mutual coupling by using the normalized mutual resistance [37].

$$\rho_c \cong r_{ij} \tag{5.16}$$

and $r_{ij} = \frac{\mathrm{Re}(Z_{ij})}{\mathrm{Re}(Z_{ij})}$ where Z_{ij} is the standard 2-port impedances.

The envelope-correlation can also be found from S-parameters measured at each antenna terminal [38].

$$\rho_e = \frac{|S_{11}^* S_{12} + S_{21}^* S_{22}|^2}{(1-(|S_{11}|^2 + |S_{21}|^2))(1-(|S_{22}|^2 + |S_{12}|^2))} \tag{5.17}$$

5.3.5 Branch Power Ratio and Mean Effective Gain (MEG)

As discussed above, the 2nd condition of getting diversity gain is that the power levels of all the antennas must not be too different. One way of illustrating this is by using the ratio of two branch power levels, *k*, as follows in linear form:

$$K = \frac{P_{\min}}{P_{\max}} \tag{5.18}$$

where P min [W] is the power from the antenna with the lower power and P max [W] is the power from the antenna with the higher power in each pair of antennas. The ratio of the two antennas' power levels, k, is multiplied by the diversity gain to obtain the new diversity gain for a selection combiner.

An alternative method to obtain the branch power ratio is derived from the Mean Effective Gain (MEG) [39] of the antennas as follows (assuming only two branches):

$$K = \min\left(\frac{MEG_2}{MEG_1}, \frac{MEG_1}{MEG_2}\right) \tag{5.19}$$

The MEG is the average gain of an antenna in a mobile environment and is defined in [25] as the ratio between the mean received power of the antenna (P_{rec}) and the total mean incident power (P_V + P_H). The MEG is a figure of merit for the average performance of an antenna on a mobile terminal taking into account the incident radio waves in the multipath environment and the gain patterns of the antenna. This parameter determines how effective the mobile terminal antenna will be in a multipath environment. It is important to evaluate the MEG of the antennas to determine their diversity performance. Taga has derived the following equation to evaluate the MEG [39].

$$MEG = \int_0^{\pi}\int_0^{2\pi}\left[\frac{XPR}{1+XPR}G_\theta(\theta,\phi)P_\theta(\theta,\phi) + \frac{1}{1+XPR}G_\phi(\theta,\phi)P_\phi(\theta,\phi)\right]\sin\theta d\phi d\theta \tag{5.20}$$

where G_θ (θ, Φ) and G_Φ (θ, Φ) are the θ and Φ components of the antenna power gain patterns respectively. P_θ (θ, Φ) and P_Φ (θ, Φ) are the θ and Φ components of the angular density functions respectively.

5.3.6 Types of Diversity Techniques

The diversity gain can be achieved by using different techniques including time, frequency and antenna diversities and/or combination of these methods.

5.3.6.1 Antenna Diversity Techniques

Antenna diversity is further characterized as space diversity, polarization diversity and pattern / angle diversity. All of these techniques are being used for obtaining diversity gain in smaller and portable terminals. These are explained in detail as follows.

5.3.6.1.1 Space Diversity

Spatial diversity utilizes more than one antennas which are sufficiently separated from each other so that the relative phases of the multipath contributions are significantly different at the two antennas. This is the most fundamental technique to achieve diversity. The phase differences between the total signals received at each of the antennas are proportional to the differences in the path lengths from the scatterers to each antenna. When large phase differences are present, they give rise to a low correlation between the signals at the antennas. Therefore it is expected that the correlation decreases with an increase in the distance between the scatterers or an increase in the distance between the antennas. By assuming angular density function to be uniform in azimuth of the mobile environment and no angular density function in elevation (i.e. Two-dimensional scenario), the correlation coefficient for a distance separation d can be obtained from the zero order Bessel function, $J_o(x)$ [25].

$$\rho_{12} = j_0(\beta d) \tag{5.21}$$

where β is the phase constant.

The angular distribution of wave arrival does affect the correlation coefficient for a given spacing d, whereby if the angular density function is

restricted to a limited range then ρ_{12} will increase [25]. Generally, spacing, d of 0.5λ is practically used to obtain two uncorrelated signals at mobile terminals.

Apart from the effect of the angular density functions $P_\theta(\theta, \Phi)$ and $P_\Phi(\theta, \Phi)$, it should be noted that since the two antennas are horizontally spaced with $d = 0.5\lambda$, mutual coupling also affects the performance of diversity as well. It has been shown in theory and experimentally that mutual coupling reduces the correlation coefficient [25]. Recently it has been reported that the MIMO capacity is still relatively large when the four antennas are closely spaced down to $d = 0.2\lambda$ in the indoor environment [39]. In the outdoor environment, the MIMO capacity for antennas with spacing of $d = 0.2\lambda$ is even larger than when the antennas spacing is $d = 2.5\lambda$ [40].

5.3.6.1.2 Pattern / Angle Diversity

Angle diversity consists of two or more receiving antenna beams with a common phase center but oriented towards different directions or at least having partially non-overlapping radiation pattern. Some researchers also refer to this as pattern diversity, whereas others use the term pattern diversity when the two or more collocated receiving antennas have different response patterns. Pattern diversity can be seen as a variation of angle diversity. Pattern diversity occurs in many instances at the mobile terminals because the antennas will pick up signals coming from different angles. Since the fading signals coming from different directions are independent then pattern diversity can be implemented. This has been considered at the base station in some cases and compared with spatial diversity [41-42].

At the mobile terminal, two omni-directional antennas interacting with each other whilst closely spaced can also obtain pattern diversity. Basically, the antennas act as parasitic elements to each other and their patterns change to allow signals to be picked up at different angles. Antennas with beam steering at the mobile terminals (by changing the feed point impedance of parasitic elements) have been developed [43]. Recent studies conducted on pattern diversity in the MIMO systems have shown that with appropriate dissimilarity in the antenna pattern, the system can achieve large channel capacity [44]. Fig. 5.12 shows the

difference between the space diversity and pattern diversity. It can be seen that space diversity is based on distance whereas the pattern diversity is achieved by placing one antenna element horizontal and the other antenna vertical so that their pattern are different in space in different directions.

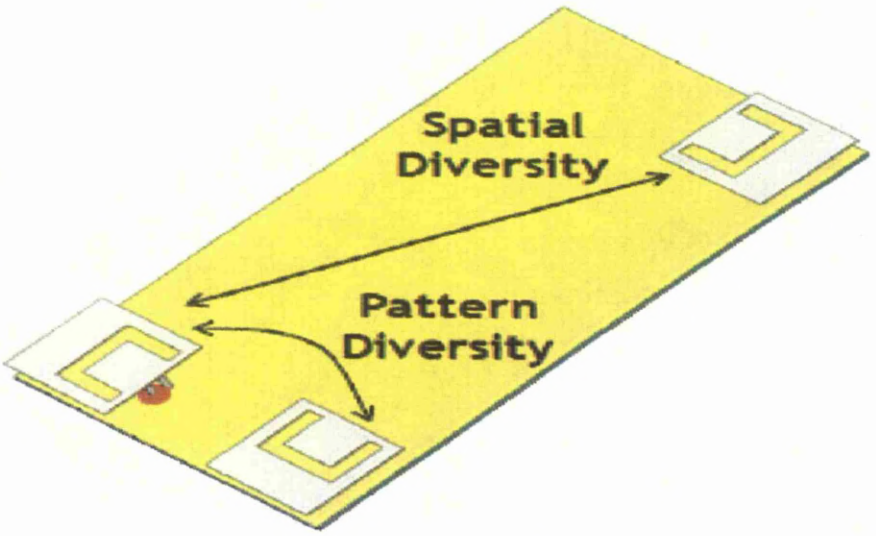

Fig. 5.11 Difference between space diversity and pattern diversity [CST]

5.3.6.1.3 Polarization Diversity

Polarization diversity can be achieved when two or more differently polarized antennas are used as the branches of a diversity receiver or transmitter. It has been reported by Lee and Yeh that the horizontal and vertical polarization paths between a mobile and a base station are uncorrelated [45]. A number of studies on polarization diversity have been carried out at the base stations [46-48]. Previously, spatial diversity has been widely used in base stations but the size of the antenna structures is too large. With the use of polarization diversity the size of the antenna structures can be reduced significantly. Early theoretical analysis has been undertaken to show that at the base station the largest diversity gain can be obtained when the two antennas are polarized at ± 45° where the vertical is used as a single reference [49-51].

Polarization diversity has emerged an attractive option to apply at the mobile terminals due to the reduced size of the antenna structures. Therefore,

recent studies on the MIMO systems have exploited the MIMO channels by using polarization diversity [52-53].

5.3.6.2 Time Diversity

The diversity can be obtained from single antenna by transmitting the signal multiple times, spaced apart in sufficiently that the channel fading is uncorrelated i.e. at least 0.5λ between antenna locations when the repeated signal is received. This is rarely used in practice, as the retransmission of information reduces the system capacity and introduces a transmission delay.

5.3.6.3 Frequency Diversity

If the two frequency components are spaced wider than the coherence bandwidth of the wideband channel, they experience uncorrelated fading providing another mean of obtaining diversity gain. However, as in time diversity the simple retransmission on two frequencies would be inefficient. That is why it is also rarely used.

References

[1] C. E. Shannon, "A Mathematical theory of communication", *Bell Syst. Tech.*, vol. 27, pp. 379-423, 623-656, July & Oct. 1948.

[2] T. S. Rappaport, *Wireless communications: principles and practice*, Prentice Hall, 2002.

[3] J. Proakis, *Digital communications*, McGraw-Hill 4th edition, 2000.

[4] J. Winters, "On the capacity of radio communication system with diversity in a Rayleigh fading environment", *IEEE Journal on Selected Areas in Communications*, vol. 5, no. 5, pp. 871-878, June 1987.

[5] G. J. Foschini, "Layered space-time architecture for wireless communication in a fading environment when using multi-element antennas," Bell Labs Tech J., vol. 1, no. 2, 41-59, 1996.

[6] G. J. Foschini and M. J. Gans, "On limits of wireless communications in a fading environment when using multiple antennas", *Wireless Personal Communications*, page(s): 311-335, March 1998.

[7] J. D. Parsons, *The mobile radio propagation channel*, New York Wiley, 2nd Edition, 2000.

[8] J. Kermoal, P. Mogensen, S. Jensen, J. Andersen, F. Frederiksen, T. Sorensen, and K. Pedersen, "Experimental investigation of multipath richness for multi-element transmit and receive antenna arrays", *IEEE 51st Vehicular Technology Conference*, vol. 3, pp. 2004-2008, May 2000.

[9] J. Kermoal, L. Schumacher, K. Pedersen, P. Mogensen, and F. Frederiksen, "A stochastic MIMO radio channel model with experimental validations", *IEEE Journal on Selected Areas in Communications*, vol. 20, no. 6, pp. 1211-1226, August 2002.

[10] J. P. Kermoal, "Measurement, modelling and performance evaluation of the MIMO radio channel," in A thesis of Aalborg University for the degree of Doctor of Philosophy, August 2002.

[11] 3GPP, URL: http://www.3gpp.org

[12] IST-IMETRA, URL: http://www.ist-imetra.org

[13] I. E. Telatar, "Capacity of multi-antenna Gaussian channels", *European Transaction on Telecommunications*, vol. 10, no. 6, pp. 585-595, November 1999.

[14] G. G. Raleigh and J. M. Cioffi, "Spatio-temporal coding for wireless communications", *IEEE Trans Communication*, vol. 46, pp. 357-366, March 1998.

[15] A. J. Paulraj, D. A. Gore, R. U. Nabar and H. Bolcskei, "An overview of MIMO communications-a key to gigabit wireless", *Proceedings of the IEEE*, vol. 92, no. 2, pp. 198-218, February 2004.

[16] H. Bölcskei, D. Gesbert and A. J. Paulraj, "On the capacity of OFDM-based spatial multiplexing systems", *IEEE Trans. Commun.*, vol. 50, pp. 225-234, Feb. 2002.

[17] R. J. Piechocki, P. N. Fletcher, A. R. Nix, C. N. Canagarajah and J. P. McGeehan, "Performance evaluation of BLAST-OFDM enhanced hiperlan/2 using simulated and measured channel data", *Electronics Letters*, vol. 37, no. 18, pp. 1947- 1951, August 2001.

[18] J. W. Wallace and M. A. Jensen, "MIMO capacity variation with SNR and multipath richness from full-wave indoor FDTD simulations," IEEE Antenna and Propagation Society International Symposium, vol. 2, pp. 523-526, June 2003.

[19] A. F. Molish and M. Z. Wi, "MIMO system with antenna selection- An overview", copyright Mitsubishi Electric Research Laboratories, Inc., 2004.

[20] D. Gesbert, M. Shafi, D. Shan, P. J. Smith and A. Naguib, "An overview of MIMO space-time coded wireless systems", *IEEE Journal on selected Areas in Communications*, vol. 21, no. 3, April 2003.

[21] N. Seshadri and J. Winters, "Two signaling schemes for improving the error performance of frequency-division-duplex (FDD) transmission system using transmitter antenna diversity", *Int. J. Wireless Inform. Networks*, vol. 1, no. 1, pp. 49-60, Jan. 1994.

[22] S. M. Alamouti, "A simple transmit diversity technique for wireless communications", *IEEE J. Select Area Commun.*, vol. 16, pp. 1451-1458, Oct. 1998.

[23] D. Chizik, G. J. Foschini, M. J. Gans and R. A. Valenzuela, "Keyholes, correlation, and capacities of multi-element transmit and receive antennas", *IEEE transaction on wireless communications*, vol. 1, no. 2, pp. 361-368, April 2002.

[24] D. Shiu, G. J. Foschini, M. J. Gans and J. M. Kahn, " Fading correlation and its effect on the capacity of multielement antenna systems", *IEEE transaction on communications*, vol. 48, no. 3, pp. 502-513, March 2000.

[25] S. R. Saunder and A. A. Zavala, *Antennas and propagation for wireless communication systems*, 2nd Edition, John Wiley & Sons Ltd, 2007.

[26] M. Tarkiainen and T. Westman, "Predictive switched diversity for slow speed mobile terminals", *IEEE Vehicular Technology Conference*, vol. 3, pp. 2042-2044, May 1997.

[27] P. S. Kildal, K. Rosengren, J. Byun and J. Lee, "Definition of effective diversity gain and how to measure it in a reverberation chamber", *Microwave & Optical Technology Letters,* vol. 34, no. 1, pp 56-59, July 5, 2002.

[28] B.M Green, M.A Jensen, "Diversity performance of dual antenna handsets near operator tissue", *IEEE Trans. Antennas & Propagation,* vol. 48, No 7, pp 1017-1023, 2000.

[29] P. Hallbjörner, K. Madsén, "Terminal antenna diversity characterization using mode stirred chamber", *Electronics Letters,* vol. 37, no. 5, pp 273-274, March 2001.

[30] Stephan J. Boyes, University of Liverpool (Private communication).

[31] K. Rosengren, P. S. Kildal, "Radiation efficiency, correlation, diversity gain, and capacity of a six-monopole antenna array for a MIMO system: theory, simulation and measurement in reverberation chamber", *IEE Proc. Microwaves Antennas & Propagation,* vol. 15, pp 7-16, 2005.

[32] C. B. Dietrich, K. Dietze, J. R. Nealy, W. L. Stutzmann, "Spatial, polarization and pattern diversity for wireless handheld terminals", *IEEE Trans. Antennas & Propagation,* vol. 49, no. 9, pp. 1271-1281, 2001.

[33] J. S. Colburn, Y. R. Samii, M. A. Jensen and G. J. Pottie, "Evaluation of personal communications dual-antenna handset diversity performance", *IEEE Trans. On Vehicular Technology*, vol. 47, no. 3, pp. 737-746, August 1998.

[34] F. Adachi, M. T. Feeney, A. G. Willianson and J. D. Parsons, "Cross correlation between the envelopes of 900 MHz signals received at a mobile radio base station site", *IEE Proceedings Radar and Signal Processing*, vol. 133, no. 6, pp. 506-512, October 1986.

[35] G. F. Pedersen and J. B. Andersen, "Handset antennas for mobile communications, integration, diversity and performance", *URSI Review of Radio Science*, pp. 119-139, 1996.

[36] S. C. K. Ko and R. D. Murch, "Compact integrated diversity antenna for wireless communications", *IEEE Transaction on Antenna and Propagation*, vol. 49, no. 6, June 2001.

[37] R. G. Vaughan and J. B. Anderson, "Antenna diversity in mobile communications", *IEEE Trans. Vehicular Technology*, vol. VT-36, pp. 147-172, November 1987.

[38] S. Blanch, J. Romeu and I. Cotbella, "Exact representation of antenna system diversity performance from input parameter description", *ELECTRONICS LETTERS*, vol. 39, no. 9, May 1, 2003

[39] T. Taga, "Analysis for mean effective gain of mobile antennas in land mobile radio environments", *IEEE Transaction on Vehicular Technology,* vol. 39, page(s): 117-131, 1990.

[40] V. Jungnukel, V. Pohl and C. V. Helmolt, "Capacity of MIMO systems with closely spaced antennas", *IEEE Communications Letters*, vol. 7, no. 8, Aug. 2003.

[41] R. G. Vaughan, "Pattern translation and rotation in uncorrelated source distributions for multiple beam antenna design", *IEEE Trans. on Antennas and propagation*, vol. 46, no. 7, pp. 982-990, July 1998.

[42] P. L. Penry, C. L. Holloway, "Angle and space diversity comparison in different mobile radio environments", *IEEE Trans. on Antennas and Propagation*, vol. 46, no. 6, June 1998.

[43] R. G. Vaughan, "Switched parasitic elements for antenna diversity", *IEEE Trans. on Antennas and Propagation*, vol. 47, no. 2, pp. 399-405, Feb. 1999.

[44] L. Dong, H. Ling, and R. W. Heath, "Multiple-input multiple output wireless communication systems using antenna pattern diversity," *IEEE Global Telecommunications Conference*, vol. 1, page(s): 997-1001, November 2002.

[45] W. C. Y. Lee and Y. S. Yeh, "Polarization diversity system for mobile radio", *IEEE Trans. Commun.*, vol. COM-20, no. 5, pp. 912-923, 1972.

[46] A. M. D. Turkmani, A. A. Arowojolu, P. A. Jefford and C. J. Kellett, "An experimental evaluation of the performance of two-branch space and polarization

diversity schemes at 1800MHz", *IEEE Trans. on Vehicular Technology*, vol. 44, no. 2, pp. 318-326, May 1995.

[47] K. Cho, T. Hori and K. Kagoshima, "Effectiveness of four-branch height and polarization diversity configuration for street microcell", *IEEE Trans. on Antenna and Propagation*, vol. 46, no. 6, pp. 776-781, June 1998.

[48] C. Beckman, U. Wahlberg, "Antenna system for polarisation diversity", Microwave Journal, page(s): 330-334, May 1997.

[49] R. G. Vaughan, "Polarisation diversity in mobile communications", *IEEE Trans Vech. Tech.*, vol. 30, no. 3, pp. 177-186, August 1990.

[50] S. Kozono, T. Tsuruhara and M. Sakamoto, "Base station polarization diversity reception for mobile radio", *IEEE Trans. Vehicular Tech.*, vol. 33, no. 4, pp. 301- 306, November 1984.

[51] P. C. F. Eggers, J. Toftgard and A. M. Opera, "Antenna systems for base station diversity in urban small and micro cells", *IEEE Journal on Selected Area in Communications*, vol. 11, no. 7, pp. 1046-1057, Sept. 1994.

[52] J. P. Kermoal, L. Schumacher, F. Frederiksen and P. E. Mogensen, "Polarization diversity in MIMO radio channels: experimental validation of a stochastic model and performance assessment," IEEE 54th Vehicular Technology Conference, vol. 1, pp. 22-26, 2001.

[53] M. J. Fakhereddin and K. R. Dandekar, "Combined effect of polarization diversity and mutual coupling on MIMO capacity," *IEEE International Symposium Antennas and Propagation Society*, vol. 2, page(s): 495-498, 22-27 June 2003.

CHAPTER

6

PIFA as a MIMO and Diversity Antenna

6.1 Introduction

The future wireless communications systems will be expected to support a wide range of high-quality services which may include data, high-quality voice, pictures, and video. These services are likely to include applications which require very high transmission data rates. A growing literature on both antenna diversity and multiple input multiple output (MIMO) systems has emerged owing to their ability to combat multipath fading and to deliver higher data rates, respectively [1-4]. In a MIMO system, several transmitters and receivers are used at each end of the radio link, and, in order to achieve a high capacity, the different signal paths between these should be uncorrelated. There are wide research and development efforts into diversity antennas for MIMO wireless communication terminals [5-7]. The essential requirements for the diversity antennas are that they must provide diverse reception, i.e. they must be capable of receiving different signals. Antenna diversity can be realized in several ways. Depending on the environment and the expected interference, designers can employ one or more of

these methods to achieve diversity gain. The most popular and effective diversity techniques include spatial, polarization and pattern diversity. Spatial diversity employs multiple antennas, usually with the same characteristics, that are physically separated from one another. Depending upon the expected incidence of the incoming signal, sometimes a space on the order of a wavelength is sufficient. Typical antennas include PIFA antennas [8-10], double folded dipole [11] and folded monopole antennas [12].

But it is quite challenging and hard to implement multiple antennas on very small devices such as mobiles, PDAs and laptops as placing multiple antenna elements increase mutual coupling and result in high correlation coefficient. Pattern diversity consists of two or more co-located antennas having different radiation patterns or a single antenna with two or more ports which differ from each other in terms of their radiation patterns. Isolated mode antenna technology (IMAT) is recently being introduced by Skycross in which a single antenna having dual or more feeds can be used to achieve diversity gain by exciting different modes for MIMO applications [13-14]. Similarly, a single element dual-feed monopole antenna is introduced by P. Hallbjoner in [15]. As we know that the inverted F antenna is now widely used in mobile and portable applications due to its simple design, lightweight, low-cost, conformal nature, attractive radiation pattern and reliable performance [16-18], there is a need to use this PIFA antenna to develop diversity antennas having two or more feeds/ports.

In this chapter, three new and novel dual-feed PIFA diversity antennas for different heights are presented taking into account pattern diversity and/or polarization diversity. In order to reduce the mutual coupling between the two ports and to increase the isolation; the portion of ground planes under the top radiating plate is modified and etched out. Here the designs of PIFA antennas for the 2.45 GHz Bluetooth/WLAN band are presented and can be used in mobile and PDA terminals as a diversity or MIMO antenna. The structures of these PIFA antennas can be modified to work for other similar frequency bands such as GSM, DCS, PCS and UMTS and 2.5 GHz- 2.7 GHz Long Term Evolution (LTE) band.

6.2 Isolation

The isolation between two antennas or two ports of a single antenna is a critical parameter in many applications and systems such as antenna arrays, diversity antennas and MIMO systems. If the two ports/antennas are strongly coupled then the most of the transmitted signal of one port/antenna will not be radiated but received/absorbed by the second port. It will decrease the antenna radiation efficiency due to the loss of the power dissipated in the coupled antenna or in the second port. So for the two ports/antennas to radiate efficiently, they should be sufficiently isolated and mutual coupling should be reduced to enable the two ports/antennas to radiate efficiently i.e. the S_{12} should be very small. In literature, different techniques have been introduced to increase isolation and reduce the mutual coupling between the two ports/antenna elements. In some techniques, ground plane is modified to increase isolation [19-21]. Some elements are introduced within the antenna elements to increase isolation such as mushroom-type composite right-/left handed transmission lines [22], inserting a suspended line between the PIFA's feedings and/or shorting points [23]. Similarly some decoupling networks are introduced in [24-25] to increase isolation.

6.3 Dual-Feed PIFA with Parallel Feed Plates for Height h = 10 mm

6.3.1 Antenna Configuration

The configuration of the dual-feed PIFA is shown in Fig. 6.1. The radiating top plate has dimensions $W \times L$ and ground plane dimensions are $W_g \times L_g$. The dielectric material used between the rectangular ground plane and the two feeds is FR-4 having a thickness t = 1.5 mm and relative permittivity ε_r = 4.4. The antenna height h is filled with air (free space). In practice, a low dielectric material may be used to support the top plate. The shorting plate has dimensions $W_s \times (h+t)$ and the widths of feed plates 1 and 2 are W_{f1} and W_{f2} respectively and both feed plates have height h. The horizontal distances of feed 1 and feed 2 from the side edge of the ground plane are L_{f1} and L_{f2} respectively and distance of feed 2 from

the upper edge of the top plate is L_u (as shown in Fig. 6.1). The PIFA antenna is fed by coaxial cables through 2 SMA connectors connected to Port 1 and Port 2. The software package used for simulation is Ansoft's High Frequency Structure Simulator (HFSS) based on the Finite Element Method.

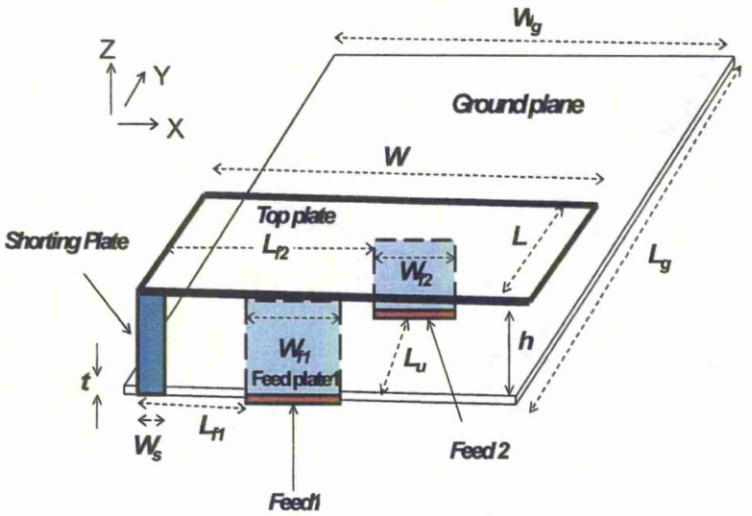

Fig. 6.1 The configuration of the dual feed PIFA antenna

Since there are many variables which can affect the antenna performance, it is challenging to obtain an optimized design. Computer aided parametric study has been conducted. The design of PIFA antenna is started initially from our work of bandwidth enhancement of PIFA by changing the widths of feed and shorting plates in which it was shown that increasing the feed plate and minimizing the width of shorting plate would result in 65% fractional bandwidth [26]. Then another feed plate of width W_{f2} is added to make this PIFA antenna a dual-feed antenna. The length of ground plane L_g is taken equal to 100 mm to make it of the same length as that of a handset mobile. A parametric study is undertaken by varying the widths of feed plate1 and feed plate 2 and position of both these feed plates under the top plate. The parameters are optimized to get the maximum bandwidth by both the ports. The optimized parameters are as follows: W_{f1}= *18 mm*, W_{f2} =*18 mm*, W_g = *40 mm*, L_g = *100 mm*, W = *40 mm*, L = *20 mm*, h = *5 mm*, W_s = *1 mm*, L_{f1} = *16 mm*, L_{f2} = *5 mm*, L_u = *17 mm* and t=*1mm*. The simulated results of this PIFA antenna are shown in Fig. 6.2. It can be observed

that the bandwidths obtained by this technique from the two ports are huge from about 0.9 GHz to 4.3 GHz and it covers all the frequency bands used now a day in mobile technology including GSM 900, PCS, DCS, UMTS, GPS, WLAN, WiMax and Bluetooth. But the problem in this design is that the transmission coefficient S_{12} is very high as can be seen from Fig. 6.2. In this case, as described earlier, the most of the signal transmitted by one of the ports will be received by the other port. So in order to make this design useful and efficient, some isolation technique must be implemented to reduce mutual coupling between the two ports. In order to identify how the ports are linked to each other, the current distribution is observed by HFSS simulations. Fig. 6.3 shows the current distribution on the top radiating plate and distribution of current on the ground plane of the antenna at 2.45 GHz at zero phases. It can be observed that most of the current flows on the ground plane. So as compared to the top plate, the two ports are found strongly linked through ground plane. So some modification of the ground plane between the two ports is required to stop the current flow from one port to the other.

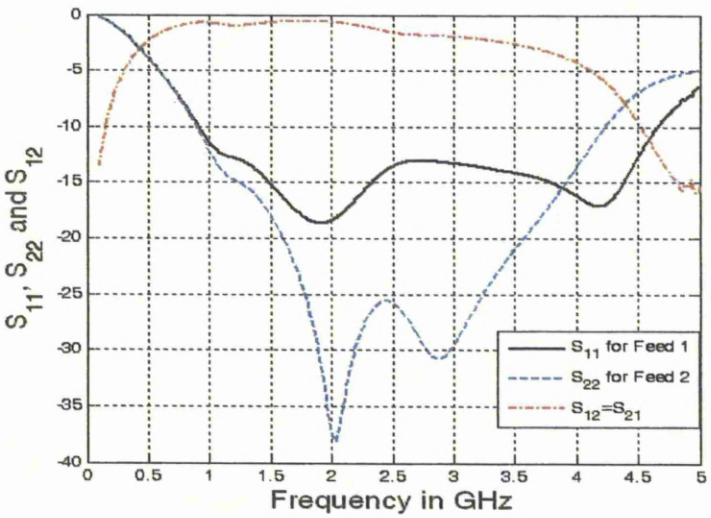

Fig. 6.2 Simulated S-parameters versus frequency in GHz

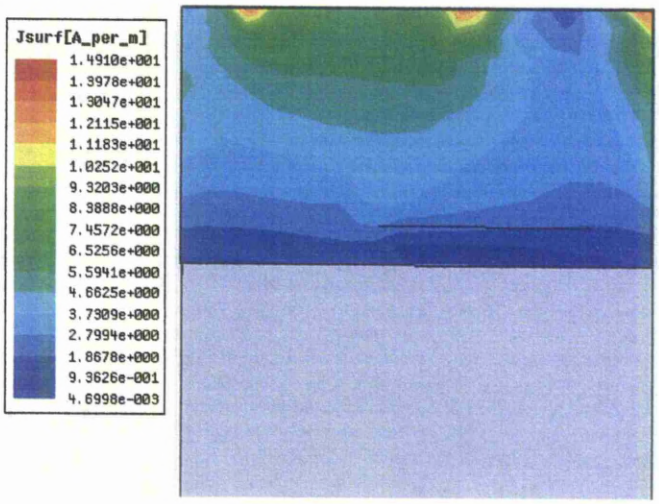

(a)

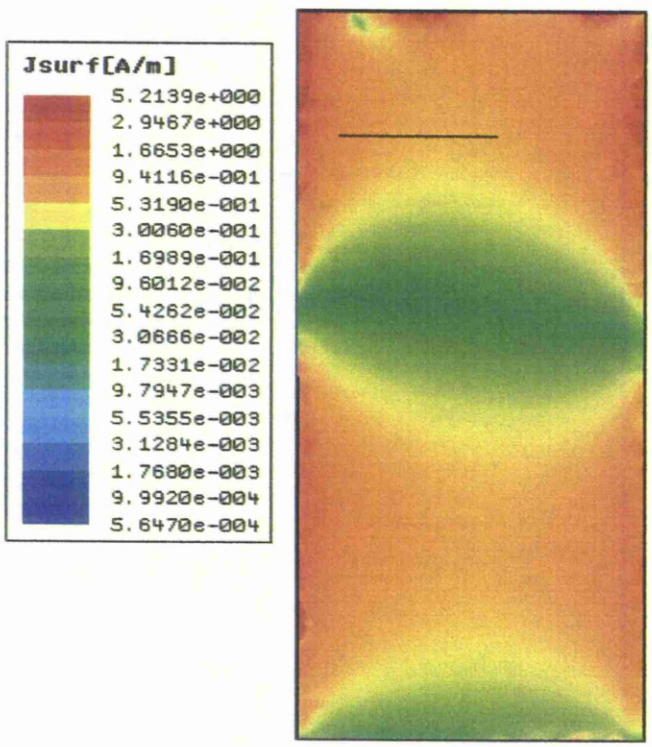

(b)

Fig. 6.3 Current distributions on (a) the top plate (b) the ground plane

Initially, the isolation technique described in [20] was implemented in which the ground plane between the two PIFA antenna elements was modified to reduce mutual coupling between the two antennas. The mutual coupling was reduced by only 1.5 dB, so ground plane is further modified through etching the

ground plane. Fig. 6.4 shows the different modifications on the ground plane between the two ports undertaken to reduce the mutual coupling. All these modifications showed reduction in mutual coupling but found not enough to achieve isolation about 10 dB. So in order to reduce the mutual coupling and to increase the isolation between the two ports, the ground plane under the top plate is amended by removing most of the conductor to reduce the current flow on the ground plane between the two ports. The bottom view of the final design of etched ground plane is shown in Fig. 6.5. The length of the etched part of the ground plane is S_{ug} *=17 mm*. The two parts of the ground plane are connected through a small strip of thickness S_x *=1 mm*. The thickness of the upper part of the ground plane to which port1 and the shorting plate are connected is also a small strip of thickness S_y *= 1 mm*. Fig. 6.6 shows the mutual coupling S_{12} with and without etching the ground plane which shows that more than 8 dB (simulated) improvement in isolation between the two ports is achieved by using this technique of etching the ground plane.

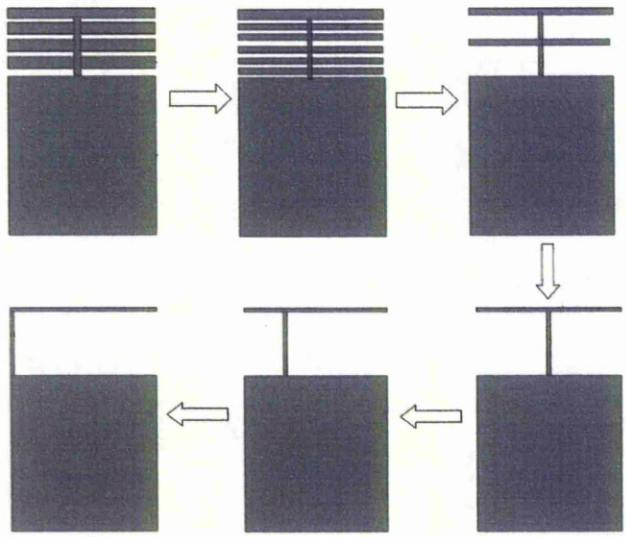

Fig. 6.4 Modifications on the ground plane between the two ports

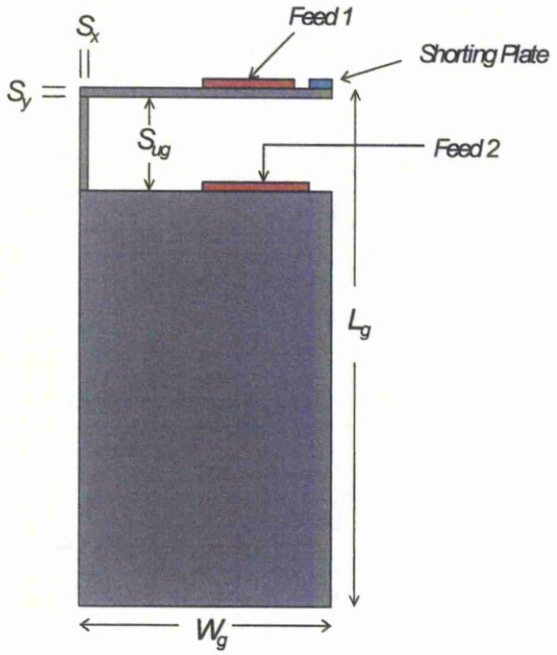

Fig. 6.5 The bottom view of the modified ground plane

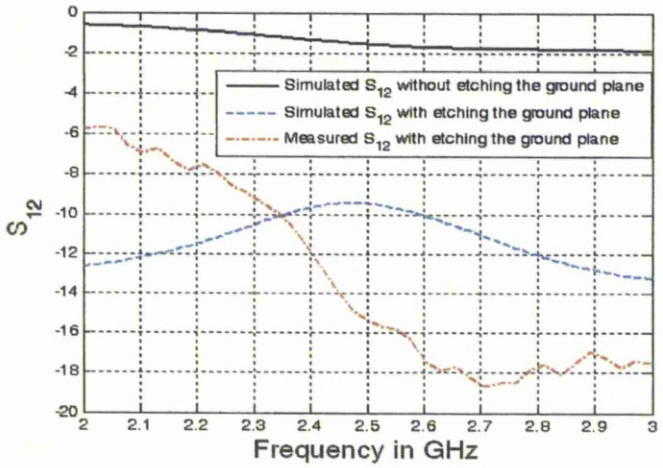

Fig. 6.6 S_{12} with and without modifying the ground plane

6.3.2 Simulated and Experimental Results

Again a parametric study is undertaken, in order to get the resonance at 2.45 GHz, by varying the widths of feed plate1 and feed plate 2 and positions of both these feed plates under the top plate while all other parameters are held fixed. The optimized parameters of this dual-feed PIFA antenna obtained for 2.45 GHz

WLAN applications are as follows: W_{f1}= *14 mm*, W_{f2} =*20 mm*, W_g = *40 mm*, L_g = *100 mm*, W = *40 mm*, L = *20 mm*, h =*10 mm*, W_s = *1 mm*, L_{f1} = *2 mm*, L_{f2} = *4 mm and* L_u = *19 mm*. The simulated and experimental results are shown in Fig. 6.7. If we compare these results with that of Fig. 6.2, it can be observed that bandwidth is much reduced now. This is due the modifications done in the ground plane to increase isolation. This is a drawback of etching the ground plane. Simulated and measured results of Fig. 6.7 are little different. The major courses for the discrepancies are (a). the cables: which are not included in the simulation but presented in the measurements; (b). the connectors: which are also not considered in the simulation; (c) The inaccuracy of the parameters in manufacturing this PIFA antenna as it is made manually in the lab. It is evident that both the branches of the antenna cover the 2.45 GHz WLAN band from 2.35 GHz to 2.55 GHz having at least a bandwidth of 200 MHz for S_{11} < *-10 dB*. The average percentage radiation efficiency of this antenna is found around 90%. The 3D simulated radiation pattern of this dual-feed PIFA with Port 1 and Port 2 alone are shown in Figs. 6.8 and 6.9 and the 2D polar plots of the measured radiation patterns of this antenna for the feed 1 and feed 2 at 2.5 GHz are shown in Fig. 6.10. It can be observed that radiation pattern of the two ports are comparatively different enough to achieve pattern diversity.

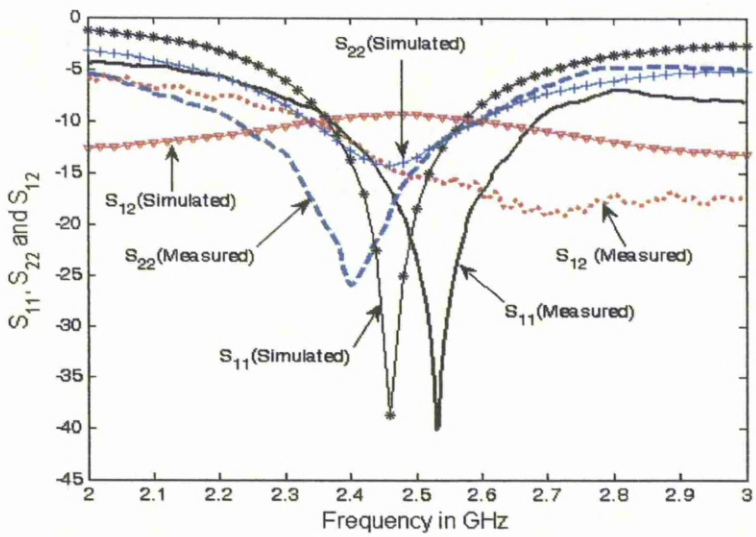

Fig. 6.7 Measured and simulated S-parameters versus frequency in GHz

Now in order to achieve a good diversity gain, this antenna must satisfy the conditions described in Eq. 5.15 in the previous chapter. Fig. 6.11 shows the graph of the envelope-correlation coefficient versus frequency in GHz. The envelope-correlation coefficients are calculated from S-parameters [29]. It is clear from the graph that maximum value of envelope correlation coefficient is below 0.04 in the region of interest. The MEGs of the two branches of the antenna are 0.56 and 0.50 and their ratio is approximately equal to unity i.e. 0.56/0.50 ≅ 1. So this antenna satisfies the two conditions of achieving a good diversity gain. Hence this single element dual-feed PIFA antenna can be used for diversity or MIMO applications.

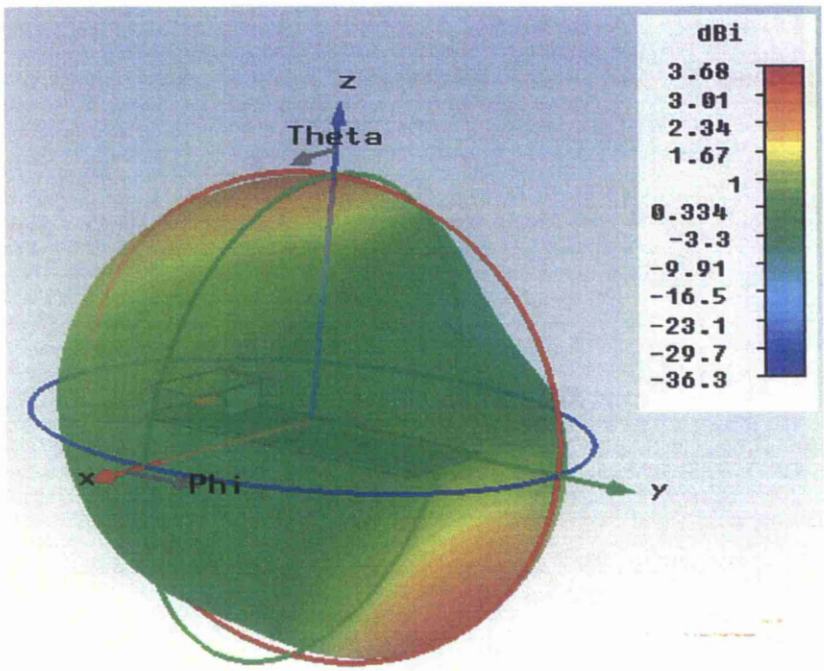

Fig. 6.8 3D simulated radiation pattern of dual-feed PIFA with Port 1 at 2.45 GHz

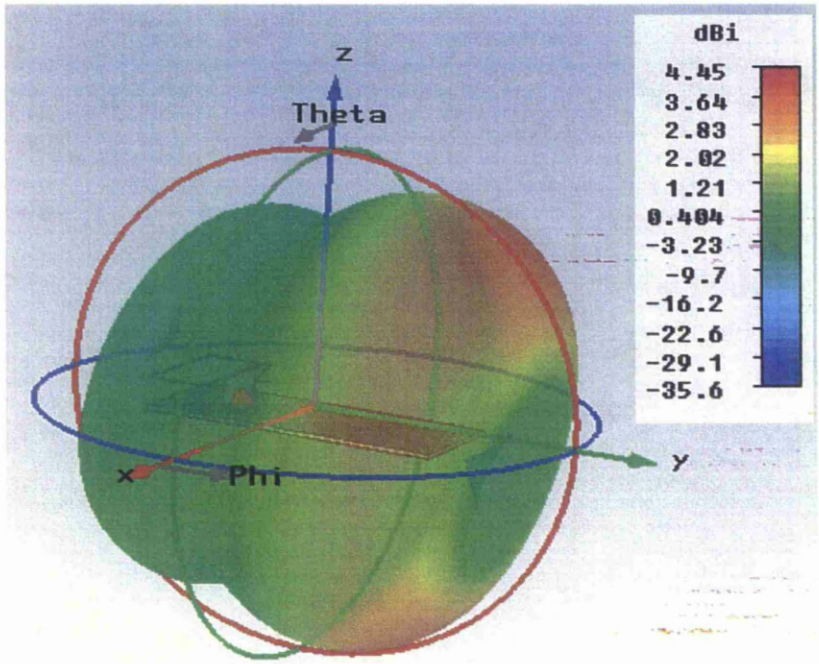

Fig. 6.9 3D simulated radiation pattern of dual-feed PIFA with Port 2 at 2.45 GHz

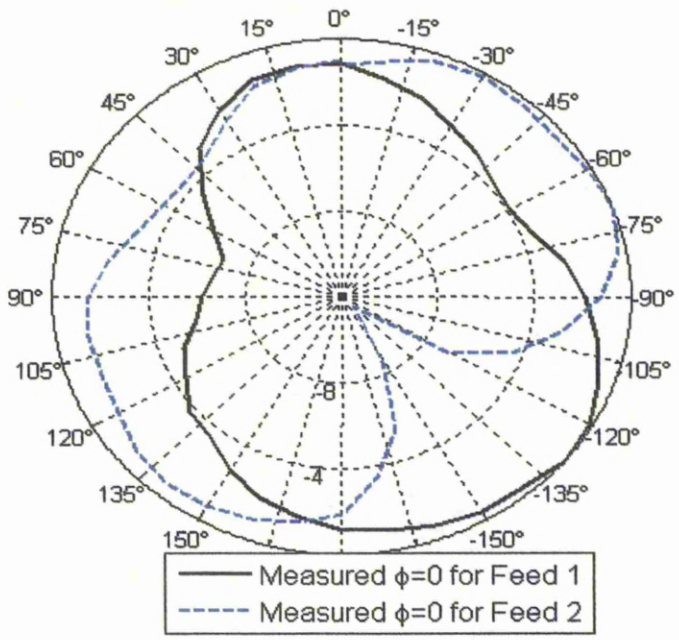

(a) XZ ($\Phi = 0°$) plane

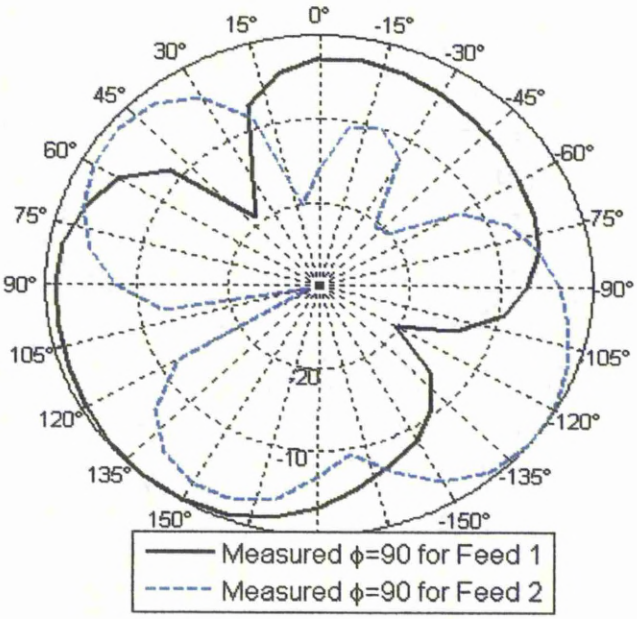

(b) YZ ($\Phi = 90°$) plane

Fig. 6.10 2D measured radiation patterns in dB scale for feed 1 and feed 2 at 2.5 GHz for different planes

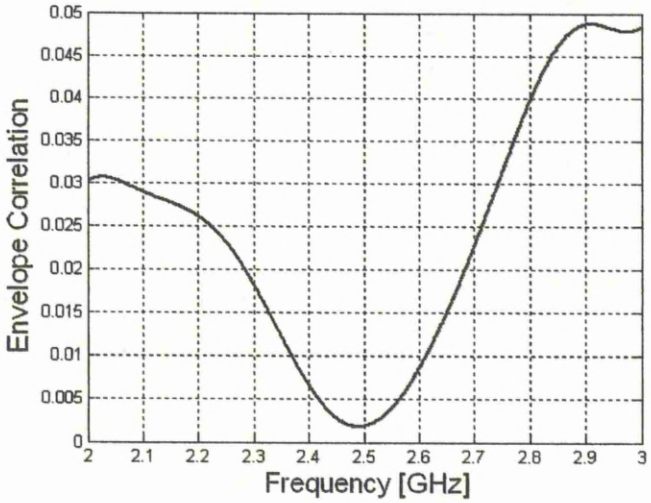

Fig. 6.11 Envelope-correlation coefficient versus frequency in GHz

6.3.3 Theory Behind the Design

Fig. 6.12 shows the current distributions on the ground plane due to the Ports 1 and 2 at 2.45 GHz. It can be seen that current due to the port 1 is minimal whereas the current density on the ground plane due to the Port 2 is high. It is

evident that the dimension of ground plane greatly affects the resonant frequency of Port 2, thus it can be concluded that Port 2 uses ground plane as well as the top plate as the radiating element. So diversity is achieved due to the fact that Port 1 has top plate as the only radiating element whereas the Port 2 is using the top plate as well as the ground plane as the radiating elements. Thus the radiation patterns produced by the two ports are different and a good diversity gain is achieved through pattern diversity. According to theory of characteristic modes, diversity gain can be achieved by exciting different modes of the radiating portion of the antenna which will produce different radiation patterns [27-28]. Here two different modes are excited to achieve diversity gain.

The isolation between the two ports is achieved by introducing an anti resonant circuit of inductor and capacitor. Fig. 6.13 shows an approximate equivalent circuit of the PIFA antenna. The value of inductor L is adjusted by the small strip which connects the upper and lower part of the ground plane and the capacitance C is introduced between small upper strip and lower part of the ground plane and etched part of ground plane acts as a dielectric.

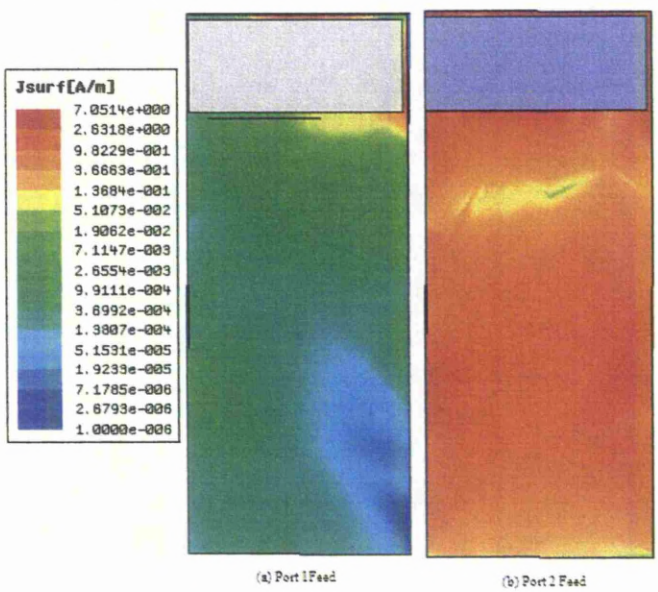

Fig. 6.12 Current distribution on the ground plane of PIFA due to Port 1 and Port 2 at 2.45 GHz

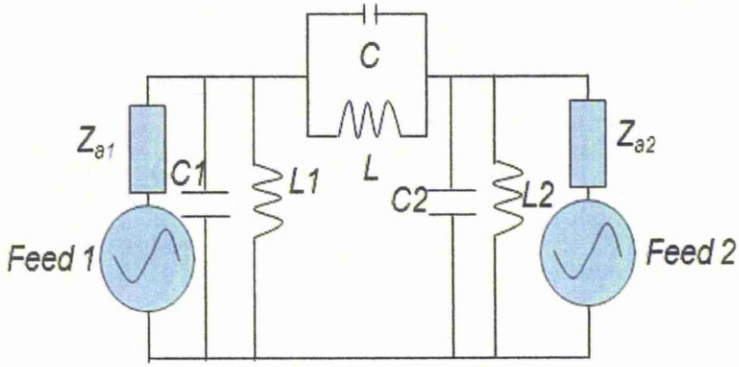

Fig. 6.13 An approximate equivalent circuit of the dual-feed PIFA

6.3.4 Parametric Study

The ground plane dimensions are varied to observe its effects on the resonant frequencies and bandwidth of ports 1 and 2. Fig. 6.14 shows the graphs of changing the length of ground plane versus the frequency in GHz for the Port 1 and Port 2. It can be seen that the resonant frequency of the Port 1 is not affected at all by the variation of length of ground plane whereas the resonant frequency and bandwidth for the Port 2 is greatly affected by the variation of ground plane. It is due to the fact that Port 1 is connected only through a small strip that is why there is no effect of changing the length of ground plane on the Port 1. The same resonant frequency and bandwidth from the Port 2 can be achieved by varying the width of second feed plate W_{f2} and the horizontal distance of feed plate 2 from the edge of the ground plane L_{f2}.

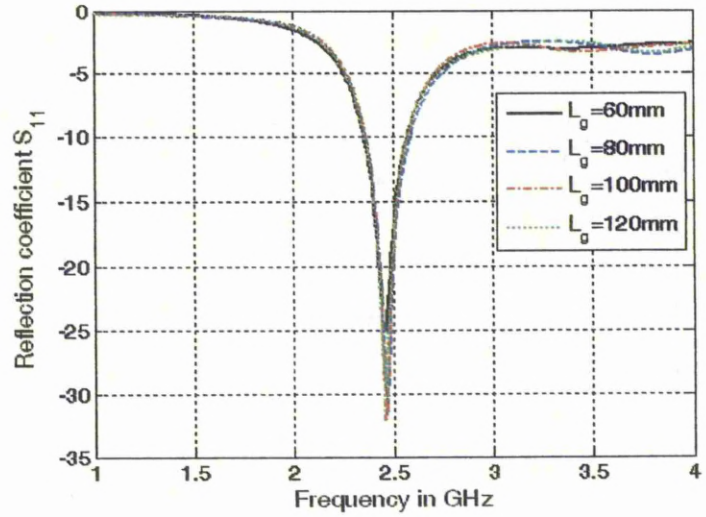

(a) S_{11}

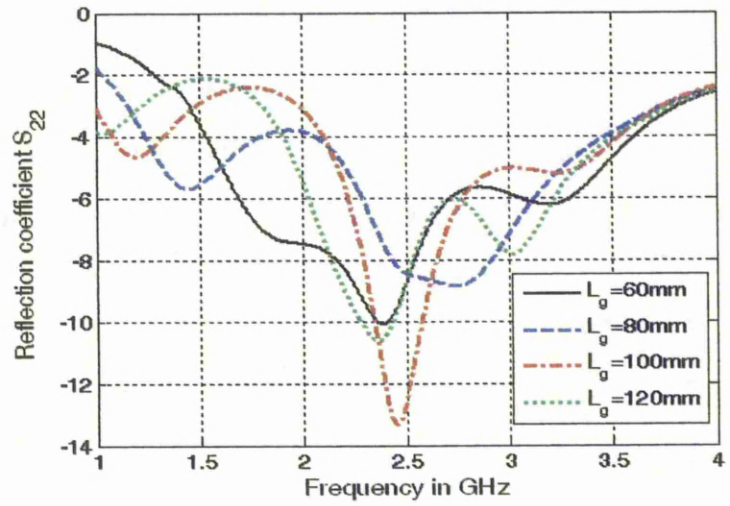

(b) S_{22}

Fig. 6.14 Reflection coefficients versus frequency in GHz for different values of L_g

The position of feed plate 1 is varied to observe its affects on the reflection coefficients S_{11} and S_{22} whereas all other parameters are held constant. Fig. 6.15 shows the reflection coefficients versus frequency in GHz for variations in position of feed plate 1. It is evident that by increasing the distance L_{f1} of feed plate 1 from the side edge of the ground plane, resonant frequency by Port 1 increases and impedance bandwidth is also changed. Changing the position of feed plate 1 also affects the reflection coefficient S_{22} which is mainly due to Port 2. It is due to the fact that the two feed plates are connected through the one common

radiating plate. So changing the position of one of the feed plate affects the reflection coefficient from the other feed as well as it changes the transmission coefficient S_{12} between the two feeds.

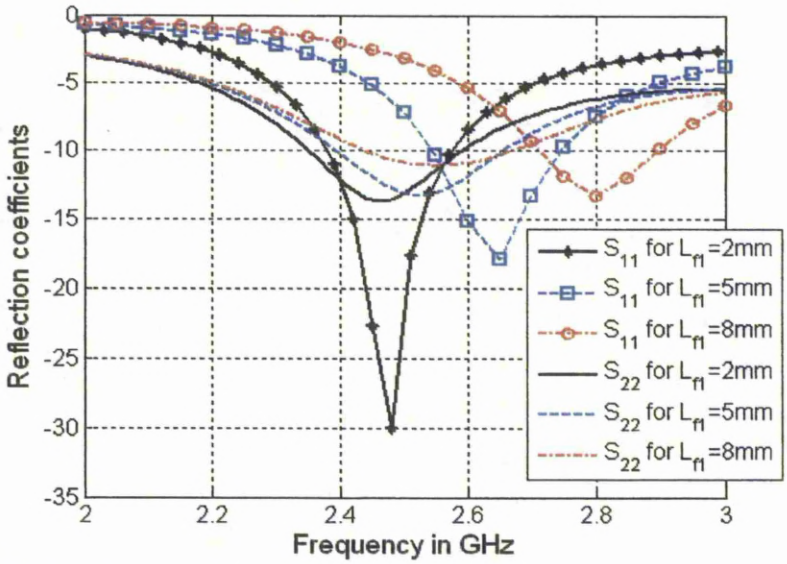

Fig. 6.15 Reflection coefficients S_{11} and S_{22} versus frequency in GHz for different values of L_{f1}

Similarly the width of feed plate 2 is varied to observe its affects on the reflection coefficients S_{11} and S_{22} whereas all other parameters are held constant. Fig. 6.16 shows the reflection coefficients versus frequency in GHz for variations in width of feed plate 2. It is evident that by increasing the width of feed plate 2 increases the resonant frequency from both the feeds and impedance bandwidth is also changed. Changing the width of feed plate 2 also affects the reflection coefficient S_{11} from the feed 1due the fact explained above. So changing the width of one of the feed plate affects the reflection coefficient from the other feed as well as it changes the transmission coefficient S_{12} between the two feeds.

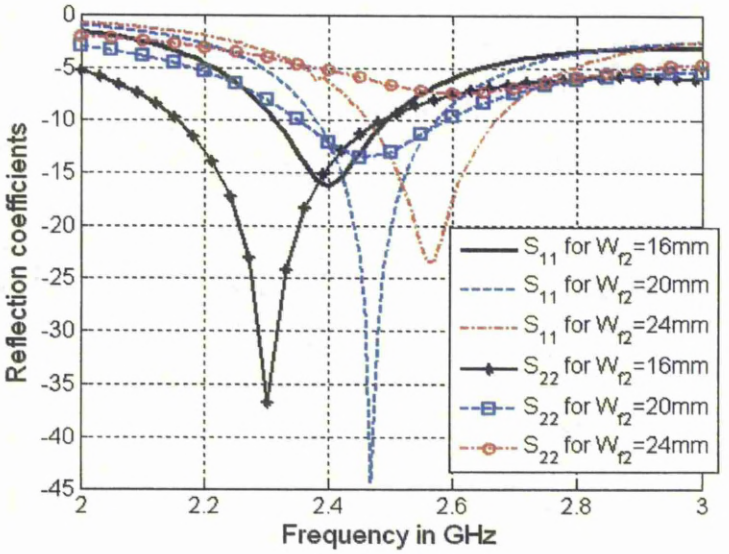

Fig. 6.16 Reflection coefficients S_{11} and S_{22} versus frequency in GHz for different values of W_{f2}

So the positions and widths of feed plates 1 and 2 need to be adjusted simultaneously for an optimized design for the required resonant frequency. This parametric study also shows that the design parameters can also be easily tuned for Long Term Evolution (LTE) 2.5 GHz-2.7 GHz band.

6.3.5 Diversity Gain Measurement

The diversity gain of the dual-feed PIFA with parallel feed plates is measured in a reverberation chamber. The measurement utilizes the reverberation chamber at the University of Liverpool. The diversity gain result for the dual-feed PIFA with parallel plates is shown in Fig. 6.18. From the plot, we can see that the diversity gain of dual-feed PIFA with parallel feed plates (co-polarized) equates to around 9 dB.

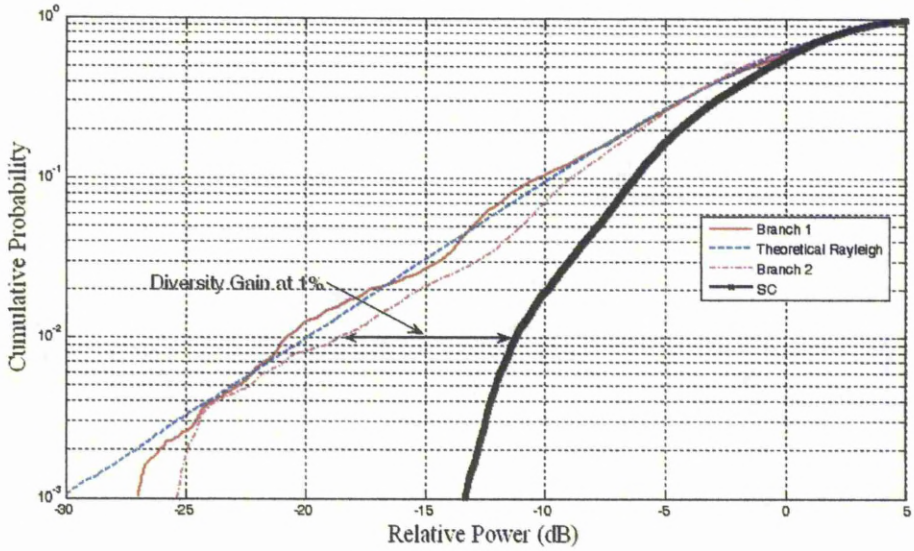

Fig. 6.17 Measured diversity gain of dual-feed PIFA with parallel feed plates

6.4 Dual-Feed PIFA with Perpendicular Feed Plates for Height h = 10 mm

The dual-feed PIFA antenna with two feed plates placed parallel to each other, as discussed above, uses only the pattern diversity to achieve diversity gain. Also the simulated S_{12} is around 10 dB as shown in Fig. 6.8. Here we present another novel dual-feed PIFA diversity antenna taking into account pattern diversity as well as the polarization diversity as the feed plates are now placed perpendicular to each other which give rise to cross polarization. Due to the two diversity techniques, diversity gain as well as the isolation between the two ports is high as compared to the antenna design discussed above. The ground plane under the main top radiating plate is modified and etched out to increase the isolation between the two ports. This PIFA antenna can cover WLAN / Wi-Fi 2.4 GHz - 2.6 GHz band or Long Term Evolution (LTE) 2.5 GHz - 2.7 GHz band and can be used in mobile and PDA terminals as a diversity or MIMO antenna.

6.4.1 Antenna Configuration

The configuration of the dual-feed PIFA is shown in Fig. 6.18. The radiating top plate has dimensions $W \times L$ and ground plane dimensions are $W_g \times L_g$.

The dielectric material used between the rectangular ground plane and the two feeds is FR-4 having a thickness t = 1.5 mm and relative permittivity ε_r = 4.4. The antenna height h is filled with air (free space). In practice, a low dielectric material may be used to support the top plate. The shorting plate has dimensions $W_s \times (h+t)$ and the widths of feed plates 1 and 2 are W_{f1} and W_{f2} respectively and both feed plates have height h. The horizontal distances of feed 1 and feed 2 from the side edge of the ground plane are L_{f1} and L_{f2} respectively and distance of feed 2 from the upper edge of the top plate is L_u. The bottom view of the modified ground plane is shown in Fig. 6.19. The ground plane is modified to improve the isolation as the two ports are strongly connected through ground plane and most of the current flows on the ground plane between the two ports as discussed in [30]. The length of the etched part of the ground plane is S_{ug}. The two parts of the ground plane are connected through a small strip of thickness S_x. The thickness of the upper part of the ground plane which is connected to shorting plate is S_y. The ground plane is extended near to that side end of ground plane where the shorting plate is placed. The distance of this extended part of the ground plane from this side end is D_c. The vertical length of this extended ground plane is equal to the width of feed plate 1 i-e W_{f1} and its thickness (width) is equal to D_x. The idea here is to introduce anti-resonance at the operational frequency 2.45 GHz between the 2 feeds – to isolate them and hence to generate the desired diversity. The PIFA antenna is fed by coaxial cables through 2 SMA connectors connected to Port 1 and Port 2.

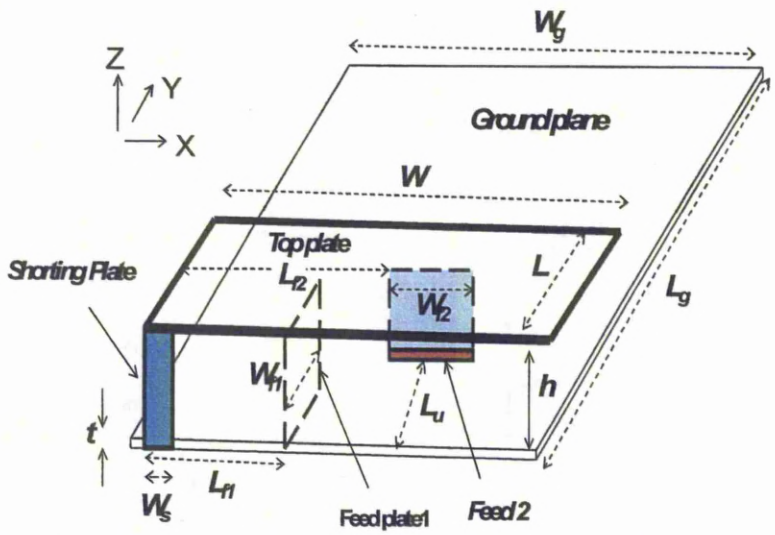

Fig. 6.18 The configuration of the dual-feed PIFA antenna with perpendicular feed plates

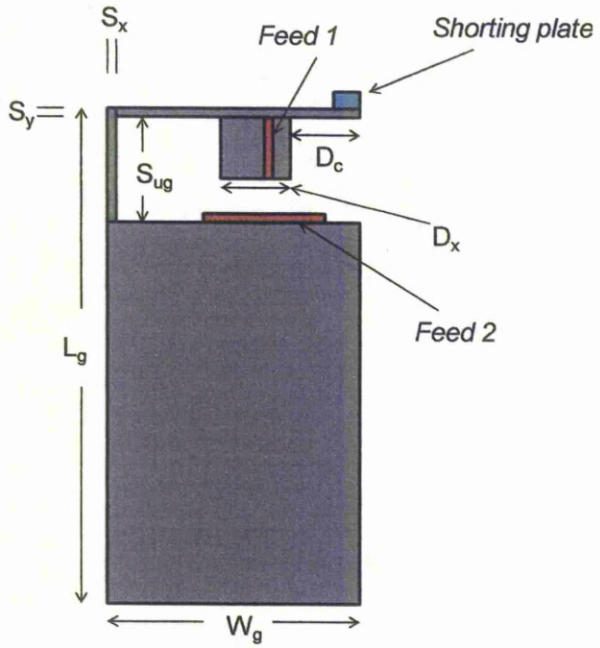

Fig. 6.19 The bottom view of the modified ground plane of the antenna

6.4.2 Simulated and Experimental Results

There are many variables which affect the PIFA antenna characteristics. In order to get the optimized design for 2.45 GHz band, some parameters are held fixed while other are varied by conducting a parametric study.

The height of PIFA, dimensions of top plate and ground plane and width of shorting plate are held fixed as follows. $W_g = 40$ *mm*, $L_g = 100$ *mm*, $W = 40$ *mm*, $L = 20$ *mm*, $h = 10$ *mm*, $W_s = 1$ *mm*, whereas the placements/positions of both feed plates L_{f1}, L_{f2} and widths of these feed plates W_{f1}, W_{f2} need to be adjusted through a parametric study to optimize these parameters. Theses parameters can also be optimized by the parametric study for LTE band from 2.5 GHz to 2.7 GHz. The remaining optimized parameters of this dual-feed PIFA antenna for 2.45 GHz WLAN band as follows: $W_{f1} = 10$ *mm*, $W_{f2} = 16$ *mm*, $L_{f1} = 11$ *mm*, $L_{f2} = 10$ *mm*, $L_u = 19$ *mm*, $S_{ug} = 17$ *mm*, $S_y = S_x = 0.5$ *mm*, $D_c = 10$ *mm* and $D_x = 5$ *mm*. The simulated and experimental results are shown in Figs. 6.20 and 6.21. The simulated and measured results are very similar. The major courses for their differences are (a) the cables: which are not included in the simulation but presented in the measurements; b) the connector: which is also not considered in the simulation; (c) The inaccuracy of exact parameters in manufacturing the PIFA as it is made manually in the lab. It is clear from the figures that both the Ports at least cover the 2.45 GHz WLAN band from 2.4 GHz to 2.6 GHz. The 3D simulated radiation pattern of this dual-feed PIFA with Port 1 and Port 2 alone are shown in Figs. 6.22 and 6.23 respectively and the 2D polar plots of the measured radiation pattern of this dual feed PIFA is shown in Fig. 6.24. It is evident that the radiation patterns by the two Ports are quite different which shows pattern diversity is present between the two Ports of the antenna. Fig. 6.25 shows the current distributions on the ground plane due to the Ports 1 and 2. It can be seen that current due to the port 1 is minimal whereas the current density on the ground plane due to the Port 2 is comparatively high. So diversity is achieved due to the fact that Port 1 has top plate as the only radiating element whereas the Port 2 is using the top plate as well as the ground plane as the radiating elements. This dual-feed also fulfils the two condition described in Eq. 5.15 which is also clear from the graph of correlation coefficient versus frequency in Fig. 6.26.

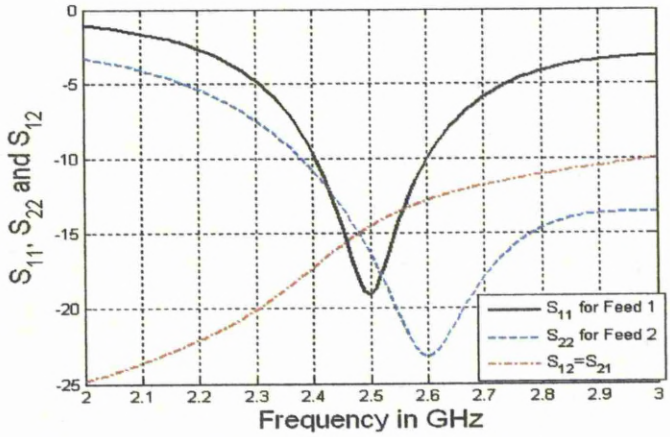

Fig. 6.20 Simulated S_{11}, S_{12} and S_{22} versus frequency in GHz

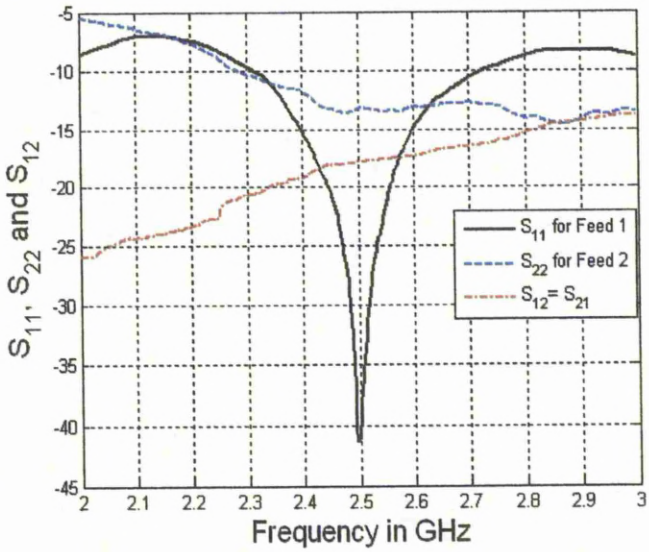

Fig. 6.21 Measured S_{11}, S_{12} and S_{22} versus frequency in GHz

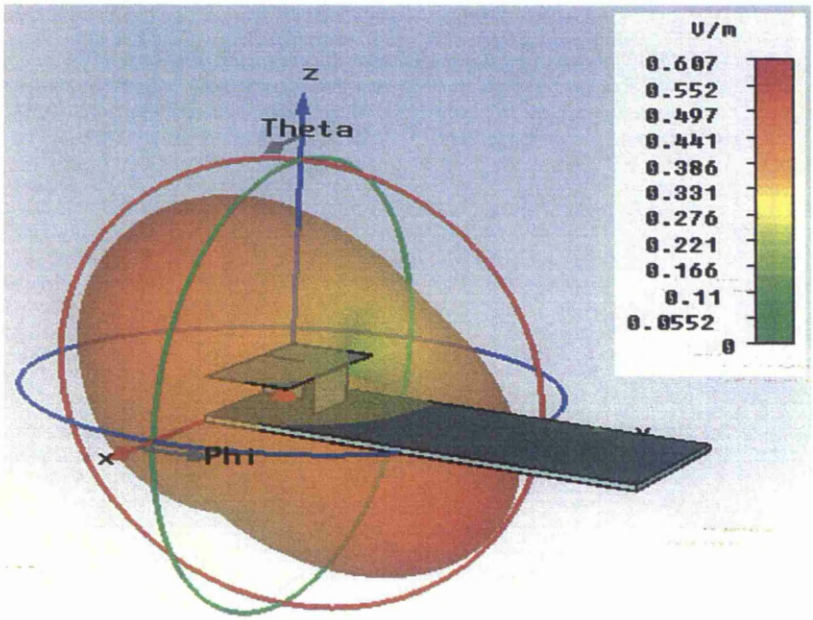

Fig. 6.22 3D simulated rad. pattern of Dual-feed PIFA with Port 1 at 2.45 GHz

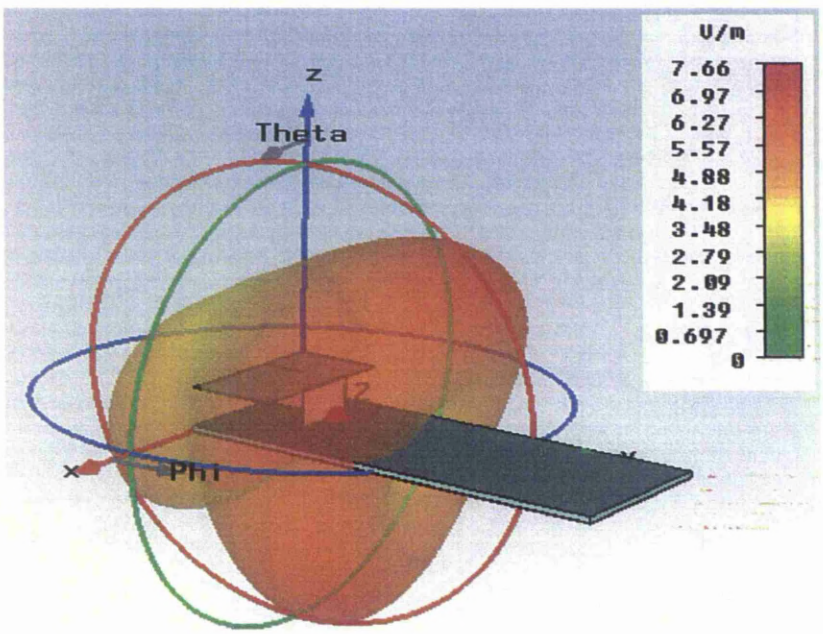

Fig. 6.23 3D simulated rad. pattern of Dual-feed PIFA with Port 2 at 2.45 GHz

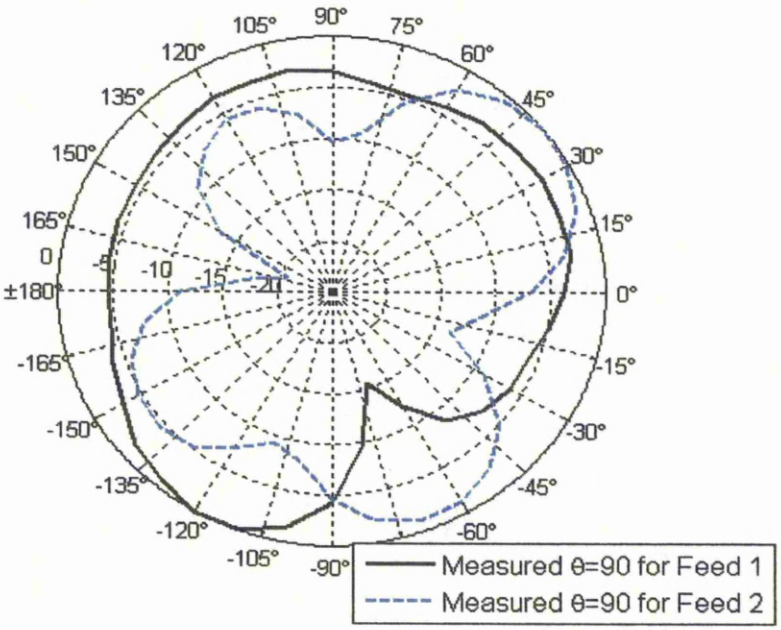

(a) XY ($\theta = 90°$)

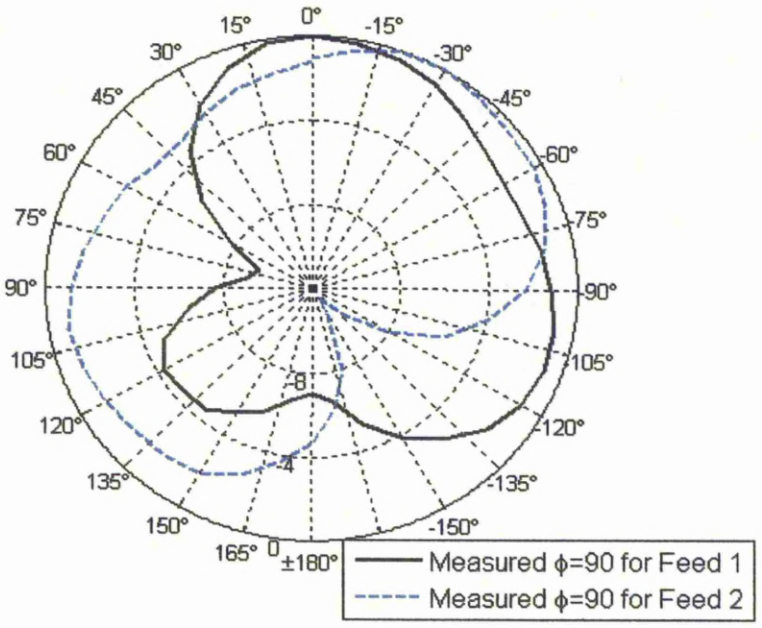

(b) YZ ($\Phi = 90°$) plane

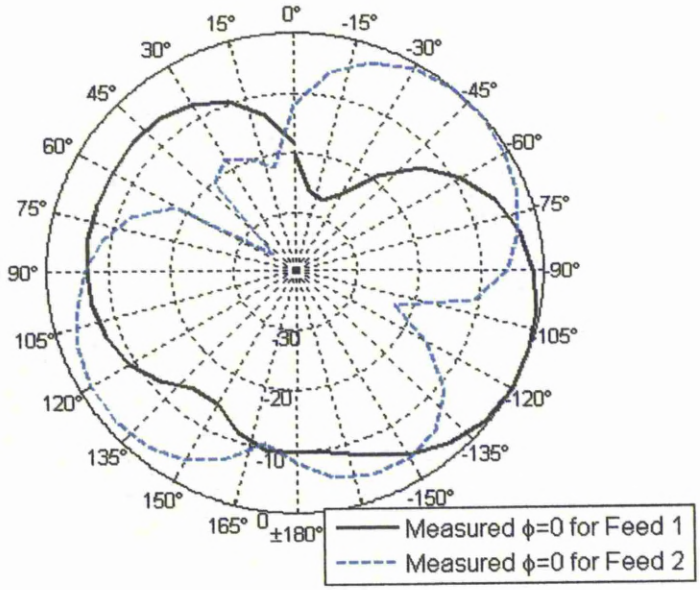

(c) XZ ($\Phi = 0°$) plane

Fig. 6.24 2D measured radiation patterns in dB scale for feed 1 and feed 2 at 2.45 GHz for different planes

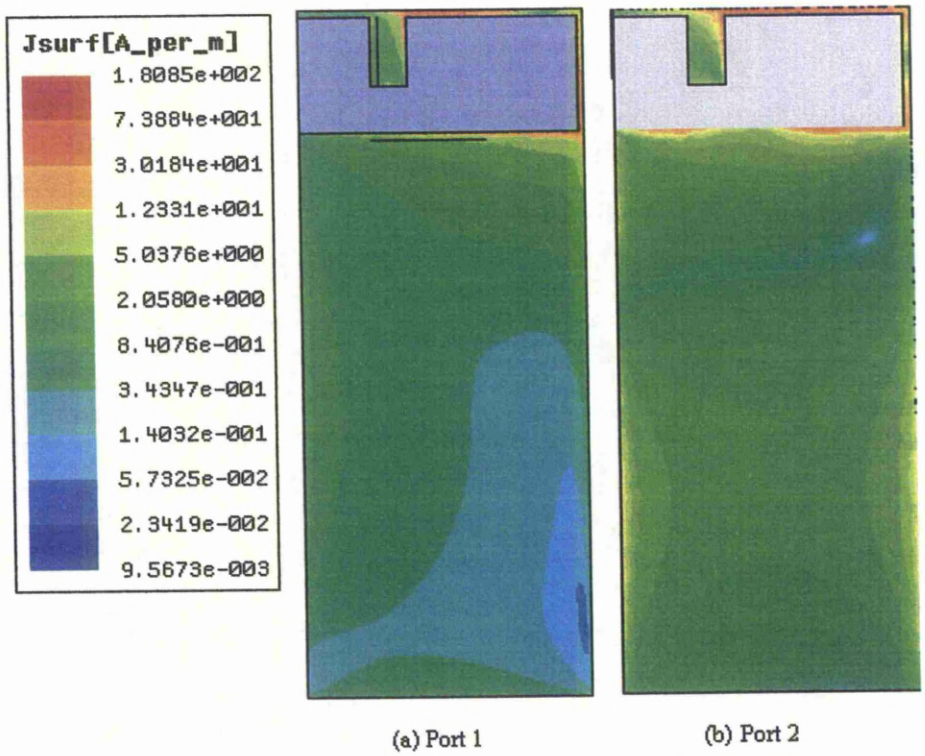

(a) Port 1 (b) Port 2

Fig. 6.25 Current Distribution on the ground plane of PIFA due to Port 1 and Port 2 at 2.45 GHz

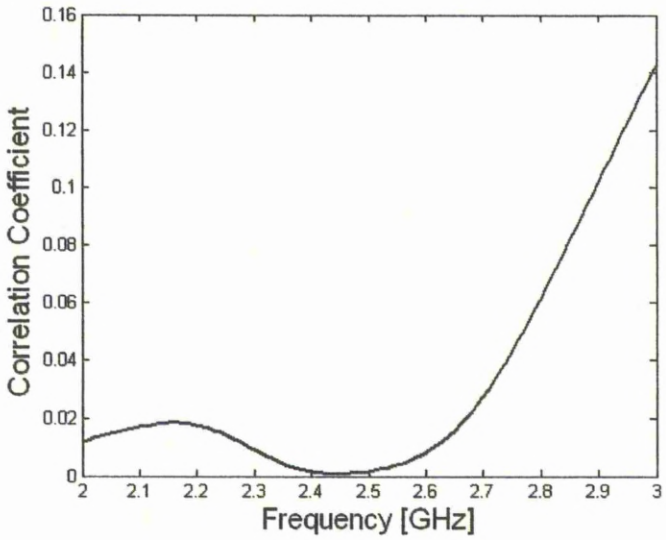

Fig. 6.26 Envelope-correlation coefficient versus frequency in GHz

6.4.3 Parametric Study

The ground plane dimensions are varied to observe its effects on the resonant frequencies and bandwidth of Ports 1 and 2. Fig. 6.27 shows the graphs of changing the length of ground plane versus the frequency in GHz for the Port 1 and Port 2 respectively. It can be seen that the resonant frequency by the Port 1 is not affected significantly by the variation of length of ground plane whereas the resonant frequency and bandwidth by the Port 2 is greatly affected by the variation of ground plane. It is due to the fact that Port 1 is connected only through a small strip to the ground plane that is why there is no significant effect of changing the length of ground plane on the Port 1. The same resonant frequency and bandwidth from the Port 2 can be achieved by varying the width of second feed plate W_{f2} and the horizontal distance of feed plate 2 from the edge of the ground plane L_{f2}. According to the theory characteristic modes, different radiation patterns can be achieved by exciting different current modes of the radiating portion of the antenna [28]. As stated above that the dimension of ground plane greatly affects the resonant frequency of Port 2 but not Port 1. So the diversity is achieved due to the fact that Port 1 uses the top plate as the main radiating element whereas Port 2 uses the top plate as well as the ground plane as the radiating elements, which is

also evident from the current distribution obtained from the simulation. Thus the radiation patterns produced by the two ports are different as shown in Fig. 6.22. Polarization diversity is achieved due to the two feed plates placed perpendicular to each other which produce cross-polarization.

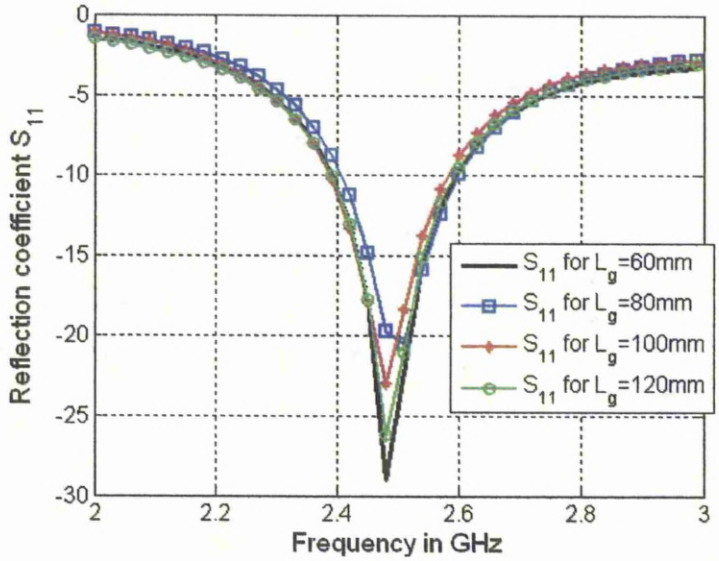

(a) S_{11}

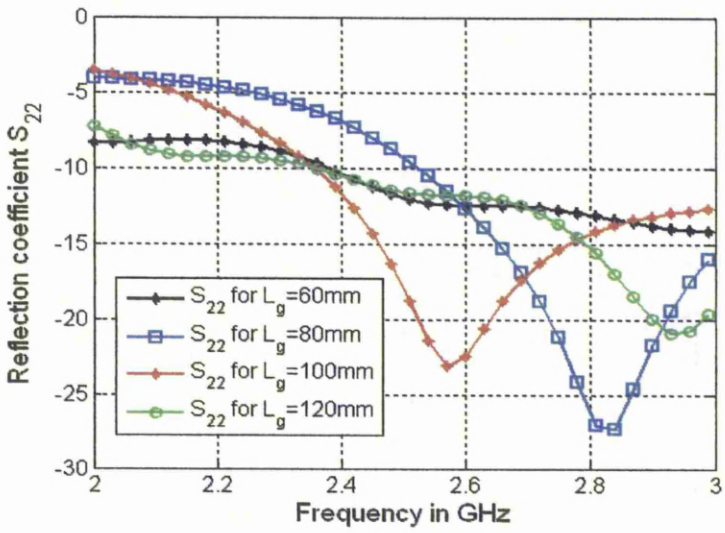

(b) S_{22}

Fig. 6.27 Reflection coefficients versus frequency in GHz for different values of L_g

6.4.4 Diversity Gain Measurement

The diversity gain of the dual-feed PIFA with perpendicular feed plates is measured in a reverberation chamber. The measurements utilize the

reverberation chamber at the University of Liverpool. The diversity gain result for the dual-feed PIFA with perpendicular plates is shown in Fig. 6.28. We can establish that diversity gain of dual-feed PIFA with perpendicular feed plates (cross-polarized) has a value of around 10 dB; an increase of around 10 % as compared to dual-feed PIFA with parallel feed plates when measured at the 1% cumulative probability level. Hence the dual-feed PIFA with perpendicular feed plates has 10 % higher diversity gain than that of with parallel feed plates due to the two diversity techniques (polarization and pattern diversity) used to produce diversity gain.

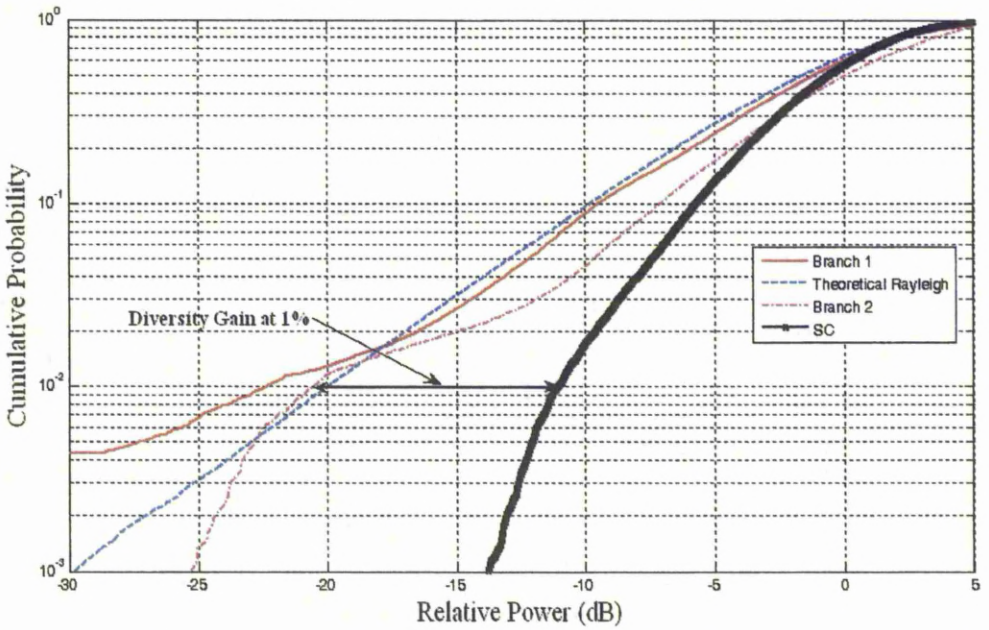

Fig. 6.28 Measured diversity gain of dual-feed PIFA with perpendicular feed plates

6.5 Dual-Feed PIFA with Parallel Feed Plates for Height h = 5 mm

We have presented above the two dual-feed PIFA antennas with a height of $h = 10$ *mm*. But these dual-feed PIFA are not suitable for some portable applications as the height is relatively large. For these applications, a thinner version of this design is required. As the dual-feed PIFA antennas discussed above are very sensitive to the height, just reducing the height does not work – many design parameters and modifications are needed to design a compact and low

profile dual-feed PIFA antenna. Here a dual feed PIFA with a height $h = 5\ mm$ is presented to produce pattern diversity. A portion of the ground plane under the top radiating plate is modified and etched out to increase the isolation between two ports/feeds. This PIFA antenna also covers the 2.45 GHz Bluetooth/WLAN band and can be used in mobile and PDA terminals as a diversity or MIMO antenna.

6.5.1 Antenna Configuration

The configuration of the dual-feed PIFA is shown in Fig. 6.29. The radiating top plate has dimensions $W \times L$ and ground plane dimensions are $W_g \times L_g$. The dielectric material used between the rectangular ground plane and the two feeds is FR-4 having a thickness $t = 1.5$ mm and relative permittivity $\varepsilon_r = 4.4$. The antenna height h is filled with air (free space). In practice, a low dielectric material may be used to support the top plate. The shorting plate has dimensions $W_s \times (h+t)$ and the widths of feed plates 1 and 2 are W_{f1} and W_{f2} respectively and both feed plates have height h. The distances of feed 1 and feed 2 from the upper edge of the ground plane are L_y and L_u respectively. The horizontal distance of feed 2 from the side edge of the ground plane is L_{f2}.The bottom view of the modified ground plane is shown in Fig. 6.30. The ground plane is modified to improve the isolation as the two ports are strongly connected through ground plane and most of the current flows on the ground plane between the two ports as discussed above. The main differences between this antenna design and the antenna designs presented above are modifications done on the ground plane and the position of feed plate 1. The length of the etched part of the ground plane is S_{ug}. The two parts of the ground plane are connected through a small strip of thickness S_x. The thickness of the upper part of the ground plane which is connected to shorting plate is S_y. The ground plane is extended opposite to that end of ground plane where a small strip connects the upper and lower part of the ground plane. The vertical extension of ground plane is D_x and its thickness is also equal to D_x. The horizontal extension of this ground plane is equal to the width of feed plate W_f and its thickness (width) is equal to D_y. The idea here is to introduce anti-resonance at the operational frequency 2.45 GHz between the 2 feeds – to isolate them and hence to generate

the desired diversity. The PIFA antenna is fed by coaxial cables through 2 SMA connectors connected to Port 1 and Port 2. The software package used for simulation is Ansoft's High Frequency Structure Simulator (HFSS) based on the Finite Element Method.

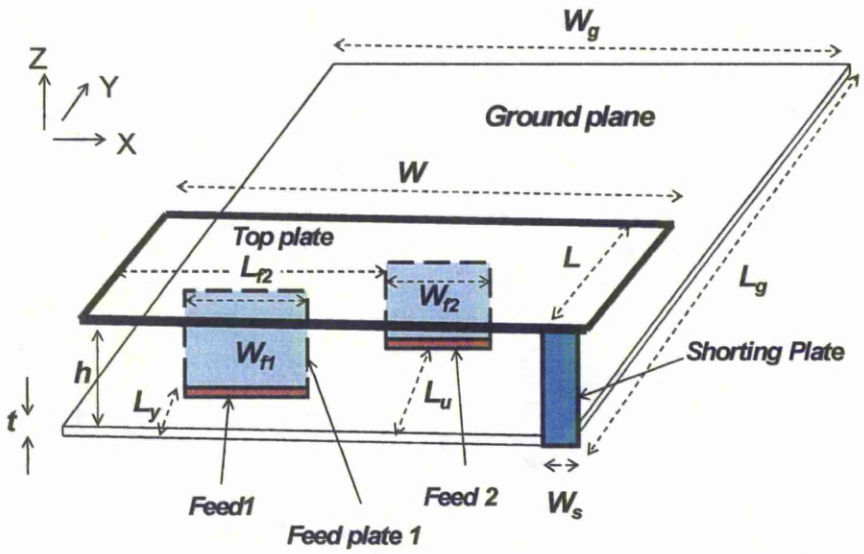

Fig. 6.29 The configuration of the dual feed PIFA antenna for *h=5mm*

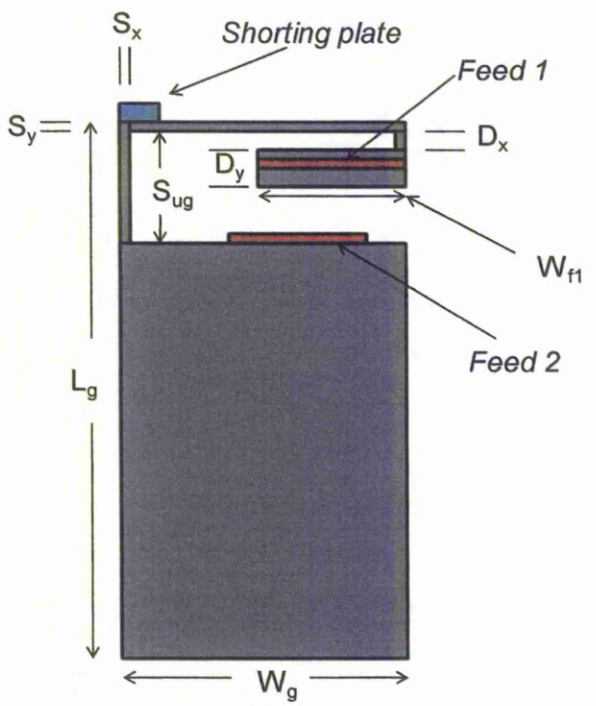

Fig. 6.30 The bottom view of the modified ground plane of the antenna

6.5.2 Simulated and Experimental Results

Due to the modifications in the ground plane and in the height of PIFA, the placements/positions of both feed plates and widths of these feed plates need to be adjusted in order to get the required resonant frequencies by both the ports. A parametric study is undertaken to optimize these parameters. All the optimized parameters of this dual-feed PIFA antenna obtained for 2.45 GHz WLAN applications are as follows: W_{f1}= *20.5 mm,* W_{f2} =*10 mm,* W_g = *40 mm,* L_g = *100 mm,* W = *40 mm,* L = *20 mm,* h = *5 mm,* W_s = *1 mm,* L_y = *2 mm,* L_{f2} = *5 mm,* L_u = *19 mm,* S_{ug} = *18 mm,* S_y = S_x = *0.5 mm,* and D_x = D_y = *1mm.* The simulated and measured results are shown in Figs. 6.31 and 6.32. It can be seen that the bandwidth achieved by port 1 is approximately 50 MHz from 2.425 GHz to 2.475 GHz (simulated) whereas the measured S_{11} is comparatively wide and measured bandwidth is around 300 MHz. The difference between them should be resulted from the connectors and cables used in the measurement. The reduced simulated bandwidth is due to the reduction in height as we know that reduction in height of PIFA reduces the bandwidth of the antenna [31]. The 3D simulated radiation pattern of this dual-feed PIFA with Port 1 and Port 2 alone are shown in Figs. 6.33 and 6.34 respectively and the 2D polar plots of the measured radiation patterns of this dual-feed PIFA are shown in Fig. 6.35. It is evident that the radiation patterns by the two ports are quite different which shows that diversity gain is achieved due to the pattern diversity. This dual-feed PIFA also fulfils the two condition described in Eq. 5.15 which is also clear from the graph of correlation coefficient versus the frequency in Fig. 6.36.

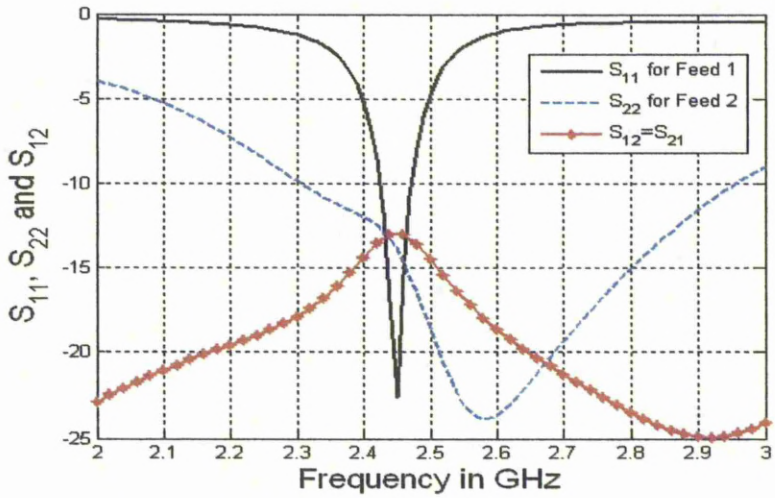

Fig. 6.31 Simulated S_{11}, S_{22} and S_{12} of low profile dual-feed PIFA

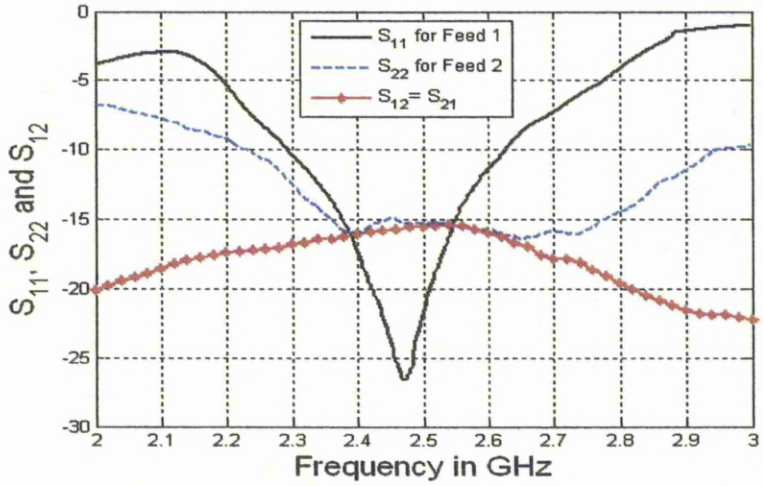

Fig. 6.32 Measured S_{11}, S_{22} and S_{12} of low profile dual-feed PIFA

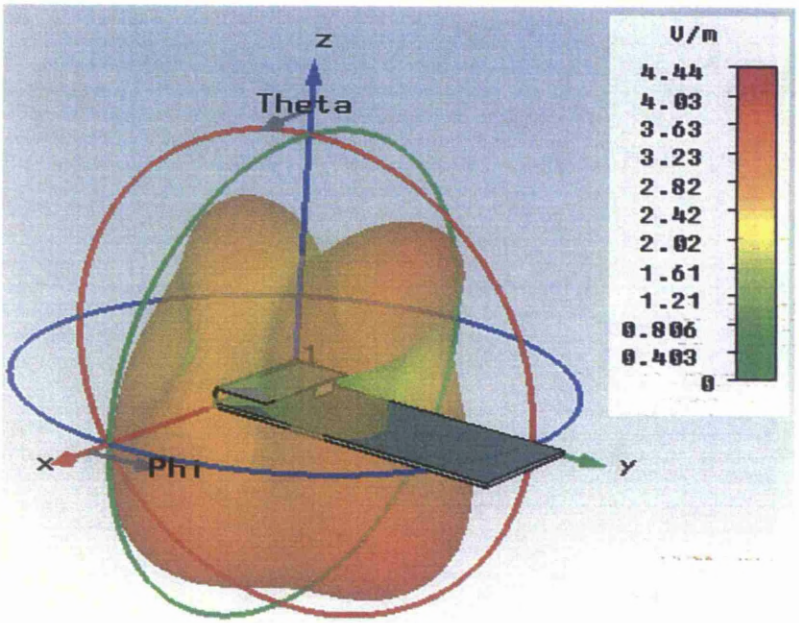

Fig. 6.33 3D simulated rad. pattern of dual-feed PIFA with Port 1 at 2.45 GHz

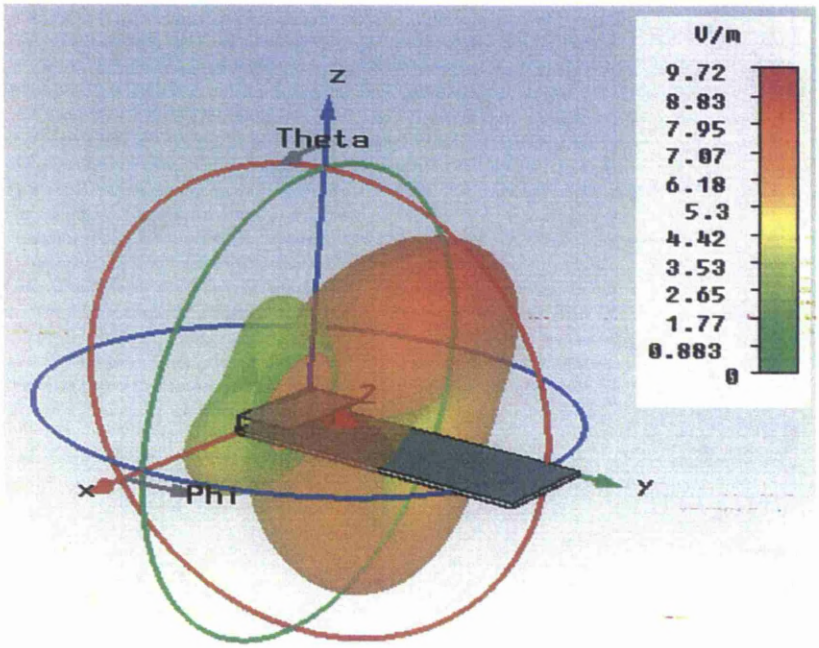

Fig. 6.34 3D simulated rad. pattern of dual-feed PIFA with Port 2 at 2.45 GHz

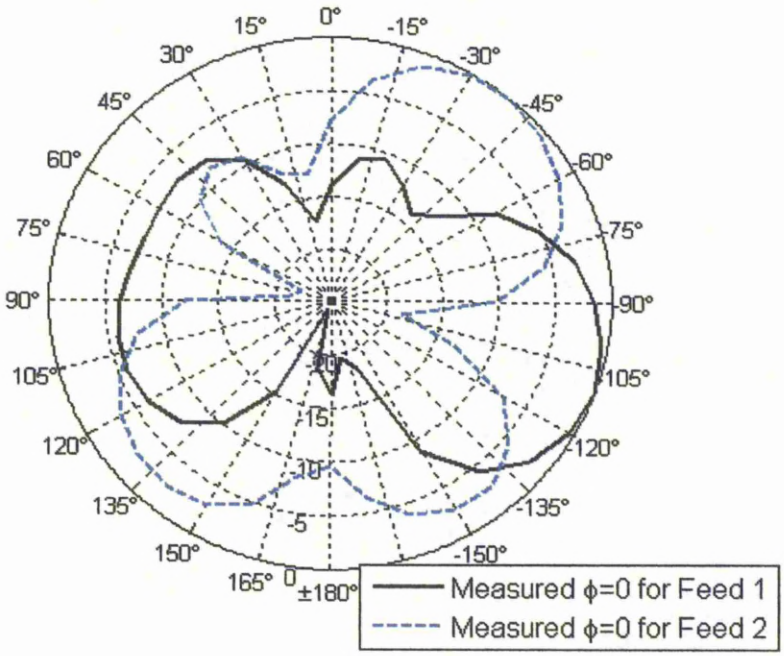

(a) XZ ($\Phi = 0°$) plane

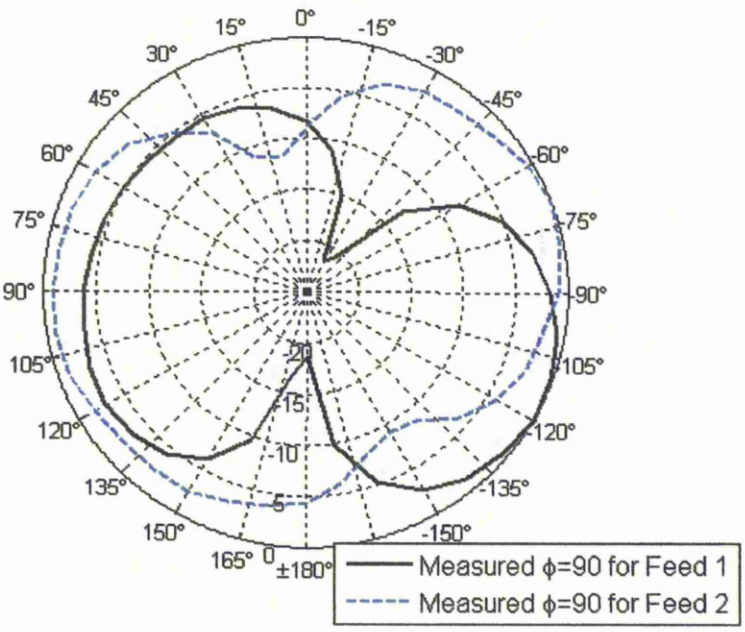

(b) YZ ($\Phi = 90°$) plane

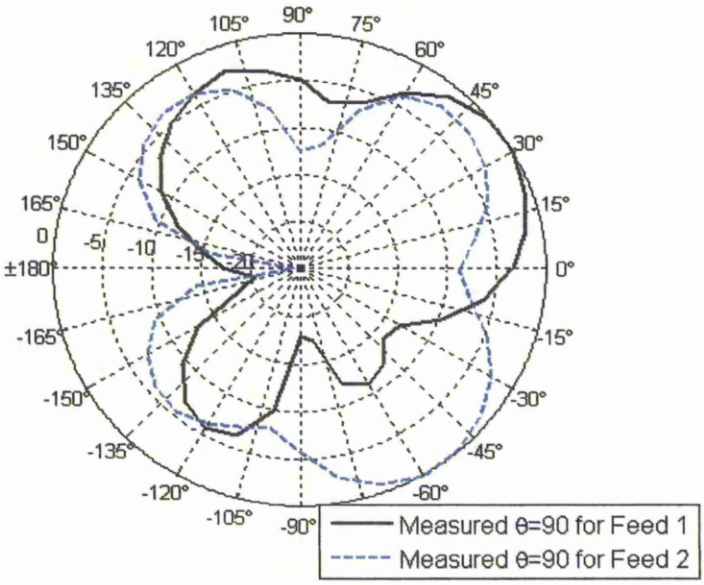

(c) XY ($\theta = 90°$) plane

Fig. 6.35 2D measured radiation patterns in dB scale for Port 1 and Port 2 at 2.45 GHz for different planes

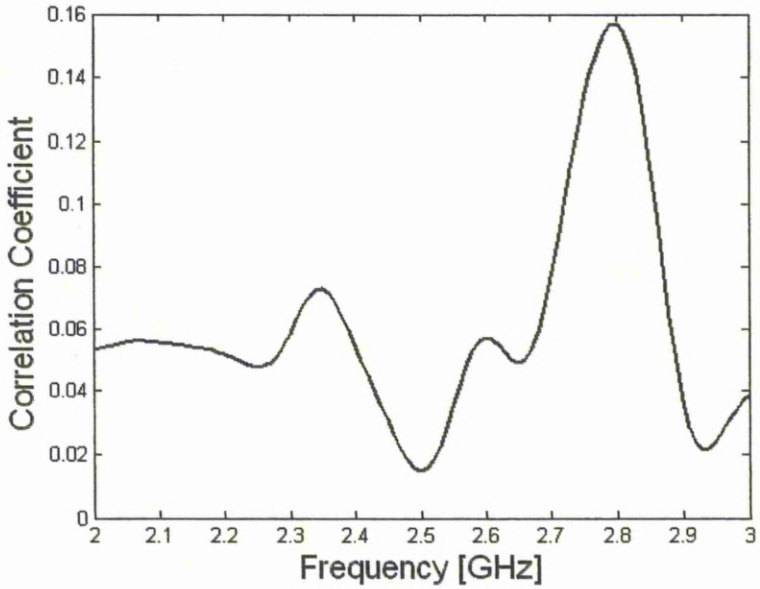

Fig. 6.36 Envelope-correlation coefficient versus frequency in GHz

6.5.3 Diversity Gain Measurement

The diversity gain of this dual-feed PIFA for h = 5 mm with parallel feed plates is measured in a reverberation chamber. The measurement utilizes the reverberation chamber at the University of Liverpool. The diversity gain result for

this dual-feed PIFA is shown in Fig. 6.37. The level of diversity gain calculated for this antenna, measured at the 1% cumulative probability, between the MRC and the strongest branch (Branch 1 in this case) is equal to 9.951 dB.

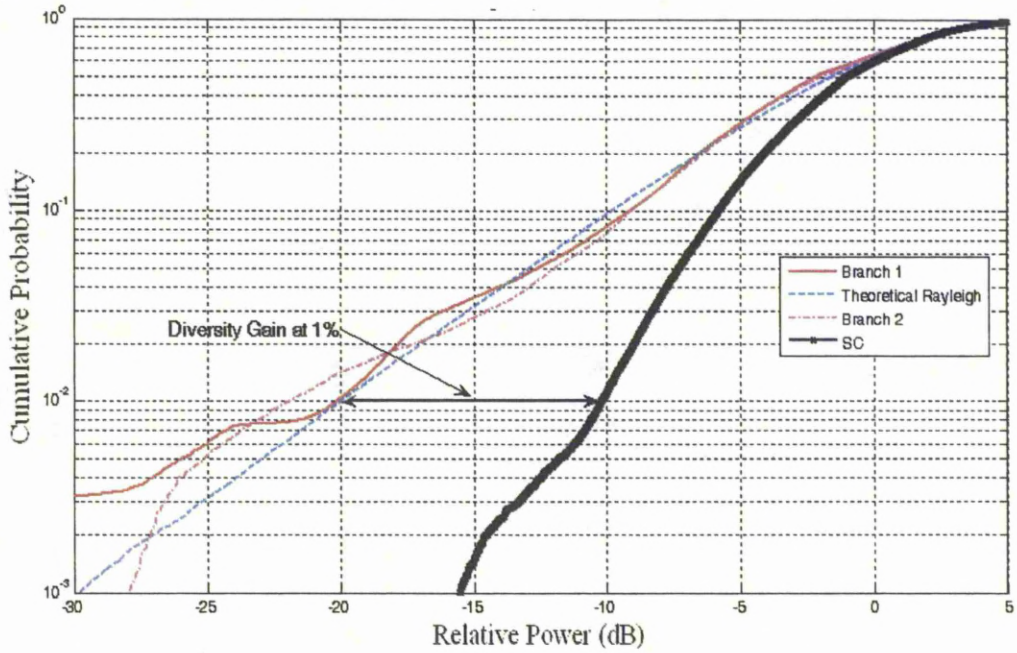

Fig. 6.37 Measured diversity gain of dual-feed PIFA for h = 5 mm with parallel feed plates

6.6 Summary

In literature, more than one PIFA antennas were used to produce diversity gain using spatial diversity. But implementation of spatial diversity in case of small portable systems such cellular mobile is very difficult as space available is very small. In this chapter, we have used pattern diversity and polarization diversity to produce diversity gain. The concept is to use one PIFA antenna with multiple feeds instead of two or more antenna elements in order to save space and cost. In order to increase the isolation and reduce the mutual coupling between the two ports, the ground planes under the top radiating plate are modified which produce anti-resonances between the two ports.

We have presented three new and compact designs of dual-feed PIFAs for different heights using pattern and polarization diversity. The designs are optimized for Bluetooth/WLAN 2.45 GHz band. Parametric studies are conducted to exhibit how resonant frequencies are affected by different parameters. And it shows that we can modify the parameters to use these PIFA designs to work for other bands such as Long Term Evolution (LTE) 2.5 GHz - 2.7 GHz band. Diversity gains are measured in a reverberation chamber which exhibit that diversity gains are achieved by these antenna designs if these antennas are utilized in portable systems for a real practical environment.

References

[1] R. G. Vaughan and J. B. Andersen, "Antenna diversity in mobile communications", *IEEE Trans. Vehicular Technology*, vol. VT-36, pp. 147–172, Nov. 1987.

[2] G. F. Pedersen and J. B. Andersen, "Handset antennas for mobile communications: Integration, diversity and performance," *Rev. Radio Sci. 1996 – 1999*, pp. 119–133, Aug. 1999.

[3] P. Mattheijssen, M. Herben, G. Dolmans and L. Leyten, "Antenna-pattern diversity versus space diversity for use at handhelds", *IEEE Transaction on Vehicular Tech,* vol. 53, no. 4, pages(s): 1035–1042, July 2004.

[4] P. S. Kildal and K. Rosengren, "Correlation and capacity of MIMO systems and mutual coupling, radiation efficiency, and diversity gain of their antennas: Simulations and measurements in a reverberation chamber", *IEEE Communication Mag.*, vol. 42, no. 12, pp. 104–112, December 2004.

[5] M. LeFevre, M. A. Jensen and M. D. Rice, "Indoor measurement of handset dual-antenna diversity performance", *47th IEEE Vehicular Technol. Conference,* vol. 3, Page(s): 1763–1767, 1994.

[6] S. C. K. Ko, and R. D. Murch, "Compact integrated diversity antenna for wireless communications", *IEEE Trans. Antennas Propagation*, vol. 49, pp. 954–960, June 2001.

[7] S. B. Yeap, X. Chen, J. A. Dupuy, C. C. Chiau and C. G. Parini, "Integrated diversity antenna for laptop and PDA terminal in a MIMO system", *IEE Proc.-Microw. Antenna Propag.,* vol. 152, No. 6, December 2005.

[8] M. Karaboikis, C. Soras, G. Tsachtsiris and V. Makios, "Compact dual-printed inverted-F antenna diversity systems for portable wireless devices", *IEEE Antennas and Wireless Prop letters,* vol. 3, page(s):9 – 14, 2004.

[9] S. Zhang, J. Hiong and S. He, "MIMO antenna system of two closely-positioned PIFAs with high isolation", *ELECTRONICS LETTERS*, vol. 45, no. 15, July 16, 2009.

[10] Y. Gao, C. C. Chiau, X. Chen and C. G. Parini, " Modified PIFA and its array for MIMO terminals", *IEE Proc.- Microw. Antenna Propagation,* vol. 152, no. 4, August 2005.

[11] S. B. Yeap, X. Chen, J. A. Dupuy, C. C. Chiau and C. G. Parini, "Low profile diversity antenna for MIMO applications", *ELECTRONICS LETTERS*, vol. 42, no. 2, January 19, 2006

[12] K. Chung and J. H. Yoon, "Integrated MIMO antenna with high isolation characteristics" *ELECTRONICS LETTERS*, vol. 43, no. 4, February 15, 2007

[13] F. M. Caimi, M. Mongomery and P. Tornatta, "Isolated Mode Antenna Technology (IMAT)", *SkyCross,* Inc. Jan, 2008.

[14] F. M. Caimi and M. Mongomery, (Skycross,USA)" Dual feed, single element antenna for WiMax MIMO application", *Hindawi Publishing Corp. Intern. Journal of Antennas and Propagation,* vol. 2008.

[15] P. Hallbjoner, "Dual feed monopole antenna" *IEE Proc.- Microw. Antenna Propagation,* vol. 150, No. 3, June 2003.

[16] K. Hirasawa and M. Haneishi, *Analysis, Design, and Measurement of Small and Low-Profile Antennas*, Artech House, 1992.

[17] P. S. Hall, E. Lee, C. T. P. Song, Planar inverted-F antennas, Chapter 7, *Printed antennas for wireless communications* Edited by R. Waterhouse, John Wiley & Sons, 2007.

[18] Y. Huang and K. Boyle, *Antennas: from theory to practice*, John Wiley & Sons, 2008.

[19] Y. Chung, S. Jeon, D. Ahn, J. Choi and T. Itoh, "High isolation dual-polarized patch antenna using integrated defected ground structure" *IEEE Microwave and Wireless Components Letters,* vol. 14, No. 1, page(s):4 – 6, January 2004.

[20] C. Chiu, C. Cheng, R. D. Murch and C. R. Rowell, "Reduction of mutual coupling between closely-packed antenna elements" *IEEE Transactions on Antennas and Propagation,* , vol. 55, no. 6, page(s):1732-1738, June 2007.

[21] K. Kim and K. Ahn, "The high isolation dual-band inverted F antenna diversity system with the small N-section resonators on the ground plane" Microwave and optical technology letters, vol. 49, No. 3, March 2007.

[22] J. Itoh, N. Michishita and H. Morishita, "Mutual coupling reduction between two inverted-F antennas using mushroom-type composite right-/left –handed transmission lines", *3rd European Conference on Antennas and Propagation (EuCAP)*, page(s):3575 – 3579, March 2009.

[23] A. Diallo, C. Luxey, P. L. Thuc. R. Staraj and G. Kossiavas, "Study and reduction of the mutual coupling between two mobile phone PIFAs operating in the DCS1800 and UMTS bands" *IEEE Transactions on Antennas and Propagation,* vol. 54, no. 11, page(s):3063 - 3074, November 2006.

[24] A. C. K. Mak, C. R. Rowell and R. D. Murch, "Isolation enhancement between two closely packed antennas" *IEEE Transactions on Antennas and Propagation,* vol. 56, no. 11, page(s): 3411 - 3419, November 2008.

[25] S. Chen, Y. Wang and S. Chung, "A decoupling technique for increasing the port isolation between two strongly coupled antennas" *IEEE Transactions on Antennas and Propagation,* Vol. 56, no. 12, page(s): 3650 - 3658, December 2008.

[26] H. T. Chattha, Y. Huang and Y. Lu, "PIFA bandwidth enhancement by changing the widths of feed and shorting plates", *IEEE Antennas & Wireless Propagation Letters*, vol. 08, page(s):637 – 640, 2009.

[27] R. F. Harrington and J. R. Mautz, "Theory of characteristic modes for conducting bodies," *IEEE Transactions on Antennas and Propagation,* AP-19, pp. 622-628, September 197 1.

[28] M. C. Fabres, E. A. Daviu, A. V. Nogueira and M. F. Bataller, "The theory of characteristic modes revisited: A contribution to the design of antennas for modern applications", *IEEE Antennas and Propagation Magazine*, vol. 49, no. 5, October 2007.

[29] S. Blanch, J. Romeu and I. Cotbella, "Exact representation of antenna system diversity performance from input parameter description", *ELECTRONICS LETTERS*, vol. 39, no. 9, May 1, 2003

[30] H. T. Chattha, Y. Huang, X. Zhu and Y. Lu, "A dual-feed PIFA diversity antenna for MIMO systems", *International Workshop on Antenna Technology (iWAT)*, pages(s): 1-4, 2010.

[31] H. T. Chattha, Y. Huang and Y. Lu, "A further study of planar inverted-F antenna", *IEEE International Workshop on Antenna Technology (iWAT)*, pp. 1-4, 2009.

CHAPTER

7

Conclusions and Future Work

7.1 Summary

The MIMO systems have shown the ability to increase the channel capacity and enhance the reliability of the wireless systems without increasing the transmitted signal power and bandwidth. The data rates and coverage of a MIMO system can be improved by using spatial multiplexing and space time coding respectively. That is the reason that MIMO systems are used in WLAN and Wimax systems and wireless mobile communication systems such as 3G and 4G will utilize the MIMO systems in near future. Future wireless communication systems will utilize MIMO and diversity antennas to increase the data rates. We have discussed different antennas which are implemented on small portable systems over the last two decades. But increasing demands of the users for the compact and low-profile portable systems have minimized the use of most of these antennas in the current and future wireless communication systems. Planar Inverted-F antenna (PIFA) is used in most of the current portable systems due to its compactness, low-profile, ease of fabrication and desired features in terms of

radiation patterns and gain etc. This features and characteristics make PIFA a very suitable candidate as a MIMO and diversity antenna. Due to these factors, PIFA was taken as a main element of study in this work.

Before using this PIFA antenna as a diversity and MIMO antenna, a comprehensive parametric study was undertaken and a new empirical equation is proposed to predict the resonant frequency of PIFA. The requirements for designing a MIMO or diversity antenna such as a high diversity gain and low mutual coupling are also addressed in this thesis. The diversity gain is a measure of the effectiveness of the diversity technique. High diversity gain can be achieved when the received signals from the antenna elements have low correlation and the power levels of the signals from these antenna elements should not be too different in a multipath environment. There are different isolation techniques introduced to achieve low mutual coupling between two antenna elements. However, it is observed that at the moment, there are no clear design criteria to achieve low mutual coupling and high isolation in a limited sized mobile terminal. The diversity technique which uses more than one antenna to transmit or receive signals, called space diversity, is utilized in space time code to exploit the MIMO channels. This is a well known method for solving the signal fading problem in multipath environment. The theoretical separation between two antenna elements is at least half-wavelength for minimum coupling. But in case of small portable systems, the space available is comparatively small so implementing more than antenna elements on such small spaces are hard to achieve. So in this thesis, the focus is given on the other antenna diversity techniques such as pattern and polarization diversities to achieve diversity gain. In order to save the space and cost, the concept of using one antenna with multiple feeds is used to achieve diversity gain. It is observed that in case of PIFA, strong current flows on the ground plane which is the PCB of a mobile terminal, so the ground plane is acting as a radiator rather than a reflector. So ground plane is modified and etched out to achieve low mutual coupling between the two ports.

Three novel designs of dual-feed PIFA for heights h = 10 mm and h = 05 mm are presented. The chosen band is Bluetooth/ WLAN 2.45 GHz band. The minimum bandwidth achieved by the two ports is at least 200 MHz. These designs can also be optimized to work for the other bands such as LTE, GSM, DCS, PCS and UMTS etc. Furthermore, the diversity performances of these antennas are evaluated with selection combiner technique in a reverberation chamber to observe the diversity gain in a real environment. It is found that reasonable diversity gains of more than 5 dB at 99 % reliability are achieved by all these antenna designs.

7.2 Key Contributions

In this thesis, three different areas related to PIFA antenna are investigated. The major contributions in this thesis are detailed in the following three sections.

Comprehensive Parametric Study and Empirical Equation of PIFA

- A comprehensive parametric study is undertaken to get the knowledge of how PIFA characteristics are affected by the change of different parameters. It was observed that partial studies were done by taking into account effects of dimension of ground plane, height of PIFA, and width of shorting plate on the characteristics of PIFA but no comprehensive parametric study existed in literature which could illustrate that how all the parameters of PIFA affect the characteristics such as the resonant frequency, impedance bandwidth and radiation pattern. This study was done by varying one parameter at a time while all other parameters were held constant.
- Then the results of this parametric study are characterized so that the PIFA designers may use the knowledge of this parametric study to develop the

PIFA antenna for the required resonant frequency and impedance bandwidth.

- It is found that impedance bandwidth can be increased by just modifying the structure of PIFA. By shortening the width of shorting plate and increasing the width of feed plate to the right value, increases the impedance bandwidth of PIFA.
- It was also observed that the empirical equation used before was also insufficient to predict the resonant frequency of PIFA as it does not include those parameters which significantly affect the resonant frequency. So based on our parametric study, a new empirical equation is proposed which can be used to predict the resonant frequency of PIFA with average error of 3 %.

Bandwidth Enhancement Techniques of PIFA

The second focus of the work was to investigate the techniques of increasing the impedance bandwidth of PIFA as this antenna was assumed a narrow band antenna. Three bandwidth enhancement techniques are proposed which significantly increase the bandwidth of PIFA.

- First technique investigates the effects of changing the widths of feed plate and shorting plate on the impedance bandwidth. It is shown that a PIFA with a much wider bandwidth (up to 65%) than previously reported can be achieved by optimizing the widths of the feed and shorting plates.
- 2nd technique introduces a PIFA antenna having a parasitic element. It is shown that due to the addition of this parasitic element, this PIFA can achieve a very wide bandwidth (more than 100%).
- The ultra wide band (UWB) systems require antennas having a very broad impedance bandwidth. The planar inverted-F antenna (PIFA) was not yet employed as an ultra wide band antenna due to its perceived narrow band characteristics. A new ultra wide band PIFA is made and tested with one parasitic element for frequencies from about 3.35 GHz to 9.4 GHz

(simulated), with a fractional bandwidth of about 102%, which is ideal for emerging ultra wide band (UWB) wireless applications.

- 3rd technique introduces another rectangular shaped parasitic element in addition to the first two techniques discussed above. The addition of this parasitic element further increases the impedance bandwidth to around 120 %.
- As UWB PIFA described above does not cover the full UWB band therefore, an UWB PIFA with two parasitic elements is also made and tested which almost cover the whole band from 3.5 GHz to 10.7 GHz (simulated).

PIFA as a Diversity and MIMO Antenna

Third work includes the use of PIFA as a diversity and MIMO antenna. Three designs have been made and tested.

- First antenna design introduces a novel dual-feed Planar Inverted-F Antenna (PIFA) suitable for wireless diversity/MIMO applications with height of PIFA h = 10 mm. By exploiting the pattern diversity, we have successfully made a provision of two isolated feeding ports using one common radiating plate. The two feed plates are placed parallel to each other. The main technique introduced is to etch the ground plane under the radiating plate to reduce the mutual coupling between the two ports. It is found that the envelope cross-correlation is less than 0.02 and the ratio of the mean effective gain between the two ports is close to unity. Thus, this new PIFA antenna can provide a better solution than two separate antennas for diversity and MIMO applications by saving the space and cost.
- 2nd design presents a new and novel dual-feed Planar Inverted-F Antenna (PIFA) suitable for wireless applications such as Wireless Local Area Network (WLAN) and Long Term Evolution (LTE) as a diversity and MIMO antenna with height of PIFA h = 10 mm. Instead of two antenna

elements, there is only one top radiating element with two isolated ports which save the space and the cost. The two feed plates are placed perpendicular to each other due to which polarization diversity as well as pattern diversity is exploited to achieve diversity gain. The isolation between the two antenna ports is achieved by the modifying the ground plane under the top radiating element.

- 3rd design introduces a new low profile dual-feed Planar Inverted-F Antenna (PIFA) suitable for wireless LAN applications with height of PIFA h = 5 mm. Pattern diversity is exploited using one common radiating plate and two isolated feeding ports. The isolation is successfully achieved mainly by modifying the ground plane under the radiating plate and producing an anti resonance between the ports. Thus, this single PIFA antenna can act as two separate antennas for diversity and MIMO applications with reduced space and cost.

7.3 Future Work

Based on the conclusions drawn and the limitations of the work presented, future work can be carried out in the following areas:

- In comprehensive parametric study of PIFA, only one parameter is changed at time while all other parameters are held constant. It would also be useful to perform tests for combinations of variations.
- For UWB antenna, the transfer function characteristics or time domain response is also important parameters for its effectiveness for UWB applications. Therefore, the transfer functions of UWB PIFAs presented in thesis can be measured to check its suitability for UWB applications.
- The isolation technique of modifying and etching out the ground plane, used in the dual-feed PIFA antenna designs presented in this thesis, has the deficiency that it reduces the bandwidth. So some other isolation techniques need to be explored to avoid reduction in bandwidth.

- It would also be interesting to increase the bandwidth with the present isolation technique used in the dual-feed PIFA designs.
- The dual-feed PIFA antenna designs need to be further reduced in height and make it more robust for practical applications
- Using the concept of producing anti resonances, the feeding ports can be increased further to work in the same frequency band.
- The concept of using one antenna element with multiple ports can be extended to other antennas such as planar monopole antennas etc.